Titre: Title:	Polluant transport in overland flow with dissolution, infiltration and adsorption effects
Auteur: Author:	Min Yan
Date:	1999
Type:	Mémoire ou thèse / Dissertation or Thesis
Référence: Citation:	Yan, M. (1999). Polluant transport in overland flow with dissolution, infiltration and adsorption effects [Thèse de doctorat, École Polytechnique de Montréal]. PolyPublie. https://publications.polymtl.ca/8791/

UNIVERSITÉ DE MONTRÉAL

POLLUTANT TRANSPORT IN OVERLAND FLOW WITH DISSOLUTION, INFILTRATION AND ADSORPTION EFFECTS

MIN YAN
DÉPARTEMENT DES GÉNIES CIVIL, GÉOLOGIQUE ET
DES MINES
ÉCOLE POLYTECHNIQUE DE MONTRÉAL

THÈSE PRÉSENTÉE EN VUE DE L'OBTENTION
DU DIPLÔME DE PHILOSOPHIAE DOCTOR (Ph.D.)
(GÉNIE CIVIL)
AOÛT 1999

UNIVERSITÉ DE MONTRÉAL

ÉCOLE POLYTECHNIQUE DE MONTRÉAL

Cette thèse intitulée:

POLLUTANT TRANSPORT IN OVERLAND FLOW WITH DISSOLUTION, INFILTRATION AND ADSORPTION EFFECTS

présentée par: **YAN Min**

en vue de l'obtention du diplôme de: Philosophiae Doctor

a été dûment acceptée par le jury d'examen constitué de:

M. CHAPUIS Robert P., Ph. D., président

M. KAHAWITA René, Ph. D., membre et directeur du recherche

M. ROUSSELLE Jean, Ph. D., membre

M. CARBALLADA Luis, Ph. D., examinateur externe

DEDICATION

To my parents Yan xushi and Zhuang Liuqing

my husband Xu Guocheng

and my beloved daughter Xu Ying

ACKNOWLEDGEMENTS

It has been my privilege to study under the Dr. Rene Kahawita's guidance during my years at Ecole Polytechnique, from whom I have learned much, his continuous support, confidence given to me and help cannot be ever properly acknowledge.

I am grateful to the members of my committee, Dr. Robert P. Chapuis, Dr. Jean Rousselle, and Dr. Luis Carballada for their valuable comments which improved the quality of this work.

I am also grateful to Dr. Jean. Rousselle for permitting to use hydrologic equipment for my experiment.

I would like to thank all my colleges and friends who contribute directly and indirectly in my study and work, including Pu Wang, Kourosh Mohammadi, André Mellado, Gilles Thériault, Yue Wang and Min Wu.

Particular thanks go to my parents, my daughter, my husband and my brother's, their love have made possible my academic endeavors that I have pursued in my life. The dedication of this thesis to them does not begin to pay my debt to them.

RÉSUMÉ

Le ruissellement de surface causé par la pluie transportant des polluants qui atteignent la surface du sol sous forme liquide ou solide est une source de pollution non ponctuelle. Le degré de pollution, provenant d'une source non ponctuelle, qui se produit à un endroit donné, dépend des conditions locales hydrologique, géographique et géologique, et varie selon les conditions climatiques régionales. Pour analyser quantitativement la source de pollution non ponctuelle dans un environnement humide, il faut simuler en même temps le champ d'éoulement et le transport de la masse en utilisant le modèle numérique approprié.

Le but de cette étude est d'améliorer de manière significative la pratique courante basée sur la modélisation mathématique du transport des polluants de source non ponctuelle présents dans le ruissellement de surface. Cette modélisation rend entièrement compte de l'évolution de la source de pollution non ponctuelle causée par le ruissellement pluvial en rapport avec l'infiltration, la dissolution et l'adsorption.

La contribution de cette étude est dans:

- L'étude des mécanismes de transport des polluants dans le ruissellement de surface en tenant compte des effects de l'infiltration, du taux de solubilité et de l'adsorption, ainsi que le développement d'un modèle numérique de simulation intégrée,

- La présentation du schéma de cannelure cubique et l'évaluation de sa mise en application comme solution technique pour le traitement numérique du modèle,
- La présentation du quelques résultats généraux qui indiquent la flexibilité du modèle et son utilité à prévoir le sort ultime d'un polluant placé sur une surface.

Le modèle numérique complet comprend les équations de St.Venant, les équations d'infiltration, l'équation du taux du solubilité, l'équation d'adsorption et l'équation du transport des polluants. Les équations bidimensionnelles de St.Venant, basées sur les principes de la continuité et de la quantité de mouvement, sont employées pour décrire la variabilité des conditions du ruissellement où sont considérées les effets de la rugosité, de l'intensité des précipitations et de l'infiltration dans le sol. Les équations de Green-Ampt et de Horton sont employées pour caractériser les processus d'infiltration. L'équation du taux de solubilité est basée sur le comportement physico-chimique du polluant dans le ruissellement et, faisant appel à l'analogie entre la masse et le transfert de quantité de mouvement, est utilisée pour simuler la transformation d'un polluant de sa phase solide à sa phase liquide. Le processus de l'adsorption-désorption peut être l'objet d'un calcul par approximation au moyen d'équations cinétiques. Quant à l'advection, l'équation de diffusion est utilisée pour suivre et tracer la migration de la concentration du polluant et, finalement, prévoir le sort ultime du polluant solide placé sur une surface.

Dans cette étude, les caractéristiques de l'entrée, de la sortie et des processus d'intervention de l'évolution des polluants dans une région donnée est directement simulée. Les entrées du modèle comportent des données des composantes spatiales, des précipitations et des conditions du sol, des polluants et de la terre ferme. Les sorties du modèle comprennent la concentration des polluants dans le ruissellement et, conséquemment, la distribution de la quantité totale des polluants.

Un ensemble d'équations régissant le système complet a été numériquement intégré en utilisant le schéma de cannelure cubique. Ce schéma est d'abord introduit pour simuler le modèle du ruissellement aqueux peu profond, lequel, selon nous, n'a pas été exploré jusqu'à maintement. Il est basé sur les rapports de cannelure cubique où l'interpolation de polynômes de niveau plus élevé peut être construite.

La praticabilité du modèle numérique a été vérifiée par trois cas pour lesquels les solutions analytiques existent et les résultats qui y apparaissent sont conformes aux solutions analytiques. En outre, le modèle a été validé de manière satisfaisante en le comparant à des données de terrain déjà publiées. Toutefois, les données comparables étant encore restreintes, des séries d'expériences de laboratoire sont entreprises à l'Ecole Polytechnique. Globalement, l'utilisation de ce modèle montre que le résultat optimal obtenu se compare favorablement aux données expérimentales existantes.

La bonne correspondance obtenue entre les résultats numériques et les données expérimentales confirme que notre modèle numérique est un outil fiable pour prédire le transport des polluants dans le ruissellement de surface. Le modèle peut être utilisé pour produire quelques résultats généraux dans la prédiction du sort final d'un polluant appliqué à une surface. On peut également conclure que le schéma de cannelure cubique est une technique de solution attrayante et flexible pour la résolution numérique du modèle en raison de sa grande précision, de son temps calcul plus court et de la facilité de son application.

ABSTRACT

Pollutants which have been applied to the soil surface in either liquid or solid form are susceptible to washoff by surface runoff caused by a rainfall episode. This contaminated runoff is usually discharged at unknown instants of time into the water system (which here is taken to mean the groundwater and surface water environment) with uncertain values of concentration. The degree of non-point source pollution that occurs at a given location is influenced by the local hydrology, geography, topography and geological conditions, and varies with the change of time and district. To quantitatively analyze non-point source pollution in the aquatic environment, both the flow field and mass transport must be simulated simultaneously using an appropriate numerical model.

The goal of this study is to make a significant improvement over current practice on numerical modeling of non-point source pollutant washoff and transport in overland flow. Specific objectives of this study are:

- to investigate pollutant transport mechanisms in overland flow,
- to develop an integrated numerical model incorporating the effects of infiltration, solubility rate, advection-diffusion and adsorption,
- to develop a variant of the cubic spline integration scheme to obtain numerical solutions to the mathematical model, resulting in greater flexibility and efficiency.

The complete numerical model consists of the St.Venant equations, plus equations describing the infiltration rate, the solubility rate, the adsorption characteristics and the pollutant transport. The two-dimensional St.Venant equations based on continuity and momentum principles are used to describe the variability of flow conditions, in which the effects of surface roughness, rainfall intensity and soil infiltration are considered. The Green-Ampt and Horton equations are used to characterize the infiltration processes. The solubility rate equation is constructed based on the physico - chemical behavior of the pollutant in overland flow. It draws on the analogy between mass and momentum transfer and is used to simulate the dissolution process of the solid pollutant into the liquid phase. The adsorption-desorption process may be approximated by equations describing the kinetics. The advection - diffusion equation is applied to trace the migration of the dissolved pollutant and finally predict the ultimate fate of the surface applied solid pollutant.

Model inputs consist of four spatial data components: rainfall, soil conditions, pollutants and land (topography) conditions. Model outputs consist of runoff and its associated pollutant concentration in the infiltrated and runoff components and consequently, the spatial and temporal distribution of the total pollutant quantity.

The set of equations governing the complete system has been integrated numerically using the cubic spline scheme. This scheme has been successfully applied to

numerically simulate the density induced circulation in estuaries. It has not however, been used to obtain solutions to the shallow water wave equations. The scheme is based on the cubic spline relationships which form the interpolating polynomials of higher order between mesh points. The main advantages of the scheme are its higher accuracy, its ability to lend itself to direct formulations in terms of the function values, first derivatives or second derivatives and lower computational time while avoiding a complex formulation.

The model was verified by three cases for which analytical solutions are available and the results are shown to be in close agreement. In addition, satisfactory validation of the model against published field data for the hydraulics of rainfall-runoff has been accomplished. Since complete data is unavailable in the open literature, a series of laboratory tests were conducted. The experimental results compare favorably with the model performance.

CONDENSÉ EN FRANÇAIS

LE TRANSPORT DES POLLUANTS DANS LE RUISSELLEMENT DE SURFACE AVEC SES EFFETS DE DISSOLUTION, D'INFILTRATION ET D'ADSORPTION

INTRODUCTION

C'est un fait inéluctable que la protection de l'environnement de l'eau est devenue une question importante dans nos vies. La plupart des concepts et des problèmes liés à la pollution de l'eau ne peuvent pas être concidérés sans une bonne compréhension de la source des polluants et de leur sort ultime dans l'environnement n'est pas acquise.

Les sources de polluants peuvent être classifiées selon deux catégories principal: les source naturelles et les source artificielles. De plus, ces catégories peuvent être subdivisées en sources dites de ponctuelle et de non ponctuelle. Les eaux de surface qui proviennent des précipitations transportant des polluants et atteignant le sol sous forme liquide ou solide, entrent dans la catégorie des sources de pollution non ponctuelle. Les facteurs externes de pollution de source non ponctuelle sont les précipitations et le ruissellement pluvial qui en résulte. La plupart des situations de pollution de source non ponctuelle ne sont pas directement contrôlables. L'analyse quantitative des polluants est

une étape du développement des techniques qui visent le contrôle de la pollution dans l'environnement humide.

Dans cette étude, les caractéristiques de l'entrée, de la sortie et du processus d'intervention des polluants pour une région sont directement simulées. La source de polluant non ponctuelle est quantitativement analysée par l'utilisation des modèles physiques conçus pour cette fin. Cependant, le transport de polluant dans le ruissellement de surface est un phénomène compliqué. Les solutions analytiques pour ce type de problème ne sont pas possibles, sauf en posant de hypothèses très restrictives. La plupart des recherches publiées traitent numériquement le phénomène en modélisant séparément l'hydraulique et les procédés de transport. Par conséquent, les modèles disponibles se limitent généralement à une description partielle des processus complexes qui se produisent, tels que l'hydraulique, le comportement d'infiltration aussi bien que l'advection et la diffusion, encore que chacun de ces processus, pris individuellement, ait déjà été bien étudié.

Notre revue de la littérature sur ces recherches indique très peu de travail a été consacré à la modélisation du ruissellement de surface et du transport des polluants de source non ponctuelle. Yan (1995), Yan et Kahawita (1997, 1998) ont développé un modèle numérique pour simuler le processus entier comprenant le reuissellement de surface et le transport de polluant non ponctuelle. Ces études ont traite du problème complexe par

une approche intégrée de modélisation du comportement hydraulique du ruissellement de surface avec infiltration, à laquelle est couplée le transport et les caractéristiques chimiques d'un polluant particulier. Cependant, il reste une certaine incertitude, particulièrement en ce qui concerne l'effet de l'adsorption et l'équation du taux de solubilité. Il y a également un réel besoin de concevoir et d'incorporer dans le modèle de simulation des traitements numériques plus efficaces et plus précis.

Ce travail actuel vise à développer un modèle numérique bidimensionnel complet pour simuler le transport des polluants de source non ponctuelle dans le ruissellement de surface, en tenant compte de comprenant l'effet de l'infiltration, de la pluie et de la solubilité. Plus spécifiquement, l'effet de l'adsorption est inséré dans le modèle en premier lieu puis le schéma de cannelure cubique est ensuite introduit pour simuler le modèle.

Les objectifs spécifiques de cette étude sont:

1) examiner les mécanismes de transport des polluants dans le ruissellement de surface en tenant compte des effets de l'infiltration, du taux de solubilité et de l'adsorption puis développer un modèle de simulation numérique intégré,
2) introduire le schéma de cannelure cubique et évaluer son exécution en tant que solution technique pour le traitement numérique du modèle.

3) présenter quelques résultats généraux qui indiquent la flexibilité du modèle et son utilité afin de prévoir le sort ultime d'un polluant placé sur une surface.

REVUE BIBLIOGRAPHIQUE

It y a une multitude de méthodes pour modéliser les caractéristiques physiques du ruissellement de surface causées par les précipitations, l'infiltration et le phénomène du transport. Cependant, la simulation numérique des polluants de source non ponctuelle dans le ruissellement de surface n'a pas beaucoup attiré l'attention des chercheur pour étudier le cas des vitesses très variables ou celui où les effets de l'infiltration, des précipitations, de la solubilité et de l'adsorption sont incorporés au modèle. Jusqu'à maintenant, la recherche s'est concentrée sur la modélisation numérique hydraulique ou sur le phénomène du transport. Le compte rendu sommaire de ces recherches apparait dans les Tableaux 1, 2, 3 et 4.

MODÈLE NUMÉRIQUE

La simulation numérique du processus complet comporte les équations de St.Venant, les équations d'infiltration, l'équation du taux de solubilité, l'équation d'adsorption et l'équation du transport des polluants. Les équations bidimensionnelles de St.Venant basées sur des principes de continuité et de quantité de mouvement sont employées pour

décrire la variabilité des conditions du ruissellement pluvial dans lesquelles sont considérées les effets de la rugosité, de l'intensité des précipitations et de l'infiltration dans le sol.

Les équations de Green-Ampt et de Horton sont employées pour caractériser les processus d'infiltration. La mise en équation du taux de solubilité est construite sur la base du comportement physico-chimique du polluant dans le ruissellement de surface et par une représentation analogique entre la masse et le transfert de la quantité de mouvement, lesquels établissent le modèle de la dissolution d'un polluant solide passant à la phase liquide. Le procédé d'adsorption-désorption peut être calculé approximativement par des équations appropriées basées sur la cinétique. Enfin, l'équation d'advection-diffusion est utilisée pour retrouver ce qu'il advient finalement du polluant.

SCHÉMA MATHÉMATIQUE

Pour obtenir une simulation correcte du modèle décrit ci-dessus, il est nécessaire d'utiliser des techniques numériques adéquates qui permettent d'évaluer le sort ultime du polluant appliqué sur la surface. La technique numérique choisie pour cette étude est le schéma d'intégration de cannelure cubique. Ce schéma a été utilisé avec succès pour résoudre une variété de problèmes d'écoulement visqueux aussi bien que des problèmes

Tableau (1) L'Examen de Modèle Ruissellement

Auteur	Année	Dimension	Physique Condition	Schéma Numérique
Liggett et Woolhiser	1967	1-D	Ruissellement avec les surfaces plates homogènes	Caractéristiques, schémas explicite et implicite
Akan et Yen	1981	1-D	Ruissellement avec les surfaces plates homogènes, écoulements souterrain et de surface ont été décrits	Un schéma de différences finies implicite à quatres-points
Chow et Ben-Zvi	1973	2-D	Ruissellement dans lequel touts les termes connexe à l'accélération convective ont été negligés	Schéma basé sur la combinaison du schéma de Lax-Wendroff avec des modifications de Burstein et de Lapidus
Wood et Arnold	1990	1-D	Approximation d'onde cinématique	Le schéma de la "boîte"
Katapodes et Strelkoff	1979	2-D	Ruissellement résultant d'une rupture de barrage	Caractéristiques
Kawahara et Yokoyama	1980	2-D	Ruissellement sans variabilité spatiale de vitesse d'infiltration et de rugosité	Méthode d'éléments finis
Zhang et Cundy	1989	2-D	Ruissellement comprenant la rugosité, l'infiltration et la microtopographie extérieures, les résultats ont été partiellement vérifiés avec des expériences sur le terrain	Exacte jusqu'au second degré Méthode explicite de MacCormack de différences finies
Tayfur et al.	1993	2-D	Équations d'ondes cinématiques comprenant la rugosité, l'infiltration et le microtopographic extérieures avec des expériences sur le terrain.	Méthode implicite de différence finie

Tableau (2) Modèle de l'Infiltration

Auteur	Année	Contenu
Mein et Larson	1973	Ils ont conçu une méthodologie pour appliquer le modèle de Green-Ampt à une entrée régulière de précipitation: Ils ont développé une procédure pour déterminer la valeur du paramètre capillaire d'aspiration utilisé dans le modèle.
Clapp et Hornberger	1978	Ils ont montré comment les équations empiriques en représentant salissent les propriétés hydrauliques.
Chu	1978	Il a démontré l'applicabilité du modèle pour l'usage dans des conditions de précipitation instable.
Rawls et al.	1983	Ils ont tracé les grandes lignes d'une procédure pour déterminer les paramètres de Green-Ampt basée sur des propriétés du sol et utilisant le spectre complet d'information d'enquête de sol.
Mullem	1991	Il indique que le modèle de Green-Ampt ont prévu le volume d'écoulement et la décharge de crête mieux que le modèle de courbe-nombre.
James et al.	1991	Ils ont développé un modèle numérique pour l'application de l'équation d'infiltration de Green-Ampt à une ligne de partage.
Corradini	1994	Il a modélisé l'infiltration pendant l'ordre complexe de précipitations, y compris la représentation d'un ordre de l'infiltration-redistribution fait un cycle avec la saturation ne menant pas à salir la saturation extérieure, et les périodes de précipitations de l'intensité moins que la capacité d'infiltration de sol.
Gupta et al	1998	L'infiltration est modélisée en tenant compte du changerment de la conductivité hydraulique sous des précipitations simulées conditionnées, le structure stochastique de la conductivité hydraulique a été incorporée dans les modèles d'infiltration Green-Ampt et de Mein-Larson.

Tableau (3) Modèles Numériques des Phénomènes de Transport

Auteur	Année	Descriptions
Siemons	1970	Modèle bidimensionnelle d'équations de diffusion sans advection ou avec l'advection unidimensionnelle.
Holly et Preissmann	1977	Discrétisation élevée d'exactitude de l'équation bidimensionnelle de diffusion et d'advection.
Li	1990	Modèle unidimensionnelle pure d'advection avec une vitesse constante.
Luk et al.	1990	Modèle bidimensionnel qui mélange des polluants dans le flux stationnaire dans un canal non prismatique natural.
Chen et Falconer	1992	Modèle bidimensionnel source-libre transport d'une masse scalaire de concentration de polluant dans un canal ouvert en utilisant l'équation d'advection.
Wu	1997	Il a développé le modèle d'équation d'ondes à l'équation multidimensionnelle de transport, la pièce d'advection résolu par l'équation d'ondes.

qui traitent des estuaires. Il n'a pas été utilisé dans les conditions d'eau peu profonde. L'avantage principal du schéma de cannelure cubique est sa grande exactitude, son temps de calcul court, son maillage variable tout évitant une formulation complexe. En raison

de ses avantages, il semble que le schéma de cannelure cubique puisse être utilisé dans toutes les disciplines.

Tableau (4) La Modèle de'Adsorption

Auteur	Année	Caractéristiques
Van Genuchten et al.	1974	Utilisée modèle de l'adsorption disponible pour évaluer des équations cinétiques et d'équilibre pour la prévision du mouvement de pesticide par des medias poreux
Melnyk	1985	A étudié les effets du comportement de sorption sur le transfert de contaminant et a examiné la nature de quelques effets
Van Der Zee	1990	Dérivées les solutions de déplacement de vague pour le cas du transport de corps dissous avec la sorption non linéaire, quand la cinétique de sorption peut être décrite avec une expression de premier ordre de cadence
Selroos et al.	1992	Modelé advection de corps dissous couplée à la cinétique de sorption dans hétérogènes des formations
Bosma et al.	1992	Proposées approximations analytiques pour le transport adsorbant non linéaire de corps dissous dans posés les sols
Barone et al.	1992	A présenté une évaluation d'diffusion-essai de laboratoire du coefficient de diffusion et du coefficient d'adsorption pour plusieurs espèces organiques volatiles dans un media saturé, relativement calme, argileux un sol
Khan et al.	1996	A développé une équation généralisée qui pourrait représenter un éventail de corps dissous organiques à plusieurs composants et dilués dans le soluté, adsorbée sur le charbon actif

VALIDATION ET VÉRIFICATION DU MODÈLE

Afin d'évaluer l'applicabilité et l'exactitude du modèle, des observations doivent être faites pour comparer la prévision numérique avec des données expérimentales et des solutions analytiques. Dans cette étude, la validité du modèle a été faire en comparant à:

- Des données analytiques de solutions,
- Des résultats expérimentaux tirés des publications scientifiques,
- Des résultats expérimentaux.

La vérification du modèle numérique est d'abord confrontée à des équations analytiques unidimensionnelles incluant les équations de transport et l'équation d'adsorption. Puis, les résultats numériques de la partie hydraulique sont comparés aux résultats en utilisant le schéma de différences finies (Yan, 1995) et aux données expérimentales tirés des publications scientifiques (Tayfur, 1993). Les résultats numériques concordent bien avec l'utilisation de la méthode numérique différent et avec les données observées. En outre, une série d'expériences au laboratoire sont conduites pour simuler le transport des polluants dans le ruissellement de surface. Le but de ces expériences est d'évaluer les capacités du modèle numérique en le comparant qualitativement avec des valeurs observées. Tous les résultats montrent que les résultats numériques s'accordent bien avec les données expérimentales. Le sommaire de deux séries de conditions de test expérimental est énumérée dans les Tableaux 5 et 6, respectivement.

Tableau (5) Sommaire des conditions des séries 1 d'expérience

No.	Surface (inférieure) rugosité	Distribution du polluant	Local du échantillon	Paramètres Expérimentaux
1	Contre-plaqué avec de petits grains de sable	NaCl appliqué uniformément	1.65m, 3.3m, 4.95m, 6.6m, 8.35m ascendante de la fin	Pente de canalisation = 0.005,
2	Contre-plaqué avec de grands grains de sable	Idem	Idem	Idem
3	Tapis d'herbe	Idem	Idem	Idem
4	Tapis d'herbe	La solution de sel est uniformément pulvérisée	Idem	Idem
5	Tapis d'herbe	Le sel est appliqué à une tache	3.335m, 4.59m, 5.995m, 7.245m, 8.35m ascendante de la fin	Pente de canalisation = 0.01

La bonne correspondance obtenue entre les solutions numériques et les données expérimentales confirme que le schéma d'intégration de cannelure cubique est un outil fiable pour prédire le transport des polluants dans le ruissellement de surface.

Tableau (6) Sommaire des conditions des séries 2 d'expérience

No	Surface (inférieure) rugosité	Simulé polluant	Solubilité g/100g	Cadence de précipitations l/s	Durée (s)	Quantité de polluant (g)
1	Tapis d'herbe	KCl	34.7	0.185	1140	20
2	Tapis d'herbe	KCl	34.7	0.175	1140	22.5
3	Tapis d'herbe	Glycerol-phosphate	10	0.175	1320	14
4	Tapis d'herbe	Glycerol-phosphate	10	0.185	1320	8
5	Tapis d'herbe	$CaCl_2$	73.5	0.185	1500	20

RÉSULTATS ET ANALYSE DE SENSIBILITÉ

Les résultats numériques montrent l'importance de la constante du taux de réaction, de la solubilité, du coefficient de diffusion et de l'adsorption. Le test de sensibilité des paramètres du modèle indique que la solubilité et la constante du taux de réaction sont des paramètres sensibles dans la modélisation de la dissolution des polluants. Les polluants qui ont une solubilité plus élevée se dissolvent plus rapidement que ceux de solubilité inférieure. La constante du taux de réaction non dimensionnelle k_2 est présumée dépendre seulement des caractéristiques de solubilité du polluant. Les polluants ayant une plus grande valeur de constante se dissolvent plus rapidement que ceux qui ont une plus petite valeur.

CONCLUSIONS

Le modèle numérique complet a été développé pour simuler le transport des polluants de source non ponctuelle dans le ruissellement de surface en tenant compte de l'infiltration, des précipitations et de la dissolution, spécifiquement avec l'effet de la vitesse de solubilité et de l'adsorption. L'applicabilité du modèle au transport bidimensionnel de polluant dans le ruissellement de surface a été démontrée compte tenu des effets de l'infiltration, de la dissolution, de la diffusion et des différents produits chimiques. Globalement, les résultats obtenus en utilisant ce modèle sont considérés comme bons.

Le modèle peut être employé pour produire quelques résultats généraux sur le sort ultime d'un polluant appliqué à une surface.

La praticabilité du modèle numérique a été vérifiée par comparaison avec des équations analytiques, des données d'observation extraites des publications scientifiques et des données obtenues à partir de séries d'expériences au laboratoire conduites à l'Ecole Polytechnique. La bonne correspondance obtenue entre les résultats numériques et les données expérimentales anisi que les solutions analytiques confirme que le modèle numérique est un outil fiable pour prédire le transport des polluants dans le ruissellement de surface.

En s'appuyant sur les résultats de notre recherche, on peut affirmer que le schéma de cannelure cubique est une technique de solution attrayante et flexible pour la solution numérique du modèle en raison de son exactitude élevée, de son temps de calcul plus court et de sa facilité d'application.

TABLE OF CONTENTS

LIST OF TABLES

LIST OF FIGURES

NOMENCLATURE

b	surface stress coefficient, [kg/kg]
C	concentration, [kg/m^3]
C^*	solubility, [kg/m^3]
d_0	infiltration depth at the start of ponding, [m]
D_p	amount of pollutant dissolved, [kg]
dt	time interval, [s]
D_x	diffusion coefficient in the x direction, [m^2/s]
D_y	diffusion coefficient in the y direction, [m^2/s]
dx	space interval in the x - direction, [m]
dy	space interval in the y - direction, [m]
f_0	initial infiltration capacity, [m/s]
f_c	a final equilibrium capacity, [m/s]
f_p	infiltration capacity, [m/s]
F	potential accumulative infiltration amount, [m]
g	gravitational acceleration, [m/s^2]
h	flow depth, [m]
k	mass transfer coefficient
k_l	hydraulic conductivity, [m/s]
k_l'	forward kinetic rate coefficient, [s^{-1}]

$k_2^{'}$	backward kinetic rate coefficient, [s^{-1}]
k_2	reaction rate constant
k_3	time rate constant, [s^{-1}]
k_4	delay time constant, [s]
k_d	distribution coefficient,
n	Manning's roughness coefficient
n_l	effective soil porosity
n_b	soil porosity
q	the discharge per unit width of slope, [$m^3/s/m$]
Q	net lateral inflow, [m/s]
Q_i	infiltration rate, [m/s]
Q_r	rainfall intensity, [m/s]
S	mass adsorbed, [kg/kg]
S_e	initial effective saturation
S_{fx}	friction slope in the x - direction
S_{fy}	friction slope in the y - direction
S_t	solubility rate, [$kg/s/m^2$]
S_x	the bed slope in the x direction
S_y	the bed slope in the y direction
t	time, [s]
T_e	equivalent time, [s]

t_p	time to ponding, [s]
u	flow velocity in the x direction, [m/s]
v	flow velocity in the y direction, [m/s]

Greek symbols

α	angle of slope in x direction
ε	kinematic eddy viscosity
ϕ	angle of slope in y direction
γ	specific weight of water, [$kg/m^2/s^2$]
θ	volumetric water content, [m^3/m^3]
ρ_s	density of solids
ρ_b	bulk density
τ	shear stress, [N/m^2]
ω	weighting coefficient
ψ_l	wetting front capillary pressure head, [m]

Subscripts

i	node number in x direction
j	node number in y direction
m	boundary node in x direction
n	boundary node in y direction

Superscripts

k	time step number

LIST OF APPENDIX

CHAPTER 1: INTRODUCTION

1.1 Generalities

It is an inescapable fact that protection of the water environment has become an important issue in our lives. Most of the important concepts and problems related to water pollution cannot be appreciated unless a good understanding of the pollutant source and its ultimate fate in the environment is acquired.

Pollutant sources fall into two basic categories: natural and artificial. They can be further subdivided into point sources and non-point sources. Surface runoff caused by rainfall carrying pollutants which have been applied to the soil surface in either liquid or solid form is under the non-point source pollution category. Non-point source pollution has the following characteristics:

1) Non-point sources of pollution are diffuse sources; the pollutants, such as fertilizes, pesticides or animal wastes with nutrient values, originate from a large area and are discharged into the water body in dilute concentrations that are dependent on the hydrological conditions.

2) Before pollutants enter the water body, there are transport processes that occur over a wide region, accompanied by dissolution, dispersion and infiltration.

3) Non-point source pollutants are usually discharged at unknown instants of time into the water system with uncertain values of concentration. These factors are influenced by unexpected natural conditions, or the accidental discharge of pollutants.

4) The degree of non-point source pollution that occurs at a given location is influenced by the local hydrology, geography and geological conditions, and varies with the change of time and district.

The external factors that cause pollutant transport are rainfall and the consequent runoff. Most situations of non-point source pollution cannot be directly controlled. The quantitative analysis of pollutants is a step in developing techniques to control pollution in the aquatic environment. In general, there are two ways to study the transport characteristics of non-point pollutant sources. One is based on the study of the output characteristics of pollutants in a region by simulating the three main links: rainfall-runoff, soil erosion and pollutant transport. The other is to analyze the water quality of the receiving water body, that is, by analyzing and calculating the quantities of pollutants in the receiving water body, this allows one to study the output characteristics of the region and then try to converge on the source of pollution. The difference between the two methods is that the former directly simulates the input, output and intervening processes, while the latter is an indirect method which seeks to control the pollution on the basis of a monitoring strategy. In this study, the former technique is used to quantitatively analyze the non-point source pollutant by the use of physically based

models for the process. Many studies have been conducted in this way with the deterministic method being usually employed. However, the pollutant transport in overland flow is a complicated phenomenon. Analytical solutions to this type of problem are not possible, except under highly restrictive assumptions. Most previous research deals with the phenomenon numerically by modeling the hydraulics and transport processes separately. The available models are therefore frequently limited to a partial description of the complex processes that occur such as the hydraulics, the infiltration behavior as well as advection and diffusion, even though these processes have been individually well studied. A perusal of the relevant literature indicates that very little work has been devoted to modeling overland flow together with non-point source pollutant transport. Yan (1995), Yan and Kahawita (1997, 1998) developed a numerical model to simulate the whole process including overland flow and non-point source pollutant transport. These studies tackled the complex problem by an integrated approach to modeling the hydraulic behavior of the overland flow with infiltration coupled with transport and chemical characteristics of the individual pollutant. However, there does remain some uncertainty particularly with respect to the effect of adsorption and the rate equation for solubility. There is also a real need for finding more efficient and accurate numerical schemes to be incorporated into the simulation model.

The present work aims to develop a complete numerical model to simulate non-point source pollutant transport in overland flow with the effect of infiltration, rainfall and

solubility. More specifically, the effect of adsorption has been incorporated into the model, and a modified version of the cubic spline scheme has been introduced to simulate the model. Figure 1.1 sketches the physical significance of pollutant transport in the rainfall-runoff process.

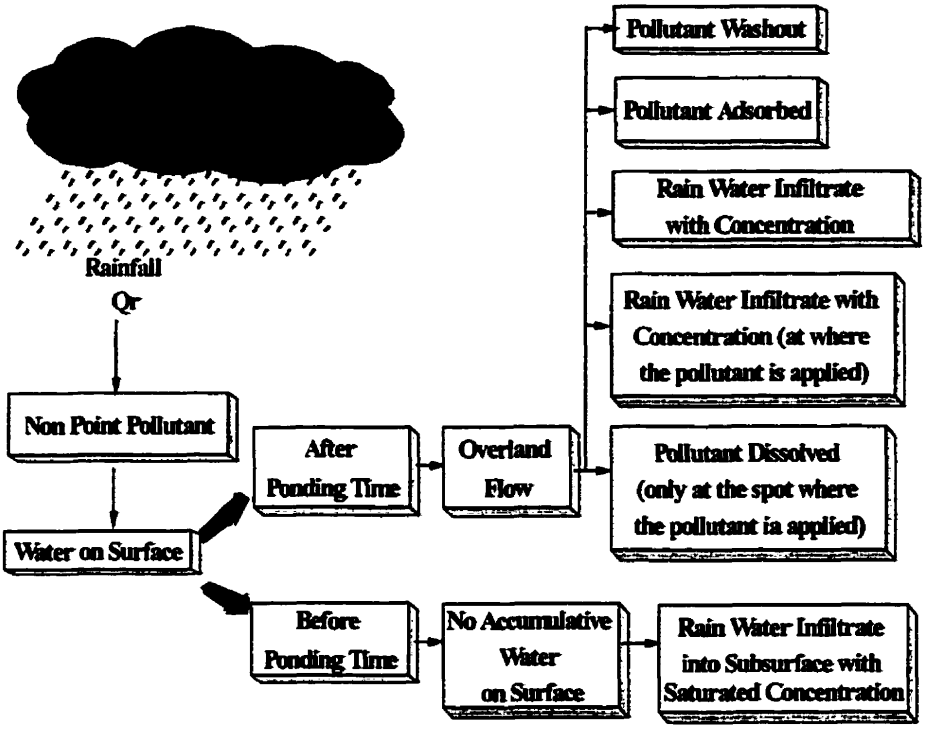

Figure 1.1 Physical description of the problem

1.2 Scope of Present Work

A two-dimensional numerical model is proposed in the present study. It focuses on the whole process of non-point source pollution caused by rainfall runoff associated with infiltration, dissolution and adsorption. Specific objectives of this study are to:

1) Investigate pollutant transport mechanisms in overland flow with the effects of infiltration, solubility rate and adsorption and develop an integrated numerical simulation model
2) Introduce the cubic spline scheme and evaluate its performance as a solution technique for the numerical solution of the model
3) Present some general results that indicate the flexibility of the model and its usefulness to predict the fate of a surface applied pollutant

The development of the mathematical model includes five steps:

1) Selection of the model variables and formulation of the mathematical equations,

2) Determination of the model parameters,

3) Numerical discretization with appropriate simulation of the input, output and intervening processes,

4) Verification of the model against available analytical and experimental results,

5) Sensitivity analyses.

The numerical simulation of the complete process consists of the St.Venant equations, the infiltration equations, the solubility rate equation, the adsorption equation and the pollutant transport equation. The two-dimensional St.Venant equations based on continuity and momentum principles are used to describe the variability of flow conditions, in which the effects of surface roughness, rainfall intensity and soil

infiltration are considered. The Green-Ampt and Horton equations are used to characterize the infiltration processes. The solubility rate equation is constructed based on the physico-chemical behavior of the pollutant in overland flow and by drawing on the analogy between mass and momentum transfer, which models the dissolution of a solid pollutant into the liquid phase. The adsorption-desorption process may be approximated by appropriate kinetics based equations. Finally, the advection-diffusion equation is used to trace the ultimate fate of the pollutant.

For proper simulation of the model cited above, it is necessary to use suitable numerical techniques with which the ultimate fate of the surface applied pollutant may be assessed. The numerical technique chosen for this study is the cubic spline integration scheme. This scheme has been successfully applied to solve a variety of viscous flow problems as well as problems relating to estuaries, it has not however, been used in the shallow water wave situation. The main advantage of the cubic spline scheme is its high accuracy, lower computational cost, and variable mesh capability while avoiding a complex formulation. Because of these benefits, it is believed that the algorithm could find application in several fields.

A series of laboratory experiments were conducted, which cover two main areas: rainfall/runoff relationship and pollutant transport in overland flow. The results were used to provide at least a partial verification of the model.

In the introductory chapter, the physics of the problem are described, and the importance of numerical models as predictive tools is indicated. The scope of the present work, in which the model development and the numerical scheme differ from previous work, is enunciated.

Chapter 2 is devoted to an examination of previous work both physical and numerical that has been accomplished in this field.

The mathematical equations used in this study such as the overland flow equations, the infiltration equations, the transport equation and the adsorption equation are presented in chapter 3. The development of the solubility rate equation is described in some details in the same chapter.

Chapter 4 is devoted to a presentation of the cubic spline scheme. The basic relations for cubic splines are given and the discretized form of the mathematical equations is illustrated. The initial and boundary conditions that must be specified are explained here.

In chapter 5, the validation and verification of the numerical models are tested and presented in three sections: 1) Analytical solutions 2) Published data 3) Laboratory Experiments. In the first section, three analytical equations are used to test the numerical

model. These equations deal with advection-diffusion and adsorption. The second section compares the numerically generated hydraulic behavior with published experimental data (Tayfur et al. 1993), as well as with the results obtained by Yan (1995) using a finite difference scheme. The third section describes the experimental setup and procedure. It includes an evaluation of the numerical model performance.

Chapter 6 incorporates a series of examples that better illustrate the cubic spline scheme as a viable tool for numerically solving the governing differential equations. The sensitivities of the reaction rate constant, the dispersion coefficient and the solubility rate are also discussed and the results related to infiltration and adsorption have been illustrated.

Chapter 7 is devoted to some concluding remarks with suggestions on how the present work may be refined and improved.

CHAPTER 2: REVIEW OF LITERATURE

2.1 Generalities

Predicting pollutant transport in surface runoff is essential for the control of non-point source pollution. The basic tools for assessing the effects of a pollutant source on the environment may be numerical modeling, use of a GIS database as well as use of statistical evaluation techniques. There exist a multitude of methods for modeling physical characteristics of surface runoff caused by rainfall, infiltration and transport phenomena. As a result, two broad classes of models may be distinguished: (1) hydrodynamic models and (2) empirical models as shown in Table 2.1.

However, numerical simulation of non-point source pollutants in overland flow where the velocities may be highly variable and where the effects of infiltration, rainfall, solubility and adsorption are incorporated into the model has not received much attention. Research has usually concentrated on numerical modeling of either the hydraulic or the transport phenomena.

2.2 Overland Flow

Much effort has been spent in modeling overland flows in the past several decades, however, most of the work has been confined to one dimension and is dominated by the use of the kinematic wave equation. The varieties of microtopography, surface roughness and hydraulic properties over distances of centimeters to meters, strongly influences the runoff characteristics. Furthermore, these spatial variations have a significant impact on soil erosion and contaminant transport.

Liggett and Woolhiser (1967) used the one-dimensional hydrodynamic equation for modeling overland flow. They conducted extensive numerical experiments to assess the behavior of different numerical schemes for solving the hydrodynamic equations. Although this study provided valuable experience and guidelines for obtaining solutions to the hydrodynamic equations for overland flow, it was limited to homogeneous plane surfaces.

Chow and Ben-Zvi (1973) proposed a two-dimensional hydrodynamic model of overland flow. They indicated the feasibility of the model in describing runoff. However, because of the required simplification of the equation, all terms related to the convective acceleration which may be significant in certain regions of the flow were dropped.

Morris and Woolhiser (1980) presented a comparison of solutions to the shallow water equations for unsteady one-dimensional flow over a plane and solutions to the diffusion and kinematic wave equations, which are approximate forms of the St.Venant equations.

Kawahara and Yokoyama (1980) presented a two-dimensional overland flow model or direct runoff flow over the watershed, which is based on a two-dimensional hydrodynamic model. In their model, the velocity of flow at any point in the watershed at any time is assumed to be expressed by its average value through depth, and spatial variability in infiltration and roughness were not included.

Akan and Yen (1981) developed a mathematical model of unsteady shallow water flow on porous media, in which both surface and subsurface flows were described by a set of dynamic wave equations. However, only a one-dimensional hydrodynamic situation with a homogeneous plane surface was considered.

In order to evaluate the models of predicted runoff for catchments dominated by overland flow effects, Hromadka et al. (1987) discussed four modeling approaches and compared a variant of the linear and nonlinear unit hydrograph methods based on the standard SCS unit hydrograph. The differences in predicted hydrologic response to variable catchment size, slopes, roughness, and the input effective rainfall intensity and temporal pattern were compared. A numerical model using the diffusion approach was

applied to a set of idealized catchments to develop synthetic unit hydrograph S-graph equivalents.

Zhang and Cundy (1989) solved the two-dimensional overland flow equation using the explicit MacCormack scheme with their results being partially verified with field experiments. These authors indicated the difficulties inherent in applying the St.Venant equations to overland flow, because of the following physical characteristics:

1) Overland flow is very shallow. It is not uncommon for the depth of overland flow to be of the order of a few centimeters or even millimeters so that very small numerical oscillations will cause failure of the solution algorithm.

2) The effect of shear stress induced by the bed roughness is larger than that in the case of deep water. This again can cause unacceptable oscillations in the computation.

3) Rainfall and infiltration respectively represent significant mathematical "source" and "sink" terms, and must be carefully treated numerically.

Govindaraju et al. (1990) provided approximate analytical solutions for overland flow using the kinematic and diffusion wave approximations under time-space varying lateral inflow. It was concluded that the analytical solutions are useful for estimating runoff from steep overland flow sections.

Table (2.1) Hydrodynamic and Empirical Models

PHYSICAL PROCESS	HYDRODYNAMIC MODELS	EMPIRICAL MODELS
Surface runoff (due to a rainfall event)	• Kinematic wave models • Diffusion wave models • St.Venant equations • Conceptual models based on systems approach	• Soil Conservation Service (SCS) method • Tennessee Valley authority (TVA)'s double triangular unit hydrograph method • Unit hydrograph method based on orthogonal functions • Rational method
Infiltration at a point under ponding	• Models based on the Richards equation • Green-Ampt model • Philip two-term model	• SCS model • HEC (Hydrologic Engineering Center) model • Algebraic equation (e.g. Kostiakov model, Haltan model, etc.)
Solute transport	• Models based on advection-diffusion • Models based on the kinematic wave theory • Fickian models	• Algebraic equations for isotherms such as the Langmuir isotherm, the Freudlich isotherm, etc. • Monte Carlo simulation-based models • Regression models

Tayfur et al. (1993) accomplished the modeling of overland flow through the numerical solution of the St.Venant equations. In their study, an implicit finite difference method was used and the solutions were examined in the light of field results. The study included the effects of variations in hillslope features such as surface roughness, infiltration and microtopography.

Katz (1995) studied the effects of surface roughness and rainfall impact on overland flow. The relationship between friction, velocity, discharge, and channel slope was examined for the case of shallow, spatially varied flow on rough surfaces. Table 2.2 summarizes previous research on overland flow.

2.3 Infiltration

Previous researchers have made systematic studies of infiltration phenomena from various points of view, this resulted in the appearance of numerous models for estimating infiltration capacity either in terms of theory or based on experiment. These investigations have summed up the advantages and limitations of each model and provided a convenient database for model applications.

Table (2.2) Overland Flow Models

Author	Year	Dimension	Physical Condition	Numerical Scheme
Liggett and Woolhiser	1967	1-D	Overland flow with homogeneous plane surfaces	Characteristics, explicit and implicit
Akan and Yen	1981	1-D	Overland flow with homogeneous plane surfaces, both subsurface and surface flows were described	A four-point implicit finite difference scheme
Chow and Ben-Zvi	1973	2-D	Overland flow in which all terms related to the convective acceleration were dropped	The scheme based on the combination of the Lax-Wendroff scheme with Burstein and Lapidus modifications
Wood and Arnold	1990	1-D	Kinematic wave approximation	Box scheme
Katapodes and Strelkoff	1979	2-D	Overland flow resulting from a dam break	Characteristics
Kawahara and Yokoyama	1980	2-D	Overland flow without spatial variability of infiltration rate and roughness	Finite element method
Zhang and Cundy	1989	2-D	Overland flow including surface roughness, infiltration and microtopography, the results were partially verified with field experiments	Second order accurate MacCormack explicit finite difference method
Tayfur et al.	1993	2-D	Kinematic wave equations including surface roughness, infiltration and microtopography with field experiments.	Implicit finite difference method

In early 1911, Green and Ampt proposed a simple infiltration equation, which was derived by applying Darcy's law to the situation of infiltration from an excess surface water supply from time zero. The variables are all predictable since they have physical significance.

In the 1930's, Horton devised a famous empirical equation according to the infiltration process. It indicates that if the rainfall supply exceeds the infiltration capacity, infiltration tends to decrease in an exponential manner. Another infiltration equation with predictable parameters for a homogeneous soil, assuming an excess of water supply at the surface, was developed by Philip in 1954.

Following the preceding works, Holtan in 1961 provided an empirical equation which expressed the infiltration capacity as a function not of time, but of the unoccupied pore space in the soil. This model is convenient for a watershed model but inconvenient to determine the control depth.

Based on the previous work, Mein and Larson (1973) developed a two-stage model for infiltration (under a constant-intensity rainfall) into a homogeneous soil with uniform initial moisture content. The first stage predicted the volume of infiltration to the moment at which surface ponding begins. The second stage, which used the Green-

Ampt model modified for infiltration prior to surface saturation, described the subsequent infiltration behavior.

Rawls et al. (1983) developed sets of average parameters based on the soil horizon or on soil texture class, or both. A procedure for determining the Green and Ampt parameters based on soil properties utilizing the full spectrum of soil survey information was outlined.

James et al. (1992) developed a computer model to calculate the rainfall excess considering infiltration, interception and surface retention. The purpose of the first phase of the study was to evaluate the application of the Green-Ampt infiltration equation to watershed hydrology. A procedure for estimating interception and surface retention using the Horton equations was developed in the second phase.

Corradini et al. (1994) extended the conceptual model of discontinuous rainfall - infiltration suitable for insertion as a modular part of complex watershed models in order to describe a large variety of real situations. The model included the representation of a sequence of infiltration-redistribution cycles with situations not leading to soil surface saturation, and rainfall periods of intensity less than the soil infiltration capacity.

The most popular equation which is widely used in the Storm Water Management Model

(SWMM) is the Green-Ampt equation. The model was confirmed to have a well-accepted physical basis and the results agreed well with those of the Richards soil moisture equation under a variety of infiltration situations studied by Akan (1986). This equation has been shown to be applicable for the conditions of constant rainfall intensity and homogeneous soil, and has been developed for determining the value of the capillary suction parameter by Mein and Larson (1973). Its applicability for use under the conditions of unsteady rainfall was demonstrated by Chu (1978). In 1991, Mullem stated that the Green-Ampt model for the prediction of both the runoff volume and peak discharge was better than other empirical equations. In 1993, Tayfur et al. modelled the processes of rainfall – infiltration; after the start of ponding, the Green-Ampt infiltration equation was used to calculate the infiltration rate.

The summary of infiltration studies is listed on Table 2.3, and typical infiltration models are shown on Table 2.4.

In the application of the Green-Ampt model, it is necessary to estimate parameters, such as the hydraulic conductivity, effective porosity and wetting front capillary pressure head. Rawls et al. (1983) have summarized a procedure for determining the Green-Ampt parameters.

Table (2.3) Review of Infiltration Studies

Author	Year	Contents
Mein and Larson	1973	Devised a methodology for applying the Green-Ampt model to a steady rainfall input; Developed a procedure for determining the value of the capillary suction parameter used in the model.
Clapp and Hornberger	1978	Showed how the empirical equations representing some soil hydraulic properties.
Chu	1978	Demonstrated the applicability of the model for use under conditions of unsteady rainfall.
Rawls et al.	1983	Outlined a procedure for determining the Green-Ampt parameters based on soil properties utilizing the full spectrum of soil survey information.
Mullem	1991	Indicates that the Green-Ampt model predicted both the runoff volume and peak discharge better than the curve-number model.
James et al.	1992	Developed a computer model for the application of the Green-Ampt infiltration equation to a watershed.
Corradini	1994	Modeling infiltration during complex rainfall sequence, including the representation of a sequence of infiltration-redistribution cycles with saturation not leading to soil surface saturation, and rainfall periods of intensity less than the soil infiltration capacity.
Gupta et al.	1998	Modeled infiltration with varying hydraulic conductivity under simulated rainfall conditions, the stochastic structure of hydraulic conductivity was incorporated in the Green-Ampt and Mein-Larson infiltration model.

Table (2.4) Lists of Typical Infiltration Models

Author	Year	Equation	Characteristic
Green and Ampt	1911	$f = k(1 + \frac{h\psi_f}{F})$	Simple and has physically based parameters, derived by applying Darcy's law
Horton	1930	$f_p = f_c + (f_0 - f_c)e^{-kt}$	Simple in form. Difficulties in determining useful values for the initial infiltration capacity and time constant restrict the use of this equation
Holtan	1961	$f = aS_a^{1.4} + f_c$ a – infiltration capacity of the average storage(in/hr.in$^{1.4}$) S_a – available storage in the surface layer	Expresses the infiltration capacity as a function not of time but of the unoccupied pore space in the soil, convenient for a watershed model, but determining the control depth is uncertain
Philip	1954	$\frac{dF}{dt} = \frac{k}{\mu}(1 + [\frac{(m - m_0)(P + H)}{F}])$ $F(t) = S\,t^{1/2} + K\,t$ $f(t) = 1/2\ S\,t^{-1/2} + K$ S –sorptivity	For a homogeneous soil with an excess supply at the surface with predictable parameters, computing these parameters is difficult and their values are more commonly obtained by fitting, a further difficulty is the assumption of an excess water supply at the surface

2.4 Transport Phenomena

Transport processes consist of advection and hydrodynamic dispersion. The term advection describes mass transport due simply to the flow of water in which the mass is dissolved. Dispersion occurs because of mechanical mixing during fluid advection and molecular diffusion. The mechanics of hydraulic dispersion is considered as being caused entirely by the motion of the fluid. Diffusion is a dispersion process of importance only at low velocities (Freeze and Cherry, 1979). A complete model for pollutant transport should account for advection, dispersion, solubility rate and chemical reactions of the pollutants as well as the hydraulic conditions of the overland flow. In recent years, the pollutant transport phenomenon has been modeled in a common effort. Many mathematical descriptions of transport processes either in overland flow, in river and channel flow or in groundwater flow are available.

Siemons (1970) attempted to solve the two-dimensional advection-diffusion equation numerically, however in the numerical solution of the two-dimensional advection-diffusion equation, advection in two dimensions was not considered.

Bresler (1973) studied simultaneous transport of solutes and water under transient unsaturated flow conditions. Theoretical and mathematical tools for analyzing transient one-dimensional (vertical) simultaneous transfer of noninteracting solute and water in

unsaturated soils were developed. It describes theoretical considerations and a numerical approach for simulating the transport of a noninteracting solute in the soil during nonsteady infiltration, redistribution, and evaporation. The combined effects of convection, ionic diffusion, and mechanical dispersion were investigated.

Li (1990) simulated the advective transport by a minimax - characteristics method, which is an explicit and efficient finite difference scheme derived from the local minimax approximation of the exact solution of the pure advection equation.

Luk et al. (1990) described a method of modeling two-dimensional mixing of pollutants in natural channels, with the use of a simple yet accurate algorithm, which overcomes most of the existing limitations. The model can be applied to steady flow in sinuous, non prismatic channels.

Chen and Falconer (1992) modeled the transient one-dimensional source-free transport of pollutant concentration in an open channel and the simplified two-dimensional advection equation. In both cases, constant velocities were used.

Aral and Liao (1996) provided the analytical solutions to the two-dimensional transport equation with time-dependent dispersion coefficients. The solutions could be used to model the transport of solute in hydrogeologic systems characterized by dispersion

coefficients that may vary as a function of travel time from the input source. In particular, he developed instantaneous and continuous point-source solutions for constant, linear, asymptotic and exponentially varying dispersion coefficients.

Wu (1997) extended the wave equation model, originally developed to solve the advection-diffusion equation, to the multidimensional transport equation in which the advection velocities vary in space and time. An operator-splitting method is adopted to solve the transport equation. The advection and the diffusion equations are solved separately at each time step. During the advection phase, the advection equation is solved using the wave equation model.

Zoppou and Knight (1997) derived the analytical solutions for the advection and the advection-diffusion equations. The analytical solutions are simple to evaluate and can be used to test numerical schemes for solving the advection and the advection-diffusion equations with spatially variable coefficients. Table 2.5 summarizes the numerical models of related transport phenomena.

However, all of the above works have their limitations. The majority of transport processes have been applied to the flow in rivers and estuaries. Furthermore, the hydraulic and transport phenomena are generally modeled separately in an uncoupled form.

Table (2.5) Numerical Models of Transport Phenomena

Author	Year	Descriptions
Siemons	1970	Model two dimensional diffusion-advection equation without advection or with advection in one dimension
Holly and Preissmann	1977	High accuracy discretisation of the two-dimensional diffusion and advection equation.
Li	1990	Model one-dimensional pure advection with constant velocity
Luk et al.	1990	Model two-dimension mixing of pollutants in steady flow in a natural non prismatic channel
Chen and Falconer	1992	Model two-dimensional source-free transport of a scalar mass of pollutant concentration in an open channel using the advection equation
Wu	1997	Extended the wave equation model to the multidimensional transport equation, the advection part being solved by the wave equation

2.5 Adsorption

Sorption deals with the interphase accumulation or concentration on the surface or interface, which is a significant phenomenon in most natural physical, chemical and biological processes and involves a series of reactions which may alter the distribution of contaminants.

Considerable effort has been focused on the investigation of adsorption behavior either in theory or in experiment or both so that many adsorption models are available, such as the Brunauer, Emmett, and Teller (BET) model, the Langmuir model and the Freundlich equation (Sundstrom and Klei, 1979). The Freundlich equation is basically empirical and has been widely used for a number of years.

Van Genuchten et al. (1974) studied how to evaluate the kinetic and equilibrium equations for the prediction of pesticide movement through porous media. The available adsorption models were used in transport equations to describe experimental laboratory data. A computer program was developed for three different adsorption models, based on the available equations.

Melnyk (1985) studied the effects of sorption behavior on contaminant migration and examined the nature of some of the effects, especially those due to sorption behavior that is dependent on the concentration of the contaminant in the groundwater. The effects are calculated using analytical solutions to the chemical equations. The hydrogeological parameters are held constant, and radioactive decay and hydrodynamic dispersion are excluded. Sorption equations in transport modeling is followed by presentation of migration results for a number of models of sorption behavior varying from linear isotherms, Langmuir, Freundlich and ion-exchange isotherms, to precipitation reactions and multiple-site sorption reactions.

Celorie et al. (1989) developed a methodology for using centrifugal modeling to determine equilibrium distribution coefficients in fine-grained soils. The method overcomes the disadvantages of common methods either by performing column studies or by batch equilibrium tests. Sorption distribution coefficients, based on the local equilibrium assumption, were computed from experimental breakthrough curves using an analytical solution to the solute transport equation.

Van Der Zee (1990) derived the traveling wave solutions for the case of solute transport with nonlinear adsorption, when adsorption kinetics may be described by a first-order rate expression. The analysis was extended for either Langmuir or Freundlich adsorption to the case of nonequilibrium interactions.

Selroos and Cvetkovic (1992) proposed a method for coupling sorption kinetics and solute advection in heterogeneous formations. The simulation results provided an indication of the coupled effects of high variability in the hydraulic parameters and sorption kinetics in heterogeneous formations. The limitation is that only equal forward and backward rate coefficients were considered, and the simulation was for two-dimensional heterogeneity with relatively simple boundary conditions.

Bosma and Van Der Zee (1992) proposed analytical approximations for nonlinear adsorbing solute transport in layered soils. The solute transport happens in a soil

consisting of two layers that have different chemical properties. The first case deals with a soil consisting of a nonlinear adsorbing layer on top of a linear adsorbing layer, whereas the second case deals with the reverse situation. The analytical solutions, which have the advantage of directly reflecting the processes underlying the phenomena and being easy to evaluate rapidly, are used to validate numerical calculations.

Barone et al. (1992) presented a laboratory diffusion-test estimation of the diffusion coefficients and the adsorption coefficients for several organic species in a saturated, relatively undisturbed, clayey soil. The results obtained from the diffusion tests were described together with the strengths and limitations of the test procedure. They also described the results of batch tests which were performed for comparison with the diffusion-test values.

Based on the collection of experimental data from the literature and on tests for various proposed models, Khan et al. (1996) developed a generalized equation which could represent the data for a wide range of multicomponent, dilute organic solutes in aqueous solution, adsorbed on activated carbon.

There has been extensive research conducted on the phenomenon of adsorption. Some of the research has been devoted to experimental investigations while the rest has relied on the development of mathematical models. Although the majority of the research has

been restricted to simple adsorption phenomena, considerable guidance to the mechanism and behavior of adsorption processes has been provided.

Table 2.6 is a non-exhaustive summary of current adsorption models.

Most of the available models cited above often emphasize either the water flow or the transport aspects. At the present time, very few models cover the hydraulic, infiltration and transport aspects in an integrated fashion. Akan (1987) presented a mathematical model for the processes of pollutant washoff by overland flow on impervious surfaces. The model is based on the kinematic description of overland flow and convective pollutant transport equations. The study addressed only a single element of the complex processes of stormwater pollutants. Thus, the model proposed could be useful only if used as part of a more comprehensive urban-runoff model.

The U.S. Environmental Protection Agency (EPA) Storm Water Management Model, SWMM, is a comprehensive water quantity and quality simulation tool. The model has been developed primarily for urban areas and uses the concepts of "blocks" that use lumped parameter systems to simulate the various processes that occur during a storm event (Singh, 1995). Pollutant transport is accounted for within the sewers comprising a drainage system in an urban area. As such, it is unsuitable for simulating the type of

processes that are studied in the present work. It is nevertheless a useful and widely accepted package for analysis of urban drainage systems.

Yan (1995) proposed a numerical model which simulated hydraulics and transport phenomena simultaneously. The two-dimensional flow model provides depth and velocity distributions in the flow domain. These distributions are used as input for a mass transport model to estimate pollutant migration in overland flow. However, in this model the effect of adsorption was not included. The model developed in this study attempts to integrate the pollutant dispersion, washoff by overland flow, infiltration into the soil and adsorption by the soil. The equations for overland flow consist of the continuity and momentum equations in which complicated physical conditions such as surface roughness, infiltration and rainfall are allowed. The equation for pollutant transport is a combination of the advection-diffusion equation with the solubility rate equation, the adsorption equation, and the effect of rainfall. The source term incorporates a solubility rate equation based on the analogy between mass and momentum transfer.

2.6 Numerical Scheme

Owing to the complexity of the phenomena involving spatial and/or temporal variation in rainfall, infiltration, surface roughness, advection, diffusion, adsorption, and so on,

analytical solutions of the governing equations are not tractable and numerical solutions are the only resort. Generally, the overland-flow equation has conventionally been solved by finite difference methods in either explicit or implicit schemes, while the QUICK (Quadratic Upstream Interpolation for Convection Kinetics) scheme (Leonard, 1979) has been widely used in solving transport problems. In explicit methods, the unknown values of the dependent variables at the new-time level occur explicitly in the difference equation and are determined sequentially. These schemes are easy to code in the solution procedure, but suffer from extreme stability restrictions (Liggett and Woolhiser 1967). The implicit method expresses unknown values in terms of other unknowns at the same time level. A set of simultaneous equations is thus obtained with the boundary conditions. Such a solution is generally stable although formal stability can only be proved for linear equations. In generally, the implicit method is suited for application to large time-scale phenomena for which explicit methods are generally found to be impractical and time-consuming. The QUICK scheme was originally developed by Leonard (1979). It uses quadratic upstream interpolation and has the benefits of mass conservation, relatively high accuracy and computational efficiency in comparison with many other higher-order-accurate schemes (Chen and Falconer, 1992). However a Von Neumann stability analysis indicates that the explicit QUICK scheme has a severe stability constraint which is dependent on the diffusion coefficient. It can be proved that this scheme is numerically unstable for the case of pure advection. As a consequence, various modified forms of the implicit QUICK scheme have been

formulated by Chen and Falconer (1992). It is claimed that these schemes overcome the stability problems of the explicit form and may be applied both to pure advection and to combined advection-diffusion.

Liggett and Woolhiser (1967) theoretically and empirically examined the convergence of the finite difference solutions and the exact solutions to the shallow-water equations. They used the method of characteristics, as well as explicit and implicit finite difference methods for modeling one-dimensional overland flow.

Amein (1968) presented the results of a study of an implicit method for the numerical solution of the complete two dimensional equations of unsteady flow. The method was successfully applied to flood routing problems. The particular requirements of this application favor methods that can provide fast and accurate solutions extending over a relatively long time scale. It was found that when the implicit method was applied to a number of representative problems in flood flows, the computations were stable and converged rapidly towards the final solutions.

Table (2.6) Adsorption Models

Author	Year	Characteristic
Van Genuchten et al.	1974	Used available adsorption models to evaluate kinetic and equilibrium equations for the prediction of pesticide movement through porous media
Melnyk	1985	Studied the effects of sorption behavior on contaminant migration and examined the nature of some effects
Van Der Zee	1990	Derived traveling wave solutions for the case of solute transport with nonlinear sorption, when sorption kinetics may be described with a first-order rate expression
Selroos and Cvetkovic	1992	Modeled solute advection coupled with sorption kinetics in heterogeneous formations
Bosma and Van Der Zee	1992	Proposed analytical approximations for nonlinear adsorbing solute transport in layered soils
Barone et al.	1992	Presented a laboratory diffusion-test estimation of the diffusion coefficient and the adsorption coefficient for several volatile organic species in a saturated, relatively undisturbed, clayey soil
Khan et al.	1996	Developed a generalized equation which could represent a wide range of multicomponent, dilute organic solutes in aqueous solution, adsorbed on activated carbon

Siemons (1970) used finite difference methods to solve the one-dimensional advection-diffusion equation and the two-dimensional advection-diffusion equation without advection.

Chow and Ben-Zvi (1973) employed a scheme based on the combination of the Lax-Wendroff scheme with Burstien and Lapudus modifications for modeling watershed flow. They obtained a solution to the two-dimensional watershed flow model that would have been extremely difficult to solve by the method of characteristics.

Holly and Preissmann (1977) explored a two-point higher-order method for calculation of advection and diffusion in one and two dimensions, and demonstrated the favorable accuracy of the method with respect to some other better known techniques.

Katopodes and Strelkoff (1979) investigated the physical and geometrical aspects of the three-dimensional (two-space dimension) method of characteristics and provided the means for developing efficient numerical approximations. Several characteristic networks were tested for their accuracy and stability, and the most accurate one was used for the simulation of a two-dimensional wave propagating on a dry bed.

Kawahara and Yokoyama (1980) proposed a methodology in which the finite element method is shown to be adaptable for solution of the direct runoff-flow process. To

discretize the time function, both one-step and two-step explicit time-integration schemes were employed. The Leap-Frog scheme and the Lax-Wendroff scheme were used in the solution procedure.

Garcia and Kahawita (1986) described the use of the MacCormack explicit time-splitting scheme in the development of a two-dimensional hydraulic simulation model. The model was able to treat rapidly varying flow problems as well as slowly varying flow problems that commonly occur in hydraulics.

Falconer and Liu (1988) modeled solute transport using the QUICK scheme. Details were provided about the refinement and application of a two-dimensional depth integrated numerical model to predict the depth mean velocity field and the spatial concentration distribution in hydraulic basins. The model includes a refined and computationally manageable third-order spatial finite-difference representation of the terms describing the advective transport of a solute, with the corresponding difference scheme being particularly suitable to modeling high solute gradients.

Zhang and Cundy (1989) solved the two-dimensional overland flow equations by using the second-order-accurate MacCormack explicit finite difference method. The accuracy of the model was tested by comparison with characteristic-based solutions and

experimental data. The results of these tests indicate that the model is accurate and has good stability and convergence properties.

Fennema and Chaudhry (1990) introduced two explicit finite-difference schemes-MacCormack and Gabutti for the solution of two-dimensional, unsteady free-surface flows. They claimed these schemes are second-order accurate in both space and time and predict the location and height of the bores without requiring shock fitting and allow simulation of both subcritical and supercritical flows, and the inclusion of initial conditions having sharp discontinuities.

Wood and Arnold (1990) modeled a one-dimensional kinematic wave equation which represents overland flow given by rainfall runoff on a sloping plane by using a box scheme. They concluded that the box scheme is one of the more popular methods because it is explicit with only one unknown per equation, and is unconditionally stable. Nevertheless, practical considerations dictate a limit on the time step.

Garcia-Navarro and Saviron (1992) described the development of a mathematical model, which solves the one-dimensional unsteady water flow equations. It is based on the McCormack second order explicit scheme, which has become an increasingly popular method for numerically integrating problems involving shocks. The treatment of the external and internal boundaries has been made by means of the method of

characteristics. The method is able to treat rapidly varying flow situations and relatively complex phenomena.

Tayfur et al. (1993) solved a two-dimensional overland flow equation by using an implicit finite difference method that does not suffer from any instability problems.

Jaque and Ball (1994) proposed a numerical scheme using a combined approach for the solution of the partial differential equation describing advection and diffusion, and provided a simple yet accurate solution algorithm for water quality modeling in open channel flows.

Holden and Stephenson (1995) presented an overall assessment of commonly used four-point difference schemes. They stated that the accuracy of finite-difference solutions to the kinematic equations to runoff modeling is affected when numerical diffusion or instability occurs. The effect of grid ratio and the spatial and temporal weighting coefficients in four-point difference schemes were discussed and a variable coefficient was suggested to eliminate uncontrolled numerical diffusion.

The emphasis of numerical solute transport models for water-quality studies in coastal and estuarine waters has focused on the numerical treatment of the advective terms in the transport equation. Komatsu et al. (1997) proposed a new refined numerical scheme for

pure advection, which prevents problems occurring when calculating advection. The scheme is based on a new concept in which the second-order wave equation of the type that describes travelling waves on a stretched string is numerically solved. This is claimed to result in higher accuracy and stability.

Lin and Falconer (1997) studied tidal flow and transport modeling using what they christen as the ULTIMATE QUICK scheme. The study describes an accurate numerical scheme for simulating two-dimensional solute transport in coastal and estuarine waters. An operator-splitting algorithm and a conventional discretization algorithm have been used to solve the solute transport equation. To avoid the occurrence of numerical oscillations, the ULTIMATE algorithm and the third-order accurate QUICKEST scheme have been used to represent the advective terms in the equation.

In this thesis, the governing equations have been numerically solved using the cubic spline method. This scheme has been increasingly used in solving the partial differential equations governing fluid flow and natural convection heat transport. The scheme was originally developed by Wang and Kahawita (1983a). They have made valuable contributions in developing the cubic spline method to solve problems of heat transfer and viscous flow with oblique shock wave. The main spline relations were presented and incorporated into solution procedures for partial differential equations. Wang and Kahawita (1983a) indicated that the method has the benefit that the approximation

possesses some of the advantages of finite element techniques without the disadvantages of high computer cost and complex problem formulation. The main advantages of using a cubic spline collocation procedure are that (Wang and Kahawita, 1983a):

1) The governing matrix system obtained is always tridiagonal thus permitting the use of the Thomas algorithm in the inversion procedure.
2) The matrix system obtained may be reduced to a scalar set of equations that either contain values of the function itself, its first derivative or its second derivative at the node points while maintaining a tridiagonal formulation.
3) The requirement of a uniform mesh is not necessary. However, for a uniform mesh, the spline approximation is fourth order accurate for the first derivatives while being third order for a non-uniform grid. The second derivative is approximated to second order for uniform as well as non-uniform grids.
4) Since the values of the first or the second derivatives may be evaluated directly, boundary conditions containing derivatives may be directly incorporated into the solution procedure, thus avoiding the difficulty that exists with conventional finite difference schemes.

The method is especially well-used to solve problems with a viscosity term such as in the heat transfer and diffusion equations. A brief review of related applications by the cubic spline scheme will be presented here.

Wang and Kahawita (1983b) developed a two-dimensional laterally integrated numerical model to represent the velocity and salinity distribution along an estuary. The governing equations which express the conservation of mass, momentum and salt or heat content were solved by a finite difference method in combination with spline functions. The influence of the convective terms on the resulting distributions of velocity and salinity was evaluated and taken into consideration.

In 1984, the same authors (Wang and Kahawita) presented the basic cubic spline formulation together with some examples of it's application. Estimates of truncation errors as well as some limited stability analyses were provided. Some test computations on Burgers equations were compared with the exact solution for the one dimensional case and with a published finite element approximate solution for the two dimensional case.

Wang (1987) proposed a spline method of fractional steps in each coordinate direction. The essential features of the method are that at every computational step, the problem is treated as a one-dimensional case in implicit form, and only one tridiagonal matrix systems is evaluated, resulting in significant savings in computer resources. As numerical examples, the computations for viscous flow with oblique shock wave and the flow in a square cavity at high Reynolds' number are performed.

Wang also attempted to explore the possibility of solving the equations of inviscid flow in 1985. The Spline Lax-Wendroff scheme and Spline Leap-Frog scheme for one-dimensional hyperbolic equations were derived, in which the artificial viscosity term was introduced. "Artificial viscosity" is a particular kind of truncation error exhibited by some finite difference analogies of advection equations. The method is to explicitly add a viscosity-like term to the inviscid dynamic equations in order to allow the computation to proceed through shock waves (Roache, 1972). The stability of the Cubic Spline schemes as well as the numerical dispersive and dissipative effects were analyzed.

Table 2.7 summarizes the characteristics of several related numerical schemes which the present author has used in modeling overland flow coupled with pollutant transport.

The stated advantages of the cubic spline scheme has led the present author to explore the possibility of using the technique to obtain numerical solutions to the governing set of equations that describe the mathematical model.

Table (2.7) Summarize the Characteristics of Related Numerical Schemes

Numerical Scheme	Characteristic
Box	Explicit with only one unknown per equation, unconditionally stable. A limit on the time step.
Explicit finite difference	Simple, only one unknown occurring explicitly, can be used to obtain the solution from the known value at the preceding time. Instability inherent at practical time steps.
Implicit Finite difference	Unconditionally stable, allows a large time step, save time. A complicated set of equations requires repetitive computations.
Quick	Mass conservation, reasonably high accuracy, computational efficiency, numerical advective stability. Numerically unstable for the case of pure advection when explicit QUICK scheme is used.
Cubic Spline	Without the high computer cost and complex problem formulation, the values of the first or the second derivatives may be evaluated directly. Boundary conditions containing derivatives may be directly incorporated into the solution procedure, thus the difficulty that exists with conventional finite difference schemes can be avoided, the matrix system obtained may be reduced to a scalar set of equations that contains values of the function itself, its first derivative or its second derivative at the node points, while maintaining a tridiagonal formulation.

CHAPTER 3: MATHEMATICAL EQUATIONS

The comprehensive model for non-point source pollutant transport in overland flow with infiltration consists of five parts: the overland flow, pollutant dissolution, pollutant adsorption by soil, the infiltration of polluted water into the subsurface, and pollutant transport by the overland flow.

3.1 Overland Flow Models

The hydrodynamic behavior of overland flow is conventionally described by the kinematic wave equations if inertial effects are small; otherwise the well-known complete St.Venant equations must be used. The two-dimensional St. Venant equations consist of a continuity equation and momentum conservation equations in the x- and y-direction. These equations may be expressed as follows (Tayfur et al. 1993):

$$\frac{\partial h}{\partial t}+\frac{\partial (hu)}{\partial x}+\frac{\partial (hv)}{\partial y}=Q\cdot\cos(\alpha)\cos(\phi) \tag{3.1}$$

$$\frac{\partial u}{\partial t}+u\frac{\partial u}{\partial x}+v\frac{\partial u}{\partial y}+\cos(\alpha)\cos(\phi)g\frac{\partial h}{\partial x}=g\sin(\alpha)-gS_{fx}-\frac{Q\cdot u}{h} \tag{3.2}$$

$$\frac{\partial v}{\partial t}+u\frac{\partial v}{\partial x}+v\frac{\partial v}{\partial y}+\cos(\alpha)\cos(\phi)g\frac{\partial h}{\partial y}=g\sin(\phi)-gS_{fy}-\frac{Q\cdot v}{h} \tag{3.3}$$

where

h is flow depth (m),

u is the component of the depth-averaged flow velocity in the x-direction (m/s),

v is the component of the depth-averaged flow velocity in the y-direction (m/s),

Q_r is the rainfall intensity (m/s),

Q_i is the infiltration rate, (m/s),

Q is the net lateral inflow (Q_r - Q_i) (m/s),

α is the slope angle with respect to the x-direction,

ϕ is the slope angle with respect to the y-direction,

g is the gravitational acceleration, (m/s^2),

S_{fx} and S_{fy} are the friction slopes in the x- and y-directions, respectively.

The friction slopes are generally represented by Manning's equation which may be expressed as:

$$S_{fx} = \frac{n^2 u\sqrt{u^2 + v^2}}{h^{4/3}} \tag{3.4}$$

$$S_{fy} = \frac{n^2 v\sqrt{u^2 + v^2}}{h^{4/3}} \tag{3.5}$$

where n is the Manning's roughness coefficient.

3.2 Infiltration Model

Infiltration is incorporated into modeling pollutant transport in overland flow, not only because it changes the distribution and decreases the magnitude of surface runoff, which in turn reduces the ability of runoff to transport pollutants, but also because many pollutants are dissolved or associated with very fine particles that move into the soil with the infiltrating water and influence the quantities of pollutant mass that penetrate the soil.

In this study, the infiltration rate is supposed to occur in two stages. The reason for using two steps to calculate infiltration was expounded by Yan (1995). At the first stage, before the start of any accumulation of water at the surface ("ponding"), the well-known Horton equation is used to predict the infiltration rate. At the second stage, defined as all times after the appearance of ponding, the Green-Ampt equation is used to describe the infiltration behavior. The ponding time t_p is the elapsed time between the start of rainfall and the time at which water begins to accumulate (ponding) at the soil surface. It may be evaluated from

$$t_p = \frac{\Psi_f \cdot n_b}{Q_r \cdot (\frac{Q_r}{k_f} - 1)} \tag{3.6}$$

with

$$n_b = (1 - S_e) \cdot n_l \tag{3.7}$$

where

t_p is the ponding time (s),

S_e is the initial effective saturation,

Q_r is the rainfall intensity (m/s),

k_l is the hydraulic conductivity of the soil (m/s),

n_l is the effective soil porosity,

n_b is the soil porosity,

ψ_l is the wetting front capillary pressure head (m).

As stated earlier, during the period leading up to ponding, Horton's equation (Viessman et al., 1989) is used:

$$f_p = f_c + (f_0 - f_c)e^{-k_3 t} \tag{3.8}$$

where

f_p is the infiltration capacity (m/s),

f_0 is the initial infiltration capacity (m/s),

f_c is the final equilibrium capacity (m/s),

k_3 is the empirical constant representing the rate of decrease in capacity (s^{-1}),

t is the time (s).

The Green-Ampt model applied during ponding is (Tayfur et al., 1993):

$$Q_i = k_1 \cdot [1 + \frac{\Psi_1}{(d_0^2 + \frac{2 \cdot k_1 \cdot \Psi_1}{n_b} \Delta t)^{1/2}}] \tag{3.9}$$

where

Q_i is the infiltration rate (m/s),

d_0 is the infiltration depth at the start of ponding (m),

Δt is the $(t-t_p)$ time increment (s).

The definitions of k_1, n_b and ψ_1 are the same as in equation (3.7). The values of ψ_1, n_1, k_1 and d_0 used in this study were from published soil properties (Rawls et al., 1983). Since the overland flow depth is small compared to the capillary head, a constant capillary pressure head ψ_1 = 0.15m ~ 0.17m is taken, the soil porosity n_b being considered equal to 0.3 ~ 0.45.

3.3 Solubility Rate Model

In most practical situations, the pollutant concentration distribution is specified as an initial condition on the basis of physical arguments. In order to simulate a specified spatial distribution of solid pollutant, the concept of solubility rate is required. When water comes into contact with the solid pollutants, dissolution of the pollutants begins and continues until equilibrium concentrations are attained, or until all the pollutants are

consumed. The solubility of a pollutant is defined as the mass of the pollutant that will dissolve in a unit volume of solution under specified conditions (Freeze and Cherry, 1979). The rate of pollutant dissolution is known as the solubility rate, which is defined as the mass of solute that will dissolve per unit time per unit area at a fixed temperature.

The model of solubility rate proposed in this study is constructed on the physico-chemical behavior of the pollutant in overland flow and by drawing on the analogy between mass and momentum transfer. When the mathematical equations governing the performance of two systems are identical in form, one system may be considered as being an analogy of the other. In this work, the analogy between mass and momentum transfer will be exploited to develop a model of the dissolution process.

The model of solubility rate is based on the following assumptions: since the solubility of solids is only slightly affected by pressure change, any pressure effects are neglected. During the process of dissolution no new substance is created and the temperature remains constant. Physical effects such as flow depth, bed shear stress and density of the pollutant, as well as chemical aspects such as solubility and reaction rate are considered.

The viscous-shear equation describes the transport of momentum under turbulent fluid conditions. It may be expressed by a generalized relation of the type:

$$\tau = \rho\varepsilon\frac{du}{dy} \tag{3.10}$$

where τ is the shear stress, ρ is a density of fluid, ε is a turbulent eddy viscosity or eddy diffusivity and du/dy is the velocity gradient in the direction of the fluid flow.

This relation may be written as

$$\frac{\tau}{\rho} = \varepsilon \frac{U}{Y} \tag{3.11}$$

where U and Y are respective characteristic velocity and length scales.

Define the friction velocity

$$u^* = \sqrt{\frac{\tau}{\rho}} \tag{3.12}$$

then

$$u^{*2} = \varepsilon \frac{U}{Y} = \varepsilon \frac{u}{h} \tag{3.13}$$

where u and h are the mean velocity and flow depth, respectively.

The rate of surface mass transfer is typically described by an equation of the form

$$\dot{m} = k \frac{C^* - C}{h} \tag{3.14}$$

where k is a surface mass transfer coefficient; C* and C are the saturated and local concentrations of the solute, respectively. Dividing equation (3.14) by (3.13) results in

$$\dot{m} = \frac{k}{\varepsilon} \frac{u^{*2}}{u} (C^* - C) \tag{3.15}$$

where k/ε is the reciprocal of the turbulent Schmidt number.

In the one dimensional case, the term u^{*2}/u may be evaluated from the Manning equation

$$\tau = \gamma \cdot R \cdot S_f \tag{3.16}$$

and

$$S_f = \frac{n^2 \cdot u^2}{h^{4/3}} \tag{3.17}$$

in which γ is the specific weight of water, R is the hydraulic radius and S_f is the friction slope. Substituting equation (3.16) and (3.17) into equation (3.12), one obtains

$$u^{*2} = \frac{\tau}{\rho} = \frac{g \cdot n^2 \cdot u^2}{R^{1/3}} \tag{3.18}$$

where R is the hydraulic radius (=h) if strictly one-dimensional flow is considered. Finally,

$$\dot{m} = \frac{k \cdot g \cdot n^2 \cdot u}{\varepsilon \cdot h^{1/3}}(C^* - C) \tag{3.19}$$

and writing this as a solubility rate equation,

$$S_t = k_2 \cdot n^2 \cdot g \frac{u}{h^{1/3}}(C^* - C) \tag{3.20}$$

The dimensionless constant k_2 is presumed to depend only on the solubility characteristics of the pollutant, it is called a reaction rate constant.

In the two-dimensional case, the total shear stress must be used:

$$\tau = \sqrt{\tau_x^2 + \tau_y^2} \tag{3.21}$$

where $\tau_x = \gamma\, h\, s_{fx}$ and $\tau_y = \gamma\, h\, s_{fy}$. Then

$$\tau = \gamma \frac{n^2}{h^{1/3}} (u^2 + v^2)^{1/2} \tag{3.22}$$

Finally,

$$\dot{m} = \frac{k}{\varepsilon} g \frac{n^2}{h^{1/3}} (u^2 + v^2)^{1/2} (C^* - C) \tag{3.23}$$

$$S_t = k_2 \cdot g \frac{n^2}{h^{1/3}} (u^2 + v^2)^{1/2} (C^* - C) \tag{3.24}$$

where

S_t is the solubility rate ($kg/m^2/s$),

h is the flow depth (m),

u, v are the components of flow velocities in the x- and y- direction, respectively (m/s),

g is the gravitational acceleration (m/s^2),

n is the Manning roughness coefficient,

C* is the solubility (kg/m^3),

C is the local concentration (kg/m^3).

Then the amount of pollutant dissolved D_p (kg) during the time interval dt in the area dxdy may be written as

$$D_p = S_t \cdot dt \cdot dx \cdot dy \tag{3.25}$$

and the amount in the total area up to time t is

$$\int_{t_p}^{t} dt \int_0^{Ly} dy \int_0^{Lx} dx \cdot S_t \tag{3.26}$$

Since a solid pollutant is considered in this study, two different initial pollutant distributions are assumed:

Case I, solid pollutant applied uniformly throughout the domain;

Case II, solid pollutant applied at a given location.

3.4 Pollutant Transport Model

Pollutant transport in the environment takes place as a result of two phenomena--advection and diffusion. Pollutants are transported by the bulk motion known as advection. Diffusion is a process in which a substance in the solution migrates in response to concentration gradients.

The starting point in the development of mathematical equations to describe the pollutant transport is to consider the physical processes that control the flux into and out of a volume element. A mass balance over a stationary control volume element, through which the fluid is flowing and pollutant is dissolving, is first established. When diffusion effects are significant, the use of Fick's law results in additional terms. Due to both advection and diffusion, mass transport takes place in the system with fluid motion

and the total flux is a combination of the advective and diffusive flux. The basic equation in two-dimensions may be written as (Yan 1995):

$$\frac{\partial C}{\partial t}+u\frac{\partial C}{\partial x}+v\frac{\partial C}{\partial y}=\frac{\partial}{\partial x}(D_x\frac{\partial C}{\partial x})+\frac{\partial}{\partial y}(D_y\frac{\partial C}{\partial y}) \tag{3.28}$$

where

C is the concentration of the pollutant (kg/m^3),

u, v are the components of the advection velocity in x- and y- direction, respectively (m/s),

D_x and D_y are diffusion coefficients in the x- and y-directions, respectively (m^2/s).

If the effects of rainfall-infiltration and solubility rate are taken into consideration in the equation, the advection-diffusion equation may be written as:

$$\frac{\partial C}{\partial t}+u\frac{\partial C}{\partial x}+v\frac{\partial C}{\partial y}=\frac{\partial}{\partial x}(D_x\frac{\partial C}{\partial x})+\frac{\partial}{\partial y}(D_y\frac{\partial C}{\partial y})+\frac{S_t}{h}-\frac{C\cdot Q_r}{h} \tag{3.29}$$

where

Q_r is the rainfall intensity (m/s),

S_t is the solubility rate ($kg/s/m^2$),

h is the flow depth (m).

In this study, constant diffusion coefficients have been assumed.

Furthermore, by considering the loss or gain of solute mass as a result of chemical reactions, the adsorption term may be included in the advection-diffusion equation. In the presence of chemical reactions, depending upon the chemical processes, a constituent may be added or removed. Then the pollutant transport equations are modified by source or sink terms.

3.5 Adsorption

Sorption is a significant phenomenon in most natural physical, chemical and biological processes and involves a series of reactions which may alter the distribution of contaminants. Sorption deals with the interphase accumulation or concentration on the surface or interface. The main cause of sorption is due to the hydrophobic property of solute to water or the high affinity of the solute for the solid particles. The term sorption which includes both adsorption and absorption, can be differentiated by the degree to which the solute molecule interacts with and is free to migrate between the sorbent phase. Absorption is a process in which solute transferred from one phase to another interpenetrates the sorbent phase by at least several manometric heads. In contrast, adsorption, i.e., solute accumulation is generally restricted to a surface or interface between the solution and adsorbent. In other words, adsorption is the accumulation of a substance at the interface between two phases. The material being adsorbed is the adsorbate or solute and the adsorbing phase is the adsorbent. Although adsorption

processes may occur at any interface between two phases, in the present study, only the case of adsorption at the liquid-solid interface is considered.

The behavior, transport and ultimate fate of distributed pollutants in overland flow may be significantly affected by their participation in sorption reactions and related phenomena. A fundamental knowledge of the behavior of sorption of contaminants onto the subsurface contaminants is thus essential for predicting their environmental impact. The degree to which the resulting effects can be quantified and predicted depends upon the extent to which certain fundamental aspects of sorption are understood, and upon the accuracy with which these phenomena can be characterized and modeled in complex surface and subsurface flow systems. In the current project, sorption phenomena are studied in some detail and incorporated into the model to understand the effect of surface adsorption.

There are different types of adsorption such as physical adsorption, chemical adsorption and electrostatic adsorption caused by the van der Waals, electrostatic and chemisorption forces. The rate of adsorption of each adsorbate depends upon the attractive forces between solute molecules, solvent molecules and the molecules of the sorbent, and upon some other effects. Adsorption processes take place in three steps: macrotransport, microtransport, and sorption.

When the adsorbate contacts a solid adsorbent, molecules of the adsorbate transfer from the solution to the solid until the concentration of the adsorbate remaining in solution is in dynamic equilibrium with the solid. The distribution of the solute between the liquid and solid phases in an adsorbent-solute-solvent system at equilibrium is termed an adsorption isotherm. The equilibrium data at a given temperature is usually represented by an adsorption isotherm, which expresses the relationship between the quantity adsorbed per unit weight of solid adsorbent and the concentration of the adsorbate in solution. To measure an adsorption isotherm, known quantities of the solid adsorbent and the solution are placed in contact at constant temperature until the solution does not change in composition with time. The adsorption isotherm can be calculated from the measured concentrations of the adsorbate in the solution at the start and at equilibrium. Available isotherms include the Freundlich isotherm, the Langmuir isotherm and the BET isotherm.

The appropriate statement of mass concentration when sorption reactions are considered in the case of one-dimensional transport is (Domenico and Schwartz, 1990):

$$D_x \frac{\partial^2 C}{\partial x^2} - u \frac{\partial C}{\partial x} \pm \frac{r}{n_b} = \frac{\partial C}{\partial t} \qquad (3.30)$$

where r is taken symbolically as the mass produced or consumed per unit volume per unit time, and may be called the rate law. The plus and minus term designates either a source or a sink and takes on different forms for different reactions. Source terms are usually specified in terms of a "rate law". This law may be expressed in terms of the rate

of decrease of a reaction, or the rate of increase of product depending on which constituent is being described by the transport equation. The rate law incorporated in this equation is a general one appropriate for both equilibrium and kinetic sorption reactions. It may be expressed as (Domenico and Schwartz 1990):

$$r = \frac{\partial C_*}{\partial t} \tag{3.31}$$

where C_* is the concentration of the solute on the solid phase.

The one-dimensional transport equation that incorporates the adsorption reaction may be expressed as:

$$\frac{1}{n_b}\frac{\partial C_*}{\partial t} + \frac{\partial C}{\partial t} + u\frac{\partial C}{\partial x} = \frac{\partial}{\partial x}\left(D_x \frac{\partial C}{\partial x}\right) + \frac{S_t}{h} - \frac{C \cdot Q_r}{h} \tag{3.32}$$

For equilibrium adsorption reactions, the concentration of adsorbed mass is a function of the mass in the solution

$$C_* = f(C) \tag{3.33}$$

then the term $\partial C_*/\partial t$ in equation (3.31) may be written in a more tractable term $\partial C/\partial t$. This produces a single differential equation containing one dependent variable. The rate of mass adsorption per unit volume of porous medium is (Domenico and Schwartz 1990):

$$\frac{\partial C_*}{\partial t} = \rho_b \frac{\partial S}{\partial t} \tag{3.34}$$

where S is the mass adsorbed per gram of soil on the surface, and ρ_b is the bulk density. Substituting equation (3.34) into equation (3.32) results in:

$$\frac{\rho_b}{n_b}\frac{\partial S}{\partial t} + \frac{\partial C}{\partial t} + u\frac{\partial C}{\partial x} = \frac{\partial}{\partial x}(D_x\frac{\partial C}{\partial x}) + \frac{S_t}{h} - \frac{C \cdot Q_r}{h} \qquad (3.35)$$

The bulk density may also be expressed as

$$\rho_b = \rho_s(1 - n_b) \qquad (3.36)$$

where ρ_s is the mass density, n_b is the porosity for a fully saturated medium, the fluid volume per unit total volume. By taking the linear Freundlich isotherm and differentiating with respect to time, the following expression may be obtained

$$\frac{\partial S}{\partial t} = k_d\frac{\partial C}{\partial t} \qquad (3.37)$$

where k_d is the distribution coefficient.

Combining equations (3.34), (3.36) and (3.37) gives

$$\frac{\partial C_s}{\partial t} = (1 - n_b)\rho_s k_d\frac{\partial C}{\partial t} \qquad (3.38)$$

Substituting equation (3.38) into equation (3.32) and rearranging terms gives transport equation for the simple case of linear sorption

$$\frac{\partial C}{\partial t}[1 + \frac{(1 - n_b)}{n_b}\rho_s k_d] = D_x\frac{\partial^2 C}{\partial x^2} - u\frac{\partial C}{\partial x} + \frac{S_t}{h} - \frac{C \cdot Q_r}{h} \qquad (3.39)$$

In the case of adsorption-desorption, the rate of sorption is a function of both the concentration of the mass in solution and the mass sorbed on the soil, i.e.,

$$\frac{\partial C_*}{\partial t} = f(C,S) \tag{3.40}$$

The following three special cases of adsorption and desorption are considered in this study.

3.5.1 Model I

A rate expression for the adsorption process which considers both the forward and backward kinetic rate coefficients on the surface of the adsorbent has been derived by Van Genuchten et al. (1973):

$$\frac{\partial S}{\partial t} = \{k_2 \exp[bS]\}\{\frac{k_1}{k_2}\exp[-2bS]\frac{\theta C}{\rho} - S\} \tag{3.41}$$

where k_1 and k_2 are the forward and backward kinetic rate coefficients, respectively. The backward rate coefficient k_2 and the partition coefficient, k_1/k_2, are independent of concentration. For equilibrium adsorption ($\partial S/\partial t = 0$), and equation (3.41) reduces to

$$S = (\theta k_1 C / \rho k_2)\exp(-2bS) \tag{3.42}$$

The values of k_1, k_2 and b may not be the same for adsorption and desorption, and hence may change with the sign according to the adsorption rate, e.g.,

$$b = \begin{cases} b_{ads} & \text{when } \dfrac{\partial S}{\partial t} > 0 \\ b_{des} & \text{when } \dfrac{\partial S}{\partial t} < 0 \end{cases} \tag{3.43}$$

where b_{ads} and b_{des} represent the values of b used to describe the adsorption and the desorption of the pollutant, respectively. Substituting equation (3.41) into equation (3.35) yields

$$\frac{\rho_b}{n_b}\{k_2 \exp(bS)[\frac{k_1}{k_2}\exp(-2bS)\frac{\theta C}{\rho_b} - S]\} + \frac{\partial C}{\partial t} = \frac{\partial}{\partial x}(D_x \frac{\partial C}{\partial x}) - u\frac{\partial C}{\partial x} + \frac{S_t}{h} - \frac{C \cdot Q_r}{h} \tag{3.44}$$

3.5.2 Model II

The second rate expression considered is (Van Genuchten et al. 1973):

$$\frac{\partial S}{\partial t} = k_2'\left[\frac{k_1'\theta}{k_2'\rho_b}C^N - S\right] \tag{3.45}$$

This equation is a first-order kinetic rate equation, with first-order forward, k'_1, and backward, k'_2, kinetic rate coefficients. For equilibrium adsorption ($\partial S/\partial t=0$), it reduces to

$$S = (k_1'\theta / k_2'\rho_b)C^N = k_d C^N \tag{3.46}$$

where k_d is the distribution coefficient.

Substituting equation (3.45) into equation (3.35) gives

$$\frac{\rho_b}{n_b} k_2' \left(\frac{k_1' \theta}{k_2' \rho_b} C^N - S\right) + \frac{\partial C}{\partial t} = \frac{\partial}{\partial x}\left(D_x \frac{\partial C}{\partial x}\right) - u \frac{\partial C}{\partial x} + \frac{S_t}{h} - \frac{C \cdot Q_r}{h} \tag{3.47}$$

3.5.3 Model III

The Freundlich equation has been shown to describe the relationship, at equilibrium, between the amount of solute in solution (C) and the amount of solute adsorbed (S). The Freundlich equation is as follows:

$$S = k_d C^N \tag{3.48}$$

Differentiating this equation with respect to time gives

$$\frac{\partial S}{\partial t} = k_d N C^{N-1} \frac{\partial C}{\partial t} \tag{3.49}$$

Substitution of this equation into equation (3.35) allows this equation to be expressed in terms of one dependent variable C:

$$\left(1 + \frac{\rho_b}{n_b} \cdot k_d \cdot N \cdot C^{N-1}\right) \frac{\partial C}{\partial t} = \frac{\partial}{\partial x}\left(D_x \frac{\partial C}{\partial x}\right) - u \frac{\partial C}{\partial x} + \frac{S_t}{h} - \frac{C \cdot Q_r}{h} \tag{3.50}$$

The complete two-dimensional pollutant transport equation which includes advection, diffusion, dissolution and adsorption processes, may then be expressed as, according to equation (3.35),

$$\frac{\rho_b}{n_b}\frac{\partial S}{\partial t}+\frac{\partial C}{\partial t}+u\frac{\partial C}{\partial x}+v\frac{\partial C}{\partial y}=\frac{\partial}{\partial x}(D_x\frac{\partial C}{\partial x})+\frac{\partial}{\partial y}(D_y\frac{\partial C}{\partial y})+\frac{S_t}{h}-\frac{C\cdot Q_r}{h}$$

(3.51)

When N = 1, substituting equation (3.49) into (3.51), one obtains

$$R_f\frac{\partial C}{\partial t}+u\frac{\partial C}{\partial x}+v\frac{\partial C}{\partial y}=\frac{\partial}{\partial x}(D_x\frac{\partial C}{\partial x})+\frac{\partial}{\partial y}(D_y\frac{\partial C}{\partial y})+\frac{S_t}{h}-\frac{C\cdot Q_r}{h} \quad (3.52)$$

where

$$R_f=1+\frac{(1-n_b)}{n_b}\rho_s k_d \quad (3.53)$$

In this study, the units are specified as follows:

$\partial S/\partial t$ is the adsorption rate,

b is the surface stress coefficient (kg/kg),

C is the concentration of the pollutant in the solution (kg/m^3),

C_* is the concentration of the solute on the solid phase (kg/m^3),

D is the diffusion coefficient (m^2/s),

k_d is the distribution coefficient,

k_1, k'_1 are forward kinetic rate coefficients (s^{-1}),

k_2, k'_2 are backward kinetic rate coefficients (s^{-1}),

S is the quantity of mass adsorbed on the surface (kg/kg),

t is the time (s),

u,v are the components of the velocities in the x- and y-directions, respectively (m/s),

x is the linear distance in the direction of the flow (m),

ρ_b is the bulk density (kg/m^3),

ρ_s is the mass density of soil (kg/m^3),

θ is the saturated water content (m^3/m^3).

CHAPTER 4: NUMERICAL SCHEME

4.1 Introduction

Following standard numerical integration techniques we consider a scheme that consists of dividing the computational domain into a collection of subintervals. A Taylor approximation to the derivatives is then constructed. In this work, the solution is approximated by a series of piecewise continuous cubic splines between each successive pair of nodes. There is sufficient flexibility in the cubic spline procedure to ensure that not only is the interpolant continuously differentiable on the interval, but also that it has a continuous second derivative on the interval.

Given a function f(x) defined on [a, b] and a set of numbers, called nodes, $a = x_0 < x_1 < \ldots < x_n = b$, a cubic spline interpolant, S(x) for f(x), is a function that satisfies the following conditions (Burden and Faires, 1993):

a. S_i denotes the cubic polynomial S(x) on the subinterval $[x_i, x_{i+1}]$ for each $i = 0, 1, \ldots n-1$;

b. $S(x_i) = f(x_i)$ for each $i = 0, 1, \ldots, n-2$;

c. $S_{i+1}(x_{i+1}) = S_i(x_{i+1})$ for each $i = 0, 1, \ldots, n-2$;

d. $S'_{i+1}(x_{i+1}) = S'_i(x_{i+1})$ for each $i = 0, 1, \ldots, n-2$;

e. $S''_{i+1}(x_{i+1}) = S''_i(x_{i+1})$ for each $i = 0, 1, \ldots, n-2$;

f. One of the following set of boundary conditions is satisfied:

(1) $S''_0(x_0) = S''_{n-1}(x_n) = 0$

(2) $S'_0(x_0) = f'(x_0)$ and $S'_{n-1}(x_n) = f'(x_n)$

Figure 4.1 shows the sketch of a cubic spline.

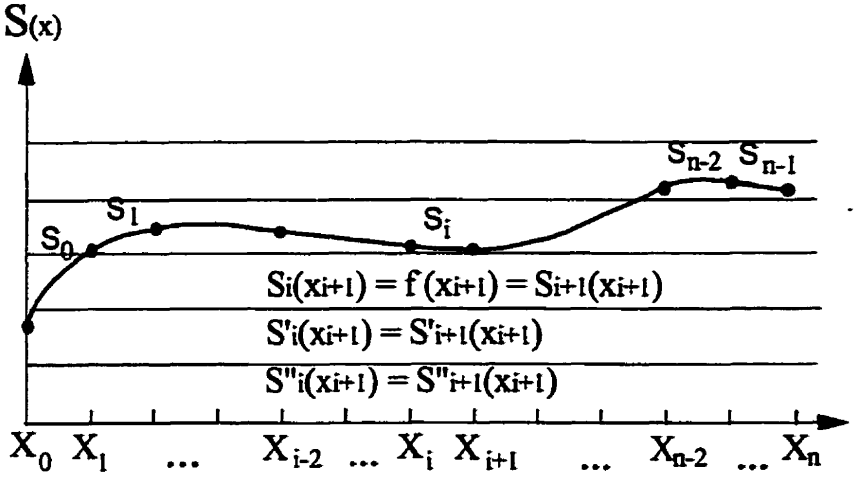

Figure 4.1 Sketch of cubic spline

4.2 Basic Relations for a Cubic Spline

To construct the cubic spline interpolant for a given function f(x), the conditions in the definition are applied to the cubic polynomials

$$S_i(x) = a_i(x - x_i)^3 + b_i(x - x_i)^2 + c_i(x - x_i) + d_i \qquad (4.1)$$

for each i = 0,1,...n-1.

$x_i \le x \le x_{i+1}$

The slope of the cubic reads:

$$S_i'(x) = 3a_i(x - x_i)^2 + 2b_i(x - x_i) + c_i \tag{4.2}$$

The second derivative of the cubic is:

$$S_i''(x) = 6a_i(x - x_i) + 2b_i \tag{4.3}$$

The coefficients a_i, b_i, c_i, and d_i may be obtained by solving the appropriate equations in the form of equations (4.1) to (4.3),

Let

$$f(x_i) = S_i(x_i) = y_i$$

$$S_i'(x_i) = m_i$$

$$S_i''(x_i) = M_i$$

Then the $S_{i-1}''(x)$ may be expressed in the subinterval $[x_{i-1}, x_i]$ as follows:

$$S_{i-1}''(x) = M_{i-1}\frac{x_i - x}{\Delta x_i} + M_i\frac{x - x_{i-1}}{\Delta x_i} \tag{4.4}$$

where $\Delta x_i = x_i - x_{i-1} > 0$

Integrating equation (4.4) twice

$$\begin{aligned} S_{i-1}(x) &= \frac{(x_i - x)^3}{6\Delta x_i}M_{i-1} + \frac{(x - x_{i-1})^3}{6\Delta x_i}M_i \\ &+ \frac{x_i - x}{\Delta x_i}\left(y_{i-1} - \frac{M_{i-1}\Delta x_i^2}{6}\right) + \left(y_i - \frac{M_i\Delta x_i^2}{6}\right)\frac{x - x_{i-1}}{\Delta x_i} \end{aligned} \tag{4.5}$$

From equation (4.5), one obtains:

$$S'_{i-1}(x) = -\frac{(x_i - x)^2}{2\Delta x_i} M_{i-1} + \frac{(x - x_{i-1})^2}{2\Delta x_i} M_i + \frac{y_i - y_{i-1}}{\Delta x_i} - \frac{M_i - M_{i-1}}{6} \Delta x_i \tag{4.6}$$

The final relationship involving the first derivatives and the second derivatives may be written as

$$\frac{\Delta x_i}{6} M_{i-1} + \frac{\Delta x_i + \Delta x_{i+1}}{3} M_i + \frac{\Delta x_{i+1}}{6} M_{i+1} = \frac{y_{i+1} - y_i}{\Delta x_{i+1}} - \frac{y_i - y_{i-1}}{\Delta x_i} \tag{4.7}$$

$$\frac{1}{\Delta x_i} m_{i-1} + 2\left(\frac{1}{\Delta x_i} + \frac{1}{\Delta x_{i+1}}\right) m_i + \frac{1}{\Delta x_{i+1}} m_{i+1} = \frac{3(y_{i+1} - y_i)}{\Delta x_{i+1}^2} + \frac{3(y_i - y_{i-1})}{\Delta x_i^2} \tag{4.8}$$

4.3 Application of Cubic Spline Scheme

Consider a second order partial differential equation of the form

$$y_t = f(y, y_x, y_{xx})$$

To construct the cubic spline interpolant for a given function y, an approximate solution may be represented as follows:

$$(y_t)_i = f(y_i, m_i, M_i)$$

The traditional finite - difference method is used to discretize the time derivative

$$y_t = \frac{y_i^{k+1} - y_i^k}{\Delta t} = (1-\omega)f^k + \omega f^{k+1} \tag{4.9}$$

where ω is a weighting coefficient. $\omega = 0$ implies an explicit scheme, $\omega = 1$ represents a fully implicit scheme. To facilitate the application of the cubic spline, equation (4.9) can be written as

$$y_i^{k+1} = F_i + R_i m_i^{k+1} + Q_i M_i^{k+1} \tag{4.10}$$

where F_i represents all the function values as well as coefficients of m_i and M_i at the previous time step k; R_i and Q_i are the coefficients of m_i and M_i at the current time step k+1, respectively.

4.4 Overland Flow Equation

4.4.1 Explicit scheme

The two-dimensional St.Venant equations are recalled

$$\frac{\partial h}{\partial t} + \frac{\partial (hu)}{\partial x} + \frac{\partial (hv)}{\partial y} = Q\cos(\alpha)\cos(\phi) \tag{3.1}$$

$$\frac{\partial u}{\partial t} + u\frac{\partial u}{\partial x} + v\frac{\partial u}{\partial y} + \cos(\alpha)\cos(\phi)g\frac{\partial h}{\partial x} = g\sin(\alpha) - gS_{fx} - \frac{Q\cdot u}{h} \tag{3.2}$$

$$\frac{\partial v}{\partial t} + u\frac{\partial v}{\partial x} + v\frac{\partial v}{\partial y} + \cos(\alpha)\cos(\phi)g\frac{\partial h}{\partial y} = g\sin(\phi) - gS_{fy} - \frac{Q\cdot v}{h} \tag{3.3}$$

They may be discretized in the cubic spline Lax-Wendroff explicit scheme (as developed by Wang, 1985) as follows:

The continuity equation (3.1) discretized along the x-direction reads

$$\frac{h_{i,j}^{k+1/2}-h_{i,j}^{k}}{\Delta t}+u_{i,j}^{k}(h_x)_{i,j}^{k}+h_{i,j}^{k}(u_x)_{i,j}^{k}=Q/2+\frac{(u^2)_{i,j}^{k}\Delta t}{2}(h_{xx})_{i,j}^{k}$$

(4.11)

In the y-direction

$$\frac{h_{i,j}^{k+1}-h_{i,j}^{k+1/2}}{\Delta t}+v_{i,j}^{k}(h_y)_{i,j}^{k}+h_{i,j}^{k+1/2}(v_y)_{i,j}^{k}=Q/2+\frac{(v^2)_{i,j}^{k}\Delta t}{2}(h_{yy})_{i,j}^{k}$$

(4.12)

where i and j are spatial node numbers in the x- and y-directions, respectively; k indicates values at the previous time step, while k+1 represents values at the current time step and Δt is the time interval. The terms $\frac{u^2\Delta t}{2}h_{xx}$ and $\frac{v^2\Delta t}{2}h_{yy}$ may be regarded as artificial viscosity terms. These terms as introduced in the shallow water equations serve to avoid numerical singularities that may arise during the process of computation. The results are unaffected by the added artificial terms; it may be mentioned that the same method was used to solve inviscid fluid flow problems by Wang and Kahawita (1984).

The discretized form of the momentum equations may be expressed in the Spline Lax-Wendroff explicit scheme as follows:

For the momentum equation (3.2) in the x-direction:

$$\frac{u_{i,j}^{k+1/2}-u_{i,j}^{k}}{\Delta t}+u_{i,j}^{k}(u_x)_{i,j}^{k}+g\cdot(h_x)_{i,j}^{k}$$
$$=g\cdot S_x-g\cdot S_{fx}-\frac{Q\cdot u_{i,j}^{k}}{h_{i,j}^{n+1}}+\frac{\Delta t\cdot(u^2)_{i,j}^{k}}{2}(u_{xx})_{i,j}^{k} \tag{4.13}$$

in the y-direction:

$$\frac{u_{i,j}^{k+1}-u_{i,j}^{k+1/2}}{\Delta t}+v_{i,j}^{k}(u_y)_{i,j}^{k}=\frac{\Delta t\cdot(v^2)_{i,j}^{k}}{2}(u_{yy})_{i,j}^{k} \tag{4.14}$$

For the momentum equation (3.3) in the x-direction:

$$\frac{v_{i,j}^{k+1/2}-v_{i,j}^{k}}{\Delta t}+u_{i,j}^{k+1}(v_x)_{i,j}^{k}+g\cdot(h_y)_{i,j}^{k}$$
$$=g\cdot S_y-g\cdot S_{fy}-\frac{Q\cdot v_{i,j}^{k}}{h_{i,j}^{n+1}}+\frac{\Delta t\cdot(u^2)_{i,j}^{k+1}}{2}(v_{xx})_{i,j}^{k} \tag{4.15}$$

and in the y-direction:

$$\frac{v_{i,j}^{k+1}-v_{i,j}^{k+1/2}}{\Delta t}+v_{i,j}^{k+1/2}(v_y)_{i,j}^{k}=\frac{\Delta t\cdot(v^2)_{i,j}^{k+1/2}}{2}(v_{yy})_{i,j}^{k} \tag{4.16}$$

In the equations above, the notations are defined as follows:

$$h_x=\frac{\partial h}{\partial x}\qquad h_y=\frac{\partial h}{\partial y}\qquad h_{xx}=\frac{\partial^2 h}{\partial x^2}\qquad h_{yy}=\frac{\partial^2 h}{\partial y^2}$$

$$u_x=\frac{\partial u}{\partial x}\qquad u_y=\frac{\partial u}{\partial y}\qquad u_{xx}=\frac{\partial^2 u}{\partial x^2}\qquad u_{yy}=\frac{\partial^2 u}{\partial y^2}$$

$$v_x=\frac{\partial v}{\partial x}\qquad v_y=\frac{\partial v}{\partial y}\qquad v_{xx}=\frac{\partial^2 v}{\partial x^2}\qquad v_{yy}=\frac{\partial^2 v}{\partial y^2}$$

The final spline approximation for the continuity equation may be expressed as

$$h_{i,j}^{k+1/2} = h_{i,j}^{k} + \Delta t\left[Q/2 - u_{i,j}^{k}(h_x)_{i,j}^{k} - h_{i,j}^{k}(u_x)_{i,j}^{k} + \frac{\Delta t \cdot (u^2)_{i,j}^{k}}{2}(h_{xx})_{i,j}^{k} \right] \tag{4.17}$$

$$h_{i,j}^{k+1} = h_{i,j}^{k+1/2} + \Delta t[Q/2 - v_{i,j}^{k}(h_y)_{i,j}^{k} - h_{i,j}^{k+1/2}(v_y)_{i,j}^{k} + \frac{\Delta t \cdot (v^2)_{i,j}^{k}}{2}(h_{yy})_{i,j}^{k}] \tag{4.18}$$

Since the friction terms in the momentum equations are nonlinear, they have been treated in semi-implicit fashion in order to avoid instabilities,

$$S_{fx} = \frac{n^2 u_{i,j}^{k+1}\sqrt{(u^2)_{i,j}^{k} + (v^2)_{i,j}^{k}}}{(h^{4/3})_{i,j}^{k}} \tag{4.19}$$

$$S_{fy} = \frac{n^2 v_{i,j}^{k+1}\sqrt{(u^2)_{i,j}^{k} + (v^2)_{i,j}^{k}}}{(h^{4/3})_{i,j}^{k}} \tag{4.20}$$

By substituting equations (4.19) and (4.20) into equations (4.13) and (4.15), and rearranging terms, the final cubic spline approximation may be written as:

$$u_{i,j}^{k+1/2} = \frac{1}{1+\dfrac{n^2 \cdot g \cdot \Delta t \sqrt{(u^2)_{i,j}^k + (v^2)_{i,j}^k}}{(h^{4/3})_{i,j}^{k+1}}} \{u_{i,j}^k + \Delta t[g \cdot S_x - \frac{Q \cdot u_{i,j}^k}{h_{i,j}^{k+1}} - u_{i,j}^k (u_x)_{i,j}^k - g \cdot (h_x)_{i,j}^k + \frac{\Delta t \cdot (u^2)_{i,j}^k}{2} (u_{xx})_{i,j}^k]\}$$

(4.21)

$$u_{i,j}^{k+1} = u_{i,j}^{k+1/2} + \Delta t \left[\frac{\Delta t \cdot (v^2)_{i,j}^k}{2} (u_{yy})_{i,j}^k - v_{i,j}^k (u_y)_{i,j}^k \right] \tag{4.22}$$

$$v_{i,j}^{k+1/2} = \frac{1}{1+\dfrac{n^2 \cdot g \cdot \Delta t \sqrt{(u^2)_{i,j}^{k+1} + (v^2)_{i,j}^k}}{(h^{4/3})_{i,j}^{k+1}}} \{v_{i,j}^k + \Delta t[g \cdot S_y - \frac{Q \cdot v_{i,j}^k}{h_{i,j}^{k+1}} - u_{i,j}^{k+1} (v_x)_{i,j}^k - g \cdot (h_y)_{i,j}^k + \frac{\Delta t \cdot (u^2)_{i,j}^{k+1}}{2} (v_{xx})_{i,j}^k]\}$$

(4.23)

$$v_{i,j}^{k+1} = v_{i,j}^{k+1/2} + \Delta t \left[\frac{\Delta t \cdot (v^2)_{i,j}^{k+1/2}}{2} (v_{yy})_{i,j}^k - v_{i,j}^{k+1/2} (v_y)_{i,j}^k \right] \tag{4.24}$$

The flow depths h^{k+1}, velocities u^{k+1} and v^{k+1} may be obtained directly together with the boundary conditions. Using the basic cubic spline relationships, the first derivative m^{k+1} of h, u or v may be obtained from

$$A_{i,j}m_{i-1,j}^{k+1} + B_{i,j}m_{i,j}^{k+1} + C_{i,j}m_{i+1,j}^{k+1} = D_{i,j} \qquad i = 1,2,...m; j = 1,2,...n \qquad (4.25)$$

The formulas for calculating coefficients $A_{i,j}$, $B_{i,j}$, $C_{i,j}$, $D_{i,j}$ and $m_{i,j}$ are given in Appendix I. Further details may be found in Wang and Kahawita (1984). The second derivative $M_{i,j}$ of h, u and v can be easily obtained from the equation

$$M_{i,j} = -\frac{4m_{i,j}}{\Delta x_{i+1,j}} - \frac{2m_{i+1,j}}{\Delta x_{i+1,j}} + 6\frac{y_{i+1,j} - y_{i,j}}{\Delta x_{i+1,j}^2} \qquad (4.26)$$

where $y_{i,j}$, represents the function, $m_{i,j}$ and $M_{i,j}$ represent coefficients of the first and the second derivatives of h, u or v at nodes i, j, respectively, and Δx is a constant spatial interval in the x-direction, while in the y-direction, Δx is replaced by Δy in equation (4.34).

4.4.2 Implicit scheme

An alternative implicit formulation of the cubic spline scheme also results in an expression of the same tridiagonal form as equation (4.10)

$$y_{i,j}^{k+1} = F_{i,j} + R_{i,j}m_{i,j}^{k+1} + Q_{i,j}M_{i,j}^{k+1}$$

As for the explicit scheme, there are two computational steps in the solution procedure of the discretized equations. The first step advances the solution to a provisional time k+1/2 which is without any practical time meaning; rather it is a predictor step. This provisional solution is based on the value at previous time step n. The second corrector

step now advances the solution to k+1, which indicates the value at present time step, the solution is based on the value of k+1/2. The solution procedure follows the order $h^{k+1/2}$, $h_x^{k+1/2}$, $h_{xx}^{k+1/2}$, $u^{k+1/2}$, $u_x^{k+1/2}$, $u_{xx}^{k+1/2}$, $v^{k+1/2}$, $v_x^{k+1/2}$, $v_{xx}^{k+1/2}$, h^{k+1}, h_y^{k+1}, h_{yy}^{k+1}, u^{k+1}, u_y^{k+1}, u_{yy}^{k+1}, v^{k+1}, v_y^{k+1}, v_{yy}^{k+1}.

The continuity equation (3.1) in the x- direction at time step k+1/2 results in:

$$\begin{aligned} h_{i,j}^{k+1/2} &= h_{i,j}^{k} - \frac{\Delta t}{2}[u_{i,j}^{k}(h_x)_{i,j}^{k+1/2} + h_{i,j}^{k}(u_x)_{i,j}^{k} + h_{i,j}^{k}(v_y)_{i,j}^{k} \\ &\quad + v\cdot(h_y)_{i,j}^{k} - \frac{Q}{2} - \frac{\Delta t(u^2)_{i,j}^{k}}{2}((h_{xx})_{i,j}^{k+1/2} + (h_{yy})_{i,j}^{k})] \\ &= F_{i,j} + R_{i,j}(h_x)_{i,j}^{k+1/2} + Q_{i,j}(h_{xx})_{i,j}^{k+1/2} \end{aligned} \tag{4.27}$$

where

$$\begin{aligned} F_{i,j} &= h_{i,j}^{k} - \frac{\Delta t}{2}[h_{i,j}^{k}(u_x)_{i,j}^{k} + h_{i,j}^{k}(v_y)_{i,j}^{k} + v_{i,j}^{k}(h_y)_{i,j}^{k} - \frac{Q}{2} \\ &\quad - \frac{\Delta t}{2}(u^2)_{i,j}^{k}(h_{yy})_{i,j}^{k}] \end{aligned} \tag{4.28}$$

$$R_{i,j} = -\frac{\Delta t}{2}u_{i,j}^{k} \tag{4.29}$$

$$Q_{i,j} = \frac{(\Delta t)^2}{4}(u^2)_{i,j}^{k} \tag{4.30}$$

The term $\Delta t\cdot u^2/2$ is regarded as an artificial viscosity term, which corresponds to the diffusivity term ν in the diffusion equation.

The momentum equations for the velocity u at time step k+1/2 are,

$$u^{k+1/2} = u^k - \frac{\Delta t}{2}[u\cdot(u_x)_{i,j}^{k+1/2} + v\cdot(u_y) + g\cdot h_x - g\cdot S_x + g\cdot S_{fx} + \frac{Q/2\cdot u}{h} - \frac{\Delta t\cdot u^2}{2}((u_{xx})_{i,j}^{k+1/2} + uy2)] \tag{4.31}$$

Substituting equation (4.19) and rearrangeing

$$u_{i,j}^{k+1/2} = \frac{1}{1+\frac{n^2\cdot g\cdot\Delta t\sqrt{(u^2)_{i,j}^k + (v^2)_{i,j}^k}}{2\cdot(h^{4/3})_{i,j}^{k+1/2}}}\{u_{i,j}^k - \frac{\Delta t}{2}[u\cdot(u_x)_{i,j}^{k+1/2} + v_{i,j}^k u_y + g\cdot(h_x)_{i,j}^{k+1/2} - g\cdot S_x + \frac{Q/2\cdot u_{i,j}^k}{h_{i,j}^{k+1/2}} - \frac{\Delta t(u^2)_{i,j}^k}{2}((u_{xx})_{i,j}^{k+1/2} + (u_{yy})_{i,j}^k)]\} = F_{i,j} + R_{i,j}(u_x)_{i,j}^{k+1/2} + Q_{i,j}(u_{xx})_{i,j}^{k+1/2} \tag{4.32}$$

where

$$F_{i,j} = \frac{1}{1+\frac{n^2\cdot g\cdot\Delta t\sqrt{(u^2)_{i,j}^k + (v^2)_{i,j}^k}}{2\cdot(h^{4/3})_{i,j}^{k+1/2}}}\left\{u_{i,j}^k - \frac{\Delta t}{2}[v\cdot u_y + g\cdot(h_x)_{i,j}^{k+1/2} - g\cdot S_x + \frac{Q/2\cdot u_{i,j}^k}{h_{i,j}^{k+1/2}} - \frac{\Delta t\cdot u^2}{2}u_{yy}]\right\} \tag{4.33}$$

$$R_{i,j} = \frac{1}{1 + \dfrac{n^2 \cdot g \cdot \Delta t \sqrt{(u^2)^k_{i,j} + (v^2)^k_{i,j}}}{2 \cdot (h^{4/3})^{k+1/2}_{i,j}}} \left(-u^k_{i,j} \cdot \frac{\Delta t}{2}\right) \tag{4.34}$$

$$Q_{i,j} = \frac{1}{1 + \dfrac{n^2 \cdot g \cdot \Delta t \sqrt{(u^2)^k_{i,j} + (v^2)^k_{i,j}}}{2 \cdot (h^{4/3})^{k+1/2}_{i,j}}} \left[(u^2)^k_{i,j} \frac{\Delta t^2}{4}\right] \tag{4.35}$$

Similarly, the momentum equation (3.3) for the velocity v in the x - direction at time step k+1/2 may be written as

$$\begin{aligned} v^{k+1/2} = v^k - \frac{\Delta t}{2}[u \cdot (v_x)^{k+1/2}_{i,j} + v \cdot v_y + g \cdot h_y - \\ g \cdot S_y + g \cdot S_{fy} + \frac{Q/2 \cdot v}{h} - \frac{\Delta t \cdot u^2}{2}((v_{xx})^{k+1/2}_{i,j} + v_{yy})] \end{aligned} \tag{4.36}$$

rearranging, equation (4.36) becomes

$$\begin{aligned} v^{k+1/2}_{i,j} = & \frac{1}{1 + \dfrac{n^2 \cdot g \cdot \Delta t \sqrt{(u^2)^{k+1/2}_{i,j} + (v^2)^k_{i,j}}}{2 \cdot (h^{4/3})^{k+1/2}_{i,j}}} \{v^k_{i,j} - \\ & \frac{\Delta t}{2}[u^{k+1/2}_{i,j}(v_x)^{k+1/2}_{i,j} + v^k_{i,j} v_y + g \cdot (h_y)^k_{i,j} \\ & - g \cdot S_y + \frac{Q/2 \cdot v^k_{i,j}}{h^{k+1/2}_{i,j}} - \frac{\Delta t \cdot (u^2)^{k+1/2}_{i,j}}{2}((v_{xx})^{k+1/2}_{i,j} + (v_{yy})^k_{i,j})]\} \\ & = F_{i,j} + R_{i,j}(v_x)^{k+1/2}_{i,j} + Q_{i,j}(v_{xx})^{k+1/2}_{i,j} \end{aligned} \tag{4.37}$$

where

$$F_{i,j} = \frac{1}{1+\dfrac{n^2 \cdot g \cdot \Delta t\sqrt{(u^2)^{k+1/2}_{i,j}+(v^2)^{k}_{i,j}}}{2\cdot(h^{4/3})^{k+1/2}_{i,j}}}$$

$$\left\{v^{k}_{i,j} - \frac{\Delta t}{2}(v\cdot v_y + g\cdot(h_y)^{k}_{i,j} - g\cdot S_y + \frac{Q/2\cdot v^{k}_{i,j}}{h^{k+1/2}_{i,j}} - \frac{\Delta t\cdot u^2}{2}v_{yy})\right\} \tag{4.38}$$

$$R_{i,j} = \frac{1}{1+\dfrac{n^2 \cdot g \cdot \Delta t\sqrt{(u^2)^{k+1/2}_{i,j}+(v^2)^{k}_{i,j}}}{2\cdot(h^{4/3})^{k+1/2}_{i,j}}}(-u^{k+1/2}_{i,j}\cdot\frac{\Delta t}{2}) \tag{4.39}$$

$$Q_{i,j} = \frac{1}{1+\dfrac{n^2 \cdot g \cdot \Delta t\sqrt{(u^2)^{k+1/2}_{i,j}+(v^2)^{k}_{i,j}}}{2\cdot(h^{4/3})^{k+1/2}_{i,j}}}[(u^2)^{k+1/2}_{i,j}\cdot\frac{\Delta t^2}{4}] \tag{4.40}$$

At the second step, the continuity equation along the y- direction at time step k+1 may be written as

$$\begin{aligned} h^{k+1}_{i,j} &= h^{k+1/2}_{i,j} - \frac{\Delta t}{2}[u^{k+1/2}_{i,j}(h_x)^{k+1/2}_{i,j} + h^{k+1/2}_{i,j}(u_x)^{k+1/2}_{i,j} + h^{k+1/2}_{i,j}(v_y)^{k}_{i,j} \\ &\quad + v^{k+1/2}_{i,j}(h_y)^{k+1}_{i,j} - \frac{Q}{2} - \frac{\Delta t\cdot(v^2)^{k+1/2}_{i,j}}{2}((h_{xx})^{k1/2}_{i,j} + (h_{yy})^{k+1}_{i,j})] \\ &= F_{i,j} + R_{i,j}(h_y)^{k+1}_{i,j} + Q_{i,j}(h_{yy})^{k+1}_{i,j} \end{aligned} \tag{4.41}$$

where

$$F_{i,j} = h_{i,j}^{k+1/2} - \frac{\Delta t}{2}[h_{i,j}^{k+1/2}(u_x)_{i,j}^{k+1/2} + h_{i,j}^{k+1/2}(v_y)_{i,j}^{k} + u_{i,j}^{k+1/2}(h_x)_{i,j}^{k+1/2} - \frac{Q}{2} - \frac{\Delta t}{2}(v_{i,j}^{k+1/2})^2(h_{xx})_{i,j}^{k+1/2}] \quad (4.42)$$

$$R_{i,j} = -\frac{\Delta t}{2} v_{i,j}^{k+1/2} \quad (4.43)$$

$$Q_{i,j} = \frac{\Delta t^2}{4}(v_{i,j}^{k+1/2})^2 \quad (4.44)$$

The momentum equation for velocity u at time step k+1 may be written as

$$u^{k+1} = u^{k+1/2} - \frac{\Delta t}{2}[u_{i,j}^{k+1/2}(u_x)_{i,j}^{k+1/2} + v_{i,j}^{k+1/2}(u_y)_{i,j}^{k+1} + g\cdot(h_x)_{i,j}^{k+1/2} - g\cdot s_x + g\cdot s_{fx} + \frac{Q/2\cdot u_{i,j}^{k+1/2}}{h} - \frac{\Delta t\cdot(v_{i,j}^{k+1/2})^2}{2}((u_{xx})_{i,j}^{k+1/2} + (u_{yy})_{i,j}^{k+1})] \quad (4.45)$$

Since S_{fy} is a semi-implicit equation, by rearranging, the following equation is obtained:

$$u_{i,j}^{k+1} = \frac{1}{1+\dfrac{n^2 \cdot g \cdot \Delta t\sqrt{(u^2)_{i,j}^{k+1/2} + (v^2)_{i,j}^{k+1/2}}}{2 \cdot (h^{4/3})_{i,j}^{k+1}}} \{u_{i,j}^{k+1/2} -$$

$$\frac{\Delta t}{2}[u_{i,j}^{k+1/2}(u_x)_{i,j}^{k1/2} + v_{i,j}^{k1/2}(u_y)_{i,j}^{k+1} + g \cdot (h_x)_{i,j}^{k+1/2} - \tag{4.46}$$

$$g \cdot S_x + \frac{Q/2 \cdot u_{i,j}^{k+1/2}}{h_{i,j}^{k+1}} - \frac{\Delta t \cdot (v_{i,j}^{k+1/2})^2}{2}((u_{xx})_{i,j}^{k+1/2} + (u_{yy})_{i,j}^{k+1})]\}$$

$$= F_{i,j} + R_{i,j}(u_y)_{i,j}^{k+1} + Q_{i,j}(u_{yy})_{i,j}^{k+1}$$

where

$$F_{i,j} = \frac{1}{1+\dfrac{n^2 \cdot g \cdot \Delta t\sqrt{(u^2)_{i,j}^{k} + (v^2)_{i,j}^{k}}}{2 \cdot (h^{4/3})_{i,j}^{k+1}}}$$

$$\cdot \{u_{i,j}^{k+1/2} - \frac{\Delta t}{2}[u_{i,j}^{k+1/2} u_x + g \cdot (h_x)_{i,j}^{k} - g \cdot S_x \tag{4.47}$$

$$+ \frac{Q/2 \cdot u_{i,j}^{k+1/2}}{h_{i,j}^{n+1}} - \frac{\Delta t \cdot (v_{i,j}^{k+1/2})^2}{2} u_{xx}]\}$$

$$R_{i,j} = \frac{1}{1+\dfrac{n^2 \cdot g \cdot \Delta t\sqrt{(u^2)_{i,j}^{k+1/2} + (v_{i,j}^{k+1/2})^2}}{2 \cdot (h^{4/3})_{i,j}^{k+1}}}(-v_{i,j}^{k+1/2}\frac{\Delta t}{2}) \tag{4.48}$$

$$Q_{i,j} = \frac{1}{1 + \frac{n^2 \cdot g \cdot \Delta t \sqrt{(u^2)_{i,j}^{k+1/2} + (v_{i,j}^{k+1/2})^2}}{2 \cdot (h^{4/3})_{i,j}^{k+1}}} [(v_{i,j}^{k+1/2})^2 \frac{\Delta t^2}{4}] \tag{4.49}$$

The momentum equation for velocity v at time step k+1 may be written as

$$\begin{aligned} v^{k+1} = v^{k+1/2} - \frac{\Delta t}{2} [& u_{i,j}^{k+1/2} (v_x)_{i,j}^{k+1/2} + v_{i,j}^{k+1/2} (v_y)_{i,j}^{k+1} \\ & + g \cdot (h_y)_{i,j}^{k+1/2} - g \cdot S_y + g \cdot S_{fy} + \frac{Q/2 \cdot v_{i,j}^{k+1/2}}{h} \\ & - \frac{\Delta t \cdot (v_{i,j}^{k+1/2})^2}{2} ((v_{xx})_{i,j}^{k+1/2} + (v_{yy})_{i,j}^{k+1})] \end{aligned} \tag{4.50}$$

Rearranging, equation (4.50) becomes

$$\begin{aligned} v_{i,j}^{k+1} = & \frac{1}{1 + \frac{n^2 \cdot g \cdot \Delta t \sqrt{(u^2)_{i,j}^{k+1} + (v^2)_{i,j}^{k+1/2}}}{2 \cdot (h^{4/3})_{i,j}^{k+1}}} \{ v_{i,j}^{k+1/2} - \\ & \frac{\Delta t}{2} [u_{i,j}^{k+1} (v_x)_{i,j}^{k+1/2} + v_{i,j}^{k+1/2} (v_y)_{i,j}^{k+1} \\ & + g \cdot (h_y)_{i,j}^{k+1/2} - g \cdot S_y + \frac{Q/2 \cdot v_{i,j}^{k+1/2}}{h_{i,j}^{k+1}} \\ & - \frac{\Delta t \cdot (v_{i,j}^{k+1/2})^2}{2} ((v_{xx})_{i,j}^{k+1/2} + (v_{yy})_{i,j}^{k+1})] \} \\ = & F_{i,j} + R_{i,j} (v_y)_{i,j}^{k+1} + Q_{i,j} (v_{yy})_{i,j}^{k+1} \end{aligned} \tag{4.51}$$

$$F_{i,j} = \frac{1}{1 + \dfrac{n^2 \cdot g \cdot \Delta t \sqrt{(u^2)_{i,j}^{k+1} + (v^2)_{i,j}^{k+1/2}}}{2 \cdot (h^{4/3})_{i,j}^{k+1}}}$$

$$\cdot \{ v_{i,j}^{k+1/2} - \frac{\Delta t}{2} [u_{i,j}^{k+1} v_x + g \cdot (h_y)_{i,j}^{k+1/2} - g \cdot S_y \qquad (4.52)$$

$$+ \frac{Q/2 \cdot v_{i,j}^{k+1/2}}{h_{i,j}^{k+1}} - \frac{\Delta t \cdot (u_{i,j}^{k+1})^2}{2} (v_{xx})_{i,j}^{k+1/2}] \}$$

$$R_{i,j} = \frac{1}{1 + \dfrac{n^2 \cdot g \cdot \Delta t \sqrt{(u^2)_{i,j}^{k+1} + (v^2)_{i,j}^{k+1/2}}}{2 \cdot (h^{4/3})_{i,j}^{k+1}}} (-v_{i,j}^{k+1/2} \frac{\Delta t}{2}) \qquad (4.53)$$

$$Q_{i,j} = \frac{1}{1 + \dfrac{n^2 \cdot g \cdot \Delta t \sqrt{(u^2)_{i,j}^{k+1} + (v^2)_{i,j}^{k+1/2}}}{2 \cdot (h^{4/3})_{i,j}^{k+1}}} [(v_{i,j}^{k+1/2})^2 \frac{\Delta t^2}{4}] \qquad (4.54)$$

By incorporating the cubic spline relations, the equations above may be transformed into a set of equations for the function $y_{i,j}$ which may represent h, u or v.

$$A_i y_{i-1,j}^{k+1} + B_i y_{i,j}^{k+1} + C_i y_{i+1,j}^{k+1} = D_i \qquad i = 1,2,...m; j = 1,2,...n \qquad (4.55)$$

The flow depth h, velocities u and v may be solved by rearranging equation (4.55) in tridiagonal matrix form. The detailed procedure for computing the first derivative $m_{i,j}$ and $M_{i,j}$ are indicated in Appendix I.

The necessary condition for stability of this scheme is (Wang, 1985)

$$\frac{u\Delta t}{\Delta x} < \frac{1}{\sqrt{3}}$$

or

$$\frac{v\Delta t}{\Delta y} < \frac{1}{\sqrt{3}}$$

4.5 Transport Equation

4.5.1 Explicit scheme

The cubic spline Lax-Wendroff explicit scheme for the transport equation (3.52) may be written as

$$\frac{C_{i,j}^{k+1/2} - C_{i,j}^{k}}{\Delta t} = \frac{1}{Rf}\left[D_x \frac{\partial^2 C_{i,j}}{\partial x^2} - u_{i,j}\frac{\partial C_{i,j}}{\partial x} + \frac{St}{h_{i,j}} - \frac{C_{i,j}Qr}{h_{i,j}}\right] \quad (4.56)$$

and

$$\frac{C_{i,j}^{k+1} - C_{i,j}^{k+1/2}}{\Delta t} = \frac{1}{Rf}\left[D_y \frac{\partial^2 C_{i,j}}{\partial y^2} - v_{i,j}\frac{\partial C_{i,j}}{\partial y}\right] \quad (4.57)$$

where

$$Rf = 1 + \frac{(1-n_b)}{n_b}\rho_s k_d$$

The final discretized form of equation (4.56) and (4.57) may be written as follows:

$$C_{i,j}^{k+1/2} = C_{i,j}^{k} + \Delta t \frac{1}{Rf}[D_x \frac{\partial^2 C_{i,j}}{\partial x^2} - u_{i,j} \frac{\partial C_{i,j}}{\partial x} + \frac{St}{h_{i,j}} - \frac{C_{i,j} \cdot Qr}{h_{i,j}}] \quad (4.58)$$

$$C_{i,j}^{k+1} = C_{i,j}^{k+1/2} + \Delta t \frac{1}{Rf}[D_y \frac{\partial^2 C_{i,j}}{\partial y^2} - v_{i,j} \frac{\partial C_{i,j}}{\partial y}] \quad (4.59)$$

The pollutant concentration $C_{i,j}^{k+1}$ can now be solved directly. The first derivative and the second derivative of the concentration may be obtained by using the same procedure of solving the continuity and momentum equations.

4.5.2 Implicit scheme

The alternative implicit scheme for the transport equation based on equation (4.10), at time step k+1/2 may be expressed as:

$$\begin{aligned} C_{i,j}^{k+1/2} &= C_{i,j}^{k} + \Delta t \frac{1}{Rf}[D_x \frac{\partial^2 C_{i,j}}{\partial x^2} - u_{i,j} \frac{\partial C_{i,j}}{\partial x} + \frac{St}{h_{i,j}} - \frac{C_{i,j} Qr}{h_{i,j}}] \\ &= F_{i,j} + R_{i,j} m_{i,j}^{k+1/2} + Q_{i,j} M_{i,j}^{k+1/2} \end{aligned} \quad (4.60)$$

where $m^{k+1/2}$ and $M^{k+1/2}$ represent $\partial C/\partial x$ and $\partial^2 C/\partial x^2$, respectively, with

$$F_{i,j} = C_{i,j}^{k} + \frac{\Delta t}{Rf}[\frac{St}{h_{i,j}} - \frac{C_{i,j} Qr}{h_{i,j}}] \quad (4.61)$$

$$R_{i,j} = -\frac{\Delta t \cdot u_{i,j}}{Rf} \quad (4.62)$$

$$Q_{i,j} = \frac{\Delta t}{Rf} D_x \tag{4.63}$$

while at time step k+1

$$\begin{aligned} C_{i,j}^{k+1} &= C_{i,j}^{k+1/2} + \Delta t \frac{1}{Rf}[D_y \frac{\partial^2 C_{i,j}}{\partial y^2} - v_{i,j} \frac{\partial C_{i,j}}{\partial y}] \\ &= F_{i,j} + R_{i,j} m_{i,j}^{k+1} + Q_{i,j} M_{i,j}^{k+1} \end{aligned} \tag{4.64}$$

where $m^{k+1/2}$ and $M^{k+1/2}$ represent $\partial C/\partial y$ and $\partial^2 C/\partial y^2$, respectively,

$$F_{i,j} = C_{i,j}^{k+1/2} \tag{4.65}$$

$$R_{i,j} = -\frac{\Delta t \cdot v_{i,j}}{Rf} \tag{4.66}$$

$$Q_{i,j} = \frac{\Delta t}{Rf} D_y \tag{4.67}$$

The equations may be transformed into a scalar set of equations by using the cubic spline relation.

$$A_i y_{i-1,j}^{k+1} + B_i y_{i,j}^{k+1} + C_i y_{i+1,j}^{k+1} = D_i$$

where $y_{i,j}$ represents concentration C at node i and j.

The concentration C, its first derivative and second derivative may be obtained by using the same procedure for solving the continuity and momentum equations.

4.6 Initial Conditions

To start the numerical calculation, all depths and velocities must be known along the land surface. In the case of overland flow developing on an initially dry surface, a very thin water layer is assumed before the flow is initiated. This assumption is necessary to overcome the numerical singularity in the solution procedure (Akan and Yen, 1981). The numerical singularity that may result from the friction slope term if the initial condition is for a dry bed surface. The results are not affected by this assumption, and the same method was employed by Liggett and Woolhiser (1967), Zhang and Cundy (1989), Chow and Ben-Zvi (1993) and Tayfur et al. (1993).

In this study, the initial conditions for the overland flow equations are

$$h(x, y, 0) = 0.00001\,m$$

$$u(x, y, 0) = 0.$$

$$v(x, y, 0) = 0.$$

the first and the second derivatives of h, u and v are set to zero.

The initial condition for the transport equation is

$$C(x, y, 0) = 0.$$

The first and the second derivatives of C are also set to zero.

4.7 Boundary Conditions

The boundary conditions on the numerical model should correspond to the existing flow regime. The upstream boundary conditions used for the overland flow equations are

$$h(0, y, t) = 0.00001$$

$$u(0, y, t) = 0$$

$$v(0, y, t) = 0$$

$$h(x, 0, t) = 0.00001$$

$$u(x, 0, t) = 0$$

$$v(x, 0, t) = 0$$

The discretized form at the upstream boundary may be written as

$$\left(\frac{\partial h}{\partial x}\right)_{i,0} = 0 \qquad \left(\frac{\partial^2 h}{\partial x^2}\right)_{i,0} = 0$$

$$\left(\frac{\partial u}{\partial x}\right)_{i,0} = 0 \qquad \left(\frac{\partial^2 u}{\partial x^2}\right)_{i,0} = 0$$

$$\left(\frac{\partial v}{\partial x}\right)_{i,0} = 0 \qquad \left(\frac{\partial^2 v}{\partial x^2}\right)_{i,0} = 0$$

$$\left(\frac{\partial h}{\partial x}\right)_{0,j} = 0 \qquad \left(\frac{\partial^2 h}{\partial x^2}\right)_{0,j} = 0$$

$$\left(\frac{\partial u}{\partial x}\right)_{0,j} = 0 \qquad \left(\frac{\partial^2 u}{\partial x^2}\right)_{0,j} = 0$$

$$\left(\frac{\partial v}{\partial x}\right)_{0,j} = 0 \qquad \left(\frac{\partial^2 v}{\partial x^2}\right)_{0,j} = 0$$

$$\left(\frac{\partial h}{\partial y}\right)_{i,0} = 0 \qquad \left(\frac{\partial^2 h}{\partial y^2}\right)_{i,0} = 0$$

$$\left(\frac{\partial u}{\partial y}\right)_{i,0} = 0 \qquad \left(\frac{\partial^2 u}{\partial y^2}\right)_{i,0} = 0$$

$$\left(\frac{\partial v}{\partial y}\right)_{i,0} = 0 \qquad \left(\frac{\partial^2 v}{\partial y^2}\right)_{i,0} = 0$$

$$\left(\frac{\partial h}{\partial y}\right)_{0,j} = 0 \qquad \left(\frac{\partial^2 h}{\partial y^2}\right)_{0,j} = 0$$

$$\left(\frac{\partial u}{\partial y}\right)_{0,j} = 0 \qquad \left(\frac{\partial^2 u}{\partial y^2}\right)_{0,j} = 0$$

$$\left(\frac{\partial v}{\partial y}\right)_{0,j} = 0 \qquad \left(\frac{\partial^2 v}{\partial y^2}\right)_{0,j} = 0$$

The discretized form for the overland flow equations at the downstream boundary may be written as

$$\left(\frac{\partial h}{\partial x}\right)_{m,j} = 0 \qquad \left(\frac{\partial^2 h}{\partial x^2}\right)_{m,j} = 0$$

$$\left(\frac{\partial u}{\partial x}\right)_{m,j} = 0 \qquad \left(\frac{\partial^2 u}{\partial x^2}\right)_{m,j} = 0$$

$$\left(\frac{\partial v}{\partial x}\right)_{m,j} = 0 \qquad \left(\frac{\partial^2 v}{\partial x^2}\right)_{m,j} = 0$$

$$\left(\frac{\partial h}{\partial y}\right)_{i,n} = 0 \qquad \left(\frac{\partial^2 h}{\partial y^2}\right)_{i,n} = 0$$

$$\left(\frac{\partial u}{\partial y}\right)_{i,n} = 0 \qquad \left(\frac{\partial^2 u}{\partial y^2}\right)_{i,n} = 0$$

$$\left(\frac{\partial v}{\partial y}\right)_{i,n} = 0 \qquad \left(\frac{\partial^2 v}{\partial y^2}\right)_{i,n} = 0$$

for each i = 0, 1, ...m; j = 0, 1, ...n.

The upstream boundary conditions for the transport equation are

$$C(x, 0, t) = 0$$

$$C(0, y, t) = 0$$

The discretized form for the transport equation at the upstream boundary may be written as

$$\left(\frac{\partial C}{\partial x}\right)_{0,j} = 0 \qquad \left(\frac{\partial^2 C}{\partial x^2}\right)_{0,j} = 0$$

$$\left(\frac{\partial C}{\partial x}\right)_{i,0} = 0 \qquad \left(\frac{\partial^2 C}{\partial x^2}\right)_{i,0} = 0$$

$$\left(\frac{\partial C}{\partial y}\right)_{0,j} = 0 \qquad \left(\frac{\partial^2 C}{\partial y^2}\right)_{0,j} = 0$$

$$\left(\frac{\partial C}{\partial y}\right)_{i,0} = 0 \qquad \left(\frac{\partial^2 C}{\partial y^2}\right)_{i,0} = 0$$

while at the downstream boundary they may be written as

$$\left(\frac{\partial C}{\partial x}\right)_{m,j} = 0 \qquad \left(\frac{\partial^2 C}{\partial x^2}\right)_{m,j} = 0$$

$$\left(\frac{\partial C}{\partial y}\right)_{i,n} = 0 \qquad \left(\frac{\partial^2 C}{\partial y^2}\right)_{i,n} = 0$$

for each $i = 0, 1, \ldots m$; $j = 0, 1, \ldots n$.

Based on the type of the equation which is obtained by converting the cubic spline formulae into three useful forms containing either the value of the function itself, its first derivative or its second derivative, the different boundary conditions were used.

CHAPTER 5: VALIDATION AND VERIFICATION OF MODELS

5.1 Generalities

In order to evaluate the scope of application and accuracy of the model, a comparison between experimentally observed data, numerical prediction and analytical solutions was made. In this chapter, the validity of the enhanced model will be compared with:

- Analytical solutions
- Data from published literature
- Experimental results obtained at the Ecole Polytechnique de Montréal.

The model was first tested against three cases where analytical equations are available. The model was then used to simulate rainfall-runoff events for which independent published data was available. Since no published data for rainfall-runoff with pollutant washoff is available, two series of laboratory experiments were designed and executed in the Hydrodynamics Laboratory at the Ecole Polytechnique de Montréal.

5.2 Analytical Solutions

Analytical solutions, if available, may be used as important tools for the preliminary validation of numerical models. In fact this step is essential if such solutions exist.

They have the added advantage of providing a deeper insight into the relevant phenomena. Furthermore, very frequently parameter sensitivity to the solution may be evaluated rapidly almost by inspection. However, analytical solutions are restricted to problems with many terms in the original equations being either simplified or totally disregarded. For this reason, checks between the numerical model and the analytical solutions may only be regarded as a partial verification.

5.2.1 Conservative transport equation

Analytical techniques for the solution of the transport equation are generally restricted to simple problems with constant coefficients. There are very few analytical solutions to the one-dimensional advection and advection-diffusion equation with variable velocity and diffusion coefficients. The analytical solution derived for the conservative and nonconservative forms of the advection and advection-diffusion equations with a particular form of spatially variable coefficients by Zoppou and Knight (1997) has been used. The particular forms of the spatially variable coefficients considered are consistent with problems of pollutant transport in an open channel where the flow in the channel is augmented by a steady, unpolluted lateral inflow distributed along the whole length of the channel. The two types of analytical solutions to the transport equations may be written as follows (Zoppou and Knight, 1997).

The first example deals with a one-dimensional conservative advection-diffusion equation; it is written as

$$\frac{\partial c}{\partial t} + \frac{\partial (cu_0 x)}{\partial x} = \frac{\partial}{\partial x}(D_0 x^2 \frac{\partial c}{\partial x}) \tag{5.1}$$

where

c = concentration of the pollutant, x = longitudinal distance, u = one-dimensional fluid velocity field, t = time, D = diffusion coefficient. The following initial and boundary conditions are imposed on:

$c(x, 0) = 0$ for $x > x_0$,

$c(x_0, t) = c_0$ for $x = x_0$,

and $c(\infty, t) = 0$

The analytical solution to equation (5.1) developed by Zoppou and Knight (1997) with the initial and boundary conditions as specified above is:

$$c(x,t) = \frac{c_0}{2}\{\frac{x_0}{x}\,\mathrm{erfc}[\frac{\ln(x / x_0) - t(u_0 + D_0)}{2\sqrt{D_0 t}}] + \exp[\frac{u_0 \ln(x / x_0)}{D_0}]\mathrm{erfc}[\frac{\ln(x / x_0) + t(u_0 + D_0)}{2\sqrt{D_0 t}}]\} \tag{5.2}$$

The parameters used for comparison with the numerical model are presented in Table 5.1.

Table (5.1) Parameters used in the Transport Equation

C_0	D_0	u_0	x_0
100	0.02	1	1

The comparison between the numerical model and the analytical solution is shown in Figure 5.1. In general, there is a good agreement between analytical and numerical solutions.

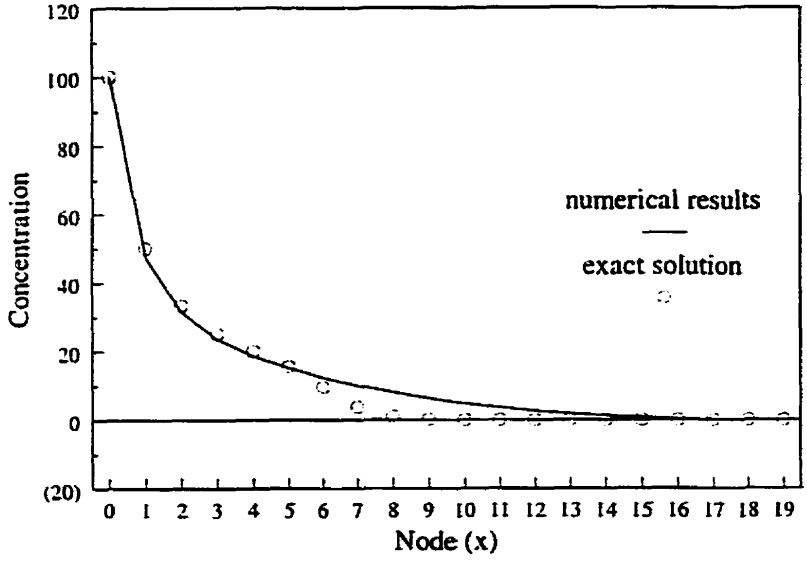

Figure 5.1 Comparison between numerical results and analytical solution for conservative advection-diffusion equation (dimensionless)

5.2.2 Non conservative transport equation

The second example is the non-conservative advection-diffusion equation, in which a variable coefficient multiplies the advection term. The equation is expressed as

$$\frac{\partial c}{\partial t} + u_0 x \frac{\partial c}{\partial x} = D_0 x^2 \frac{\partial^2 c}{\partial x^2} \tag{5.3}$$

with $c(x_0, t) = c_0$, and $x_0 > 0$.

The analytical solution to equation (5.3) is

$$\begin{aligned} c(x, t) &= \frac{c_0}{2} \operatorname{erfc}\left[\frac{\ln(x / x_0) - u_0 t}{2\sqrt{D_0 t}}\right] \\ &+ \frac{c_0}{2} \exp\left[\frac{u_0 \ln(x / x_0)}{D_0}\right] \operatorname{erfc}\left[\frac{\ln(x / x_0) + u_0 t}{2\sqrt{D_0 t}}\right] \end{aligned} \tag{5.4}$$

where, x_0, u_0, c_0 and D_0 are constants. The same values for these constants as listed in Table 5.1 were used. The concentration profile at t = 2s obtained by numerical simulation and analytical solution is compared in Figure 5.2. The appearance of small negative values of concentration may be caused by the numerical grid-scale oscillation. The good agreement between the numerical and analytical solution is obtained.

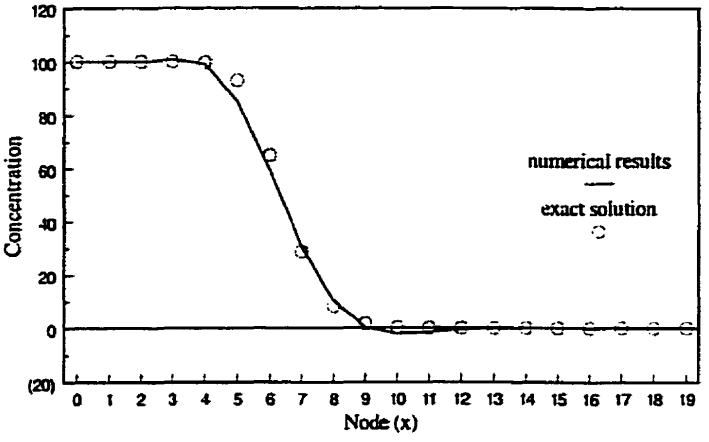

Figure 5.2 Comparison between numerical results and analytical solution for non-conservative advection-diffusion equation (dimensionless)

5.2.3 Adsorption equation

The third example of an analytical approximation to the adsorption equation is the case of linear adsorption, which may be expressed by the following equation:

$$\theta\frac{\partial c}{\partial t} + k_d\frac{\partial c}{\partial t} = \theta D\frac{\partial^2 c}{\partial x^2} - \theta u\frac{\partial c}{\partial x} \tag{5.5}$$

The analytical solution for this transport equation with adsorption was given by Bosma et al. (1992):

$$c(x,t) = c_0\left[\frac{1}{2}\mathrm{erfc}\left\{\frac{R_t x - ut}{2(DR_t t)^{1/2}}\right\} + \frac{1}{2}\exp(ux/D)\mathrm{erfc}\left\{\frac{R_t x + ut}{2(DR_t t)^{1/2}}\right\}\right] \tag{5.6}$$

where

$$R_l = 1 + k_d / \theta \tag{5.7}$$

here, c = concentration of the pollutant, x = longitudinal distance, u = fluid velocity in the x direction, t = time, D = diffusion coefficient, k_d = distribution coefficient, θ = water content, c_0 = initial concentration, R_l = linear retardation factor.

The initial and boundary conditions for the concentration c are specified as:

$$c(x, t) = 0 \qquad x > 0, \qquad t = 0$$

$$c(x, t) = c_0 \qquad x = 0, \qquad t > 0$$

The values used in the test are indicated in Table 5.2. Figure 5.3 presents the comparison between the numerically predicted concentration profile for the adsorption equation and its analytical solution.

Table (5.2) Parameters used in the Adsorption Equation

Parameter	Value
Initial concentration C_0 (kg/m^3)	10
Constant diffusion coefficient D (m^2/s)	0.2
Constant velocity u_0 (m/s)	0.05
Bulk density ρ (kg/m^3)	2650
Adsorption coefficient k_d	0.0000001

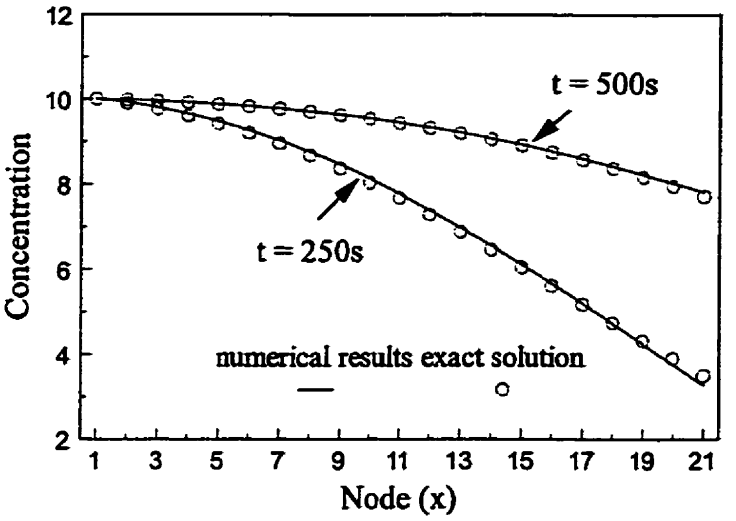

Figure 5.3 Comparison between numerical results and analytical results for adsorption equation (dimensionless)

Again, excellent agreement between the analytical and numerical results is obtained.

5.3 Comparison with Published Field Data

Tayfur et al. (1993) conducted a series of overland flow measurements on experimental plots at the small hill-slope scale. Their runoff values are used here to verify the numerical results of the present scheme. Furthermore, the earlier numerical results obtained by the present author (Yan, 1995) using finite differences have also been used to compare with the results obtained using the cubic spline scheme. A summary of the

test parameter values is shown in Table 5.3. The unified units (meter and second) are used.

Table (5.3) Computation Conditions for Numerical Test

Rainfall intensity Qr	0.0000071m/s
Infiltration rate Qi	0.0000019m/s
Dimension (d * l)	14*72
S_{ox}	0.0086
S_{oy}	0.086
Manning coefficient	0.04
Rainfall duration	5400s

Figure 5.4 compare the numerical results obtained using the finite difference and cubic spline schemes with the experimental data of Tayfur et al. (1993). Clearly, the numerical and experimental results are in good agreement.

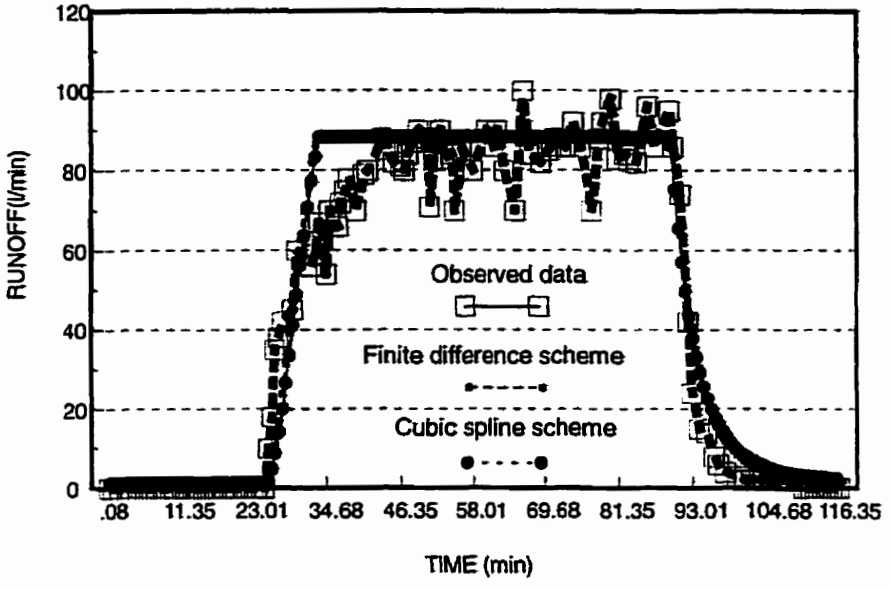

Figure 5.4 Comparison between numerical results with the data of Tayfur (1993)

5.4 Laboratory Experiments

A search of the literature failed to provide any published data on the rainfall-runoff process with infiltration and pollutant washoff. It was therefore decided to execute a series of simple experiments that would combine the three processes, hopefully resulting in useful data that could be used to asses the performance of the complete model. The experiments were realized in the Hydrodynamics Laboratory of the Ecole Polytechnique de Montréal.

5.4.1 The purpose of the experiments

The purpose of the series of laboratory experiments conducted in the present study was to evaluate and validate the numerical model by qualitative/quantitative comparison with observed values. Since it is impossible to experimentally test all possible scenarios for which a model may be applied, model validation is necessarily restricted to certain conditions. Two series of experiments were performed. In the first experiment, different values of surface roughness and initial distribution of pollutant was applied, while other factors such as slope and rainfall intensity were kept constant. The experimental setup ensured that the pollutant concentration in the runoff could be measured. The second one is two-dimensional experiment, in which rainfall-runoff relationships and pollutant transport in overland flow were investigated. Three different chemicals were used to simulate the pollutant. The design of the experiment was conceived so that the following quantities could be evaluated:

- Determination of runoff
- Construction of curves for pollutant concentration
- Investigation of the behavior of pollutant transport in overland flow

5.4.2 Experimental setup

Experiment 1

The first series of experiments were conducted in a laboratory flume of adjustable slope. The bottom of the flume is an impervious plate so that no infiltration can take place. The channel is 0.38 m wide with a total length of 11 m. The plate was lined with plywood, with sand grains glued in place to form a uniformly rough surface. Rainfall was supplied with tap water through a rotameter so that the total discharge may be measured and maintained constant. Uniform rainfall was simulated using a row of 27 atomizer nozzles over the usable flume length of 8.35 m. A 30 min to 60 min rainfall of 126 mm/hr mean intensity was applied to the flume, with intensity varying slightly between treatments. Runoff was collected at the downstream end of the channel and measured volumetrically. The flow rate was calculated by dividing the collected runoff volume by the elapsed time. When the initial runoff reached the edge of the flume at the downstream end, the time clock for the measurements was started. The simulated pollutant was common table salt (NaCl). In order to examine the effects of different surface roughness, two different grain sizes were used for the experiments. The effective sizes of the grains were 0.25 mm and 0.65 mm corresponding to fine and coarse sands, respectively. The maximum thickness of the layer for each case was 10 mm. In addition, a third value of surface roughness was simulated by replacing the sand grain surface with a polypropylene grass carpet. The roughness used in these experiments

corresponded to values of the well-known Manning coefficient of: 0.012, 0.025 and 0.05, respectively. Figure 5.5 shows a sketch of experiment 1.

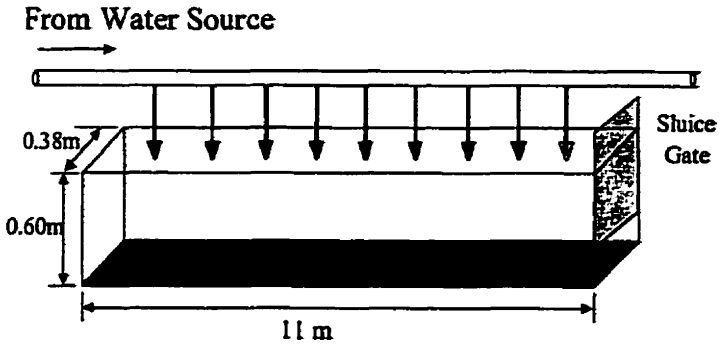

Figure 5.5 Schematic of experimental flume

The first series of experiments were comprised of five tests. In the first test, the smaller sand grains were used. Powdered salt with a total mass of 525g was spread uniformly over the flume. The slope of the flume was adjusted to 0.005. Rainfall was initiated and the experiment conducted in accordance with the methodology described earlier. The saline concentration in the runoff was measured by collecting 15 ml samples using syringes at stations situated 1.65, 3.3, 4.95, 6.6 and 8.35 m from the upstream end of the channel. For the second test, the large sand grains were used with other parameters being kept the same as in the first test. In the third test, the bottom roughness was simulated with the polypropylene grass carpet. The initial pollutant distribution, rainfall intensity and channel slope were similar to those used in the first test. A slightly different procedure for pollutant application was followed in the fourth test. The grass carpet was again used as the bed surface, however 525g of solid salt was first dissolved

in water to form a solution, which was then uniformly sprayed over the bed and allowed to dry. All other conditions were the same as in test 3. In the fifth test, the grass carpet was used again, this time with 525g of solid salt being applied at a single station 3.3 m from the upstream end. The slope of the flume was 0.01. Measuring stations for this experiment were located at 3.335, 4.59, 5.995, 7.246, and 8.35m from the upstream end. A comprehensive summary of the test conditions for experiment 1 is given in Table 5.4.

Experiment 2

The second series of experiments were conducted in a small hydrology simulation tank Model S12 manufactured by Armfield Technical Education Co. The land surface is represented by a shallow tank, which is made of stove enameled mild steel and is mounted on a free standing frame. Uniform rainfall may be simulated using 2 rows of 8 spray nozzles above the tank and the run-off is led to a measuring system at one end of the equipment. The rain water supply to the equipment is provided by tap water. The bottom surface of the tank may be covered with any type of soil to simulate infiltration. In this experiment the polypropylene grass carpet was used to simulate an impermeable surface. The run-off leaves the tank by an outflow weir at the sump end of the equipment. A metal gauze covers this outlet thus preventing the soil being washed from the tank. Provision is made to enable the slope of the tank to be adjusted within limits by the use of leveling screws fitted under the equipment frame. The salient parameters of the equipment are shown in Table 5.5.

The rainfall intensity is determined from an inline rotameter. The runoff discharge is measured with a weir at the outflow. It is also possible to collect water at the outlet and measure average discharge volumetrically.

The bottom surface of the tank was divided into 200 meshes, 20 in the x direction and 10 in the y direction. Each mesh measures 0.1 by 0.1 meters. The pollutant was carefully applied to the mesh (6,3), the measurement stations were chosen at mesh (13,3) (position A), (18,8) (position B) and at the outlet. Figure 5.6 is a plan view of the experimental setup.

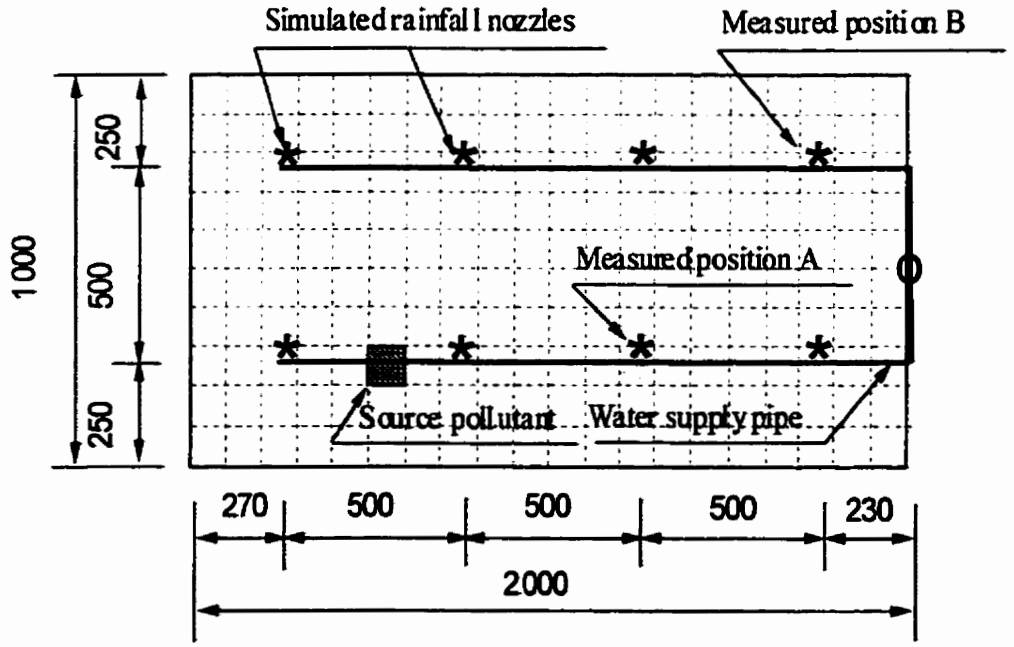

Figure 5.6 Sketch of experiment two (units: mm)

Table (5.4) Summary of Conditions for Experiment 1

No.	Surface (bottom) roughness	Pollutant Distribution	Location of Sampling	Experimental Parameters
1	Plywood with Small sand grains	Solid salt Uniformly applied	1.65m, 3.3m, 4.95m, 6.6m, 8.35m from the upstream end	Flume slope = 0.005,
2	Plywood with Large sand grains	Same as above	Same as above	Same as above
3	Grass carpet	Same as above	Same as above	Same as above
4	Grass carpet	Salt Solution Uniformly sprayed	Same as above	Same as above
5	Grass carpet	Solid salt Applied at one spot	3.335m, 4.59m, 5.995m, 7.245m, 8.35m from the upstream end	Flume slope = 0.01

Five tests were conducted as part of the second series of experiments. The grass carpet was installed in the basin to simulate a surface roughness corresponding to a Manning coefficient of 0.05. Three types of chemicals were used to simulate pollutants; Potassium Chloride (KCl), Glycerol-Phosphate and Calcium Chloride ($CaCl_2$). Concentration was measured by collecting 25ml samples using syringes. Measurements at position A commenced 30 seconds after rainfall initiation and 60 seconds at the outlet and position B. Generally speaking, it took about 3-seconds to complete taking samples between position B and the outlet. Thereafter, the time interval for taking samples was 30s for each station. The rainfall intensity used in the experiments is controlled by the water tap, which is based on the operating flow rotameter. The value of rainfall intensity ensured that the concentration of sample in the runoff water could be sucked by syringes. The measured room temperature in the experiments is around 24^{o}C, and the measured water temperature is around 22^{o}C.

Table (5.5) Parameters of Hydrology Equipment

Equipment	Dimensions
Height of working surface	1.5m
Width of working section	1m
Length of working section	2m
Maximum depth of water or soil	0.18m
Rotameter	0 ~ 18 IGPM

In the first test, 20g of solid Potassium Chloride (KCl) with solubility 347kg/m^3 was applied at the "source point", 0.525m from the upstream end of the tank and 0.25m from the left side of the tank, i.e., at mesh (6,3). Rainfall intensity was 0.0000925m/s with a duration of 1140s. In the second test, 22.5g of solid Potassium Chloride was applied at the pollutant source. The rainfall intensity was 0.0000875m/s with a duration of 1140s. In the third test, 14g of powdered Glycerol-Phosphate with solubility 100kg/m^3 was applied at the pollutant source. Rainfall intensity was 0.0000875m/s with a duration of 1320s. In the fourth test, 8g powdered Glycerol-Phosphate was applied at the pollutant source. Rainfall intensity was 0.0000925m/s with a duration of 1320s. In the fifth test, 20g solid Calcium Chloride $CaCl_2$ with a solubility of 735kg/m^3 was applied at the pollutant source. Rainfall intensity was 0.0000925m/s with a duration 1500s. The unit of rainfall intensity (m/s) is used in order to unify the system of unit through the dissertation. Details are summarized in Table 5.6. All samples were analyzed using an electric conductivity meter and converted to concentration based on an experimentally known relationship between conductivity and concentration.

5.4.3 The relationship determined experimentally between conductivity and concentration

The measured pollutant concentration was determined using a calibrated conductivity meter (Fisher Model 152). The Model 152 conductivity meter is a portable battery

operated instrument for measuring the electrical conductivity of aqueous solutions over the 0 to 100,000 microsiemens/cm range. The probe supplied is specially designed to cover this entire operating range and function within a temperature range of 0°C to 40°C due to a built in temperature compensation circuit. It can measure and record solution temperature at the time the conductivity measurement is taken and will automatically correct the measured conductivity of a solution and indicate what that conductivity would be if the test solution was at the reference temperature of 25°C, regardless of its actual temperature. Before making sample measurements, the instrument/probe combination is calibrated using a standard solution of known value. The most accurate results will be obtained using a standard solution having a conductivity value close to that of the solutions to be tested. In our case, the samples taken from the experiment is first measured. Then based on this known (approximate) conductivity, a standard solution is provided. Using known concentration values of KCl, $CaCl_2$ and β-Glycerol-Phosphate, a standard relationship between electrical conductivity and concentration is established. Figures 5.7 to 5.9 indicate the relationships between concentration and conductivity for β-Glycerol-Phosphate, KCl and $CaCl_2$, respectively.

Table (5.6) Parameters for Experiment 2

No	Surface roughness	Pollutant used for simulation	Solubility g/100g	Rainfall intensity m/s	Duration (s)	Amount of pollutant (g)
1	Grass carpet	KCl	34.7	0.0000925	1140	20
2	Grass carpet	KCl	34.7	0.0000875	1140	22.5
3	Grass carpet	Glycerol-phosphate	10	0.0000875	1320	14
4	Grass carpet	Glycerol-phosphate	10	0.0000925	1320	8
5	Grass carpet	$CaCl_2$	73.5	0.0000925	1500	20

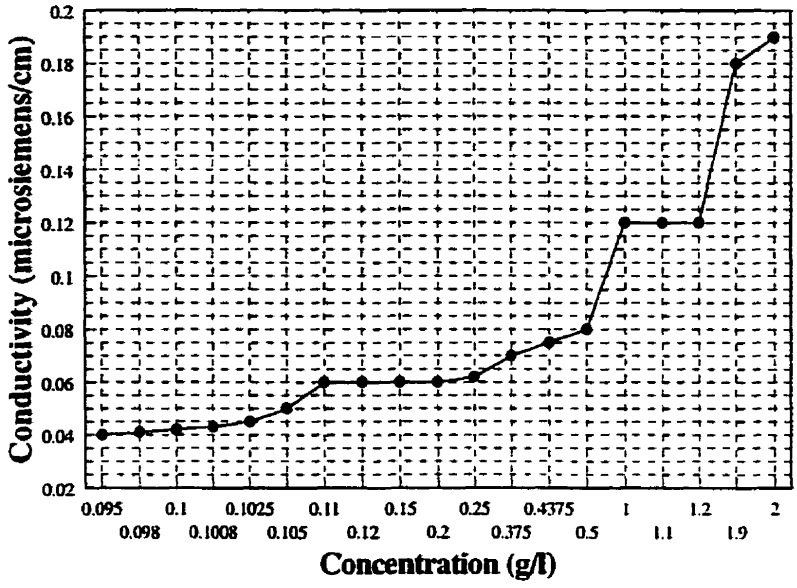

Figure 5.7 Calibration standard line of conductivity-concentration for Glycerol-phosphate

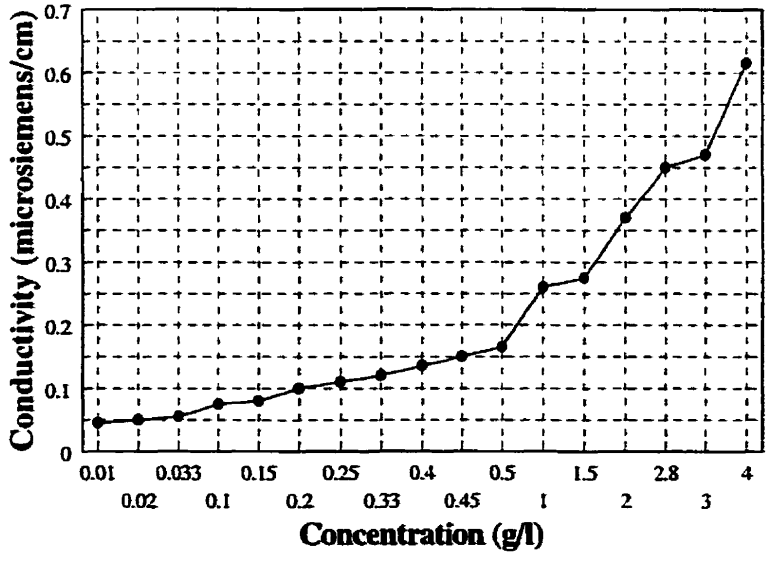

Figure 5.8 Calibration standard line of conductivity-concentration for $CaCl_2$

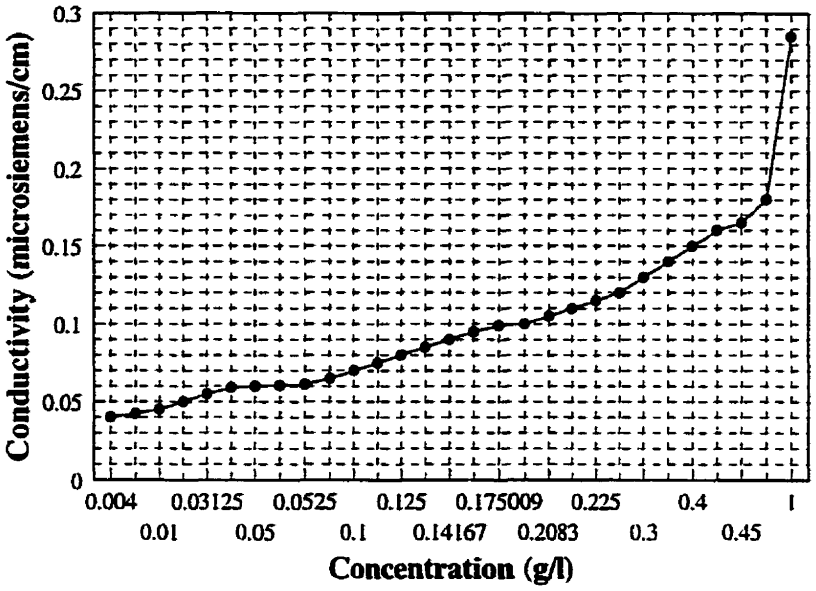

Figure 5.9 Calibration standard line of conductivity-concentration for KCl

5.4.4 Evaluation of numerical model performance

Comparison of numerical results with experimental data for the first set of experiments I are presented from Figures 5.10 to 5.14. Recall that this series of tests were conducted exclusively with Sodium Chloride. The concentration is plotted against distance. Displayed distances and concentrations are dimensionless. The x-axis represents distance divided by the total length of the flume, while the y-axis is the concentration obtained at the fixed measurement locations divided by the maximum measured concentration. Each line illustrates the concentration distribution along the channel corresponding to different times. The results of the longitudinal distribution of saline concentration for test I in experiment I are given in Figure 5.10. The solid line

represents the numerical results at time 360s, circles represent experimental results at time 360s. Figure 5.11 is the saline concentration along the flume for test 2 of experiment 1 as a function of distance. Figure 5.12 gives the saline concentration along the flume for test 3 of experiment 1 as a function of distance. Figure 5.13 presents the results of saline concentration along the flume for test 4 of experiment 1. These figures illustrate the comparison between the numerical and experimental results under the conditions of different surface roughness and initial pollutant distribution. The tendency of the numerical and experimental results is essentially qualitatively consistent. However, quantitative discrepancies exist between the numerical and experimental results. Some of the reasons for the discrepancies may be attributed to measurement bias. A more significant reason may be due to the electric conductivity meter. It was discovered that the batteries installed were defective. After changing the batteries in the unit the final test was conducted. The results from this test are summarized in Figure 5.14. Clearly, the experimental results are better approximated by the numerical model.

Comparisons of numerical results with experimental data for the second set of experiment 2 are presented in Figures 5.15 to 5.19. Again, the dimensionless concentration is plotted against time. The x-axis represents time and the y-axis is the concentration obtained at different times divided by the maximum measured concentration. Figure 5.15 is a comparison between measured concentration with numerical results for Potassium Chloride KCl in test 1 of experiment 2. The rainfall is

supplied at an intensity of 0.0000925m/s and 20g KCl is applied. The measurement station is located at position A and at the outlet.

Figure 5.16 shows the simulated and measured concentration profiles of KCl with respect to time in test 2 of experiment 2 at position outlet, A and B, respectively. The rainfall is supplied at an intensity 0.0000875m/s and 22.5g KCl is applied. These figures demonstrate that both simulated and measured values exhibit a similar concentration distribution pattern.

For β-Glycerol-Phosphate, the same trend is observed at position A and at the outlet shown in Figures 5.17 and 5.18. The rainfall intensity in Figure 5.17 is 0.0000875m/s, 14g powdered β-Glycerol-Phosphate is applied, and the rainfall intensity in Figure 5.18 is 0.0000925m/s, 8g powdered β-Glycerol-Phosphate is applied.

Figure 5.19 shows the comparison between measured concentration with numerical results for $CaCl_2$ in test 5 of experiment 2. The rainfall is supplied at an intensity 0.0000925m/s and 20g $CaCl_2$ is applied.

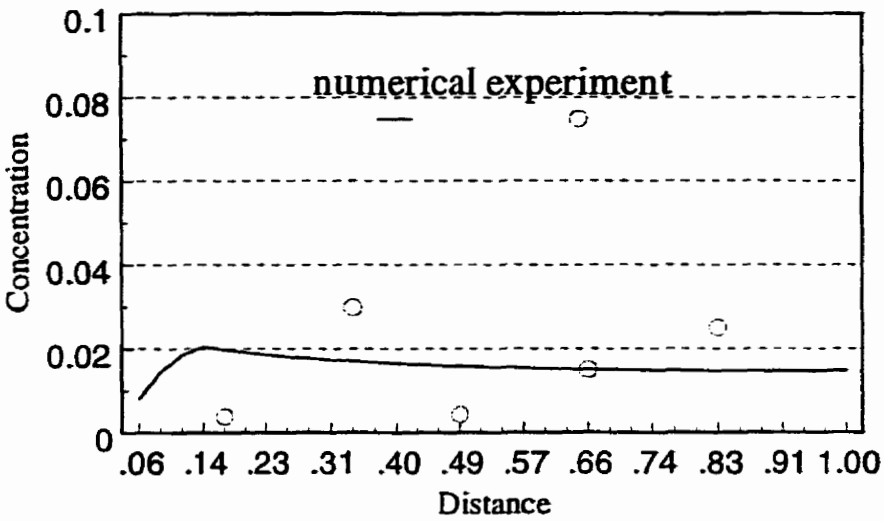

Figure 5.10 Longitudinal distribution of saline concentration t = 360s

(test 1 for experiment 1)

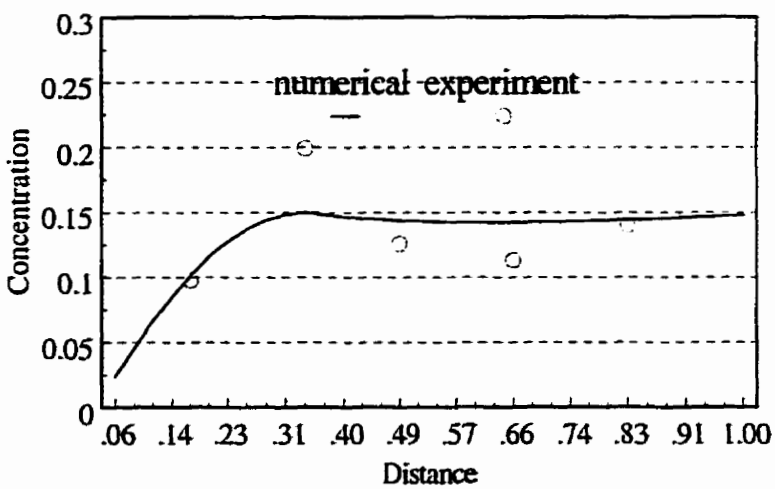

Figure 5.11 Saline concentration along flume t = 360s (test 2 for experiment 1)

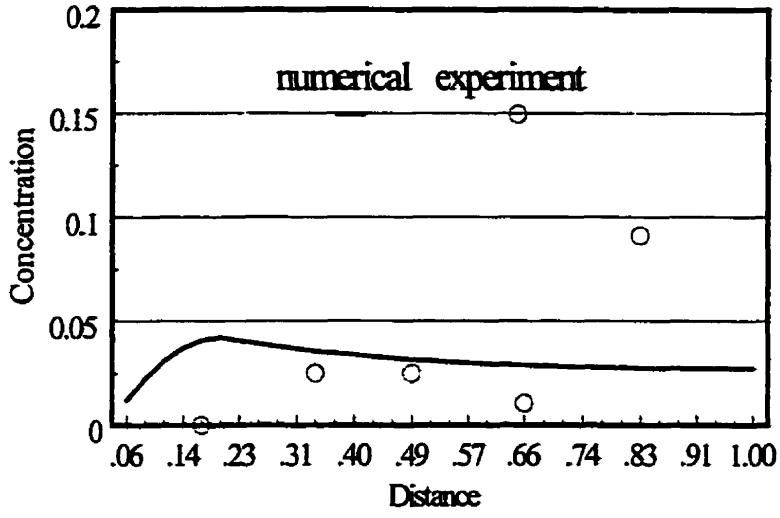

Figure 5.12 Saline concentration along flume t = 660s (test 3 for experiment 1)

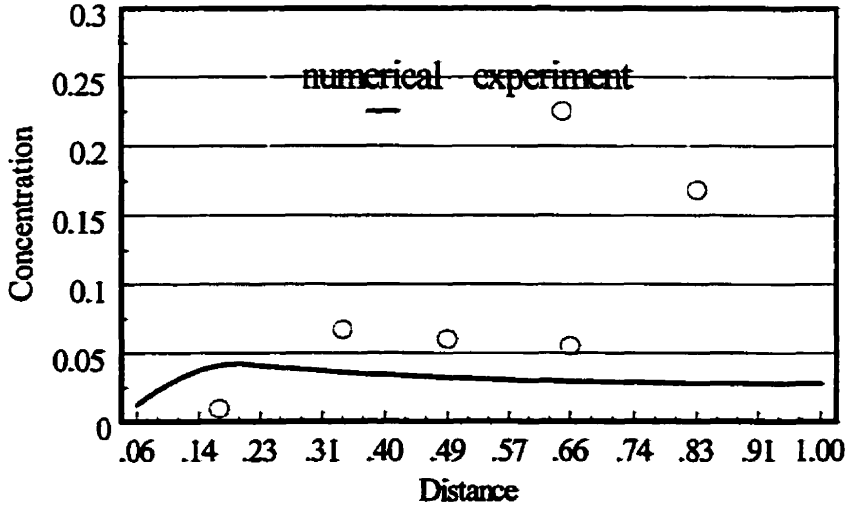

Figure 5.13 Saline concentration along flume t = 420s (test 4 for experiment 1)

Generally, the numerical simulation displays satisfactory agreement with the experimental data. Not surprisingly, given the true complexity of the process, there is some degree of deviation between simulated and measured concentration. Some of the discrepancies may also be attributed to errors associated with the difficulties encountered during the experimental procedure.

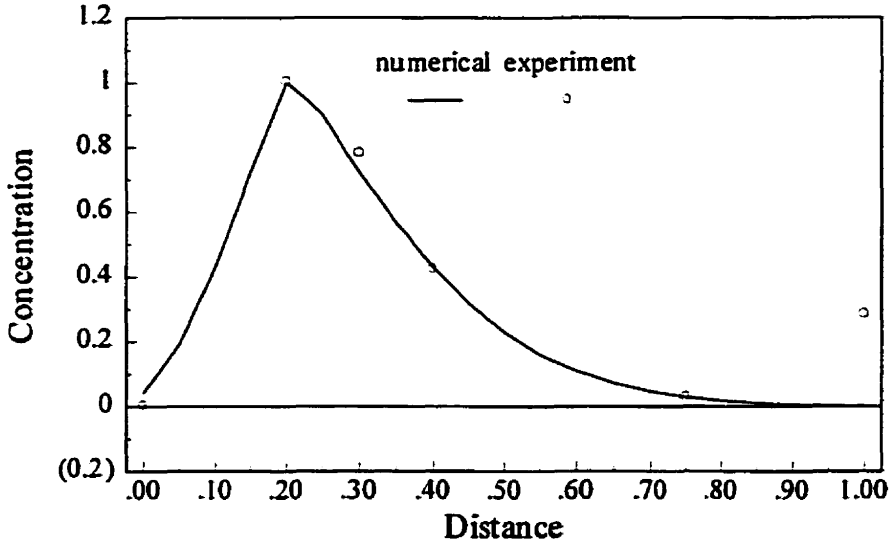

Figure 5.14 Saline concentration along flume t = 240s (test 5 for experiment 1)

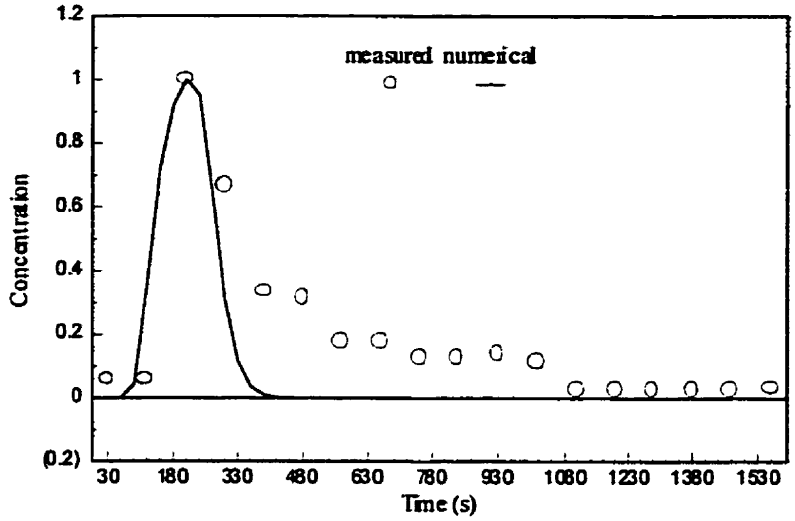

Outlet

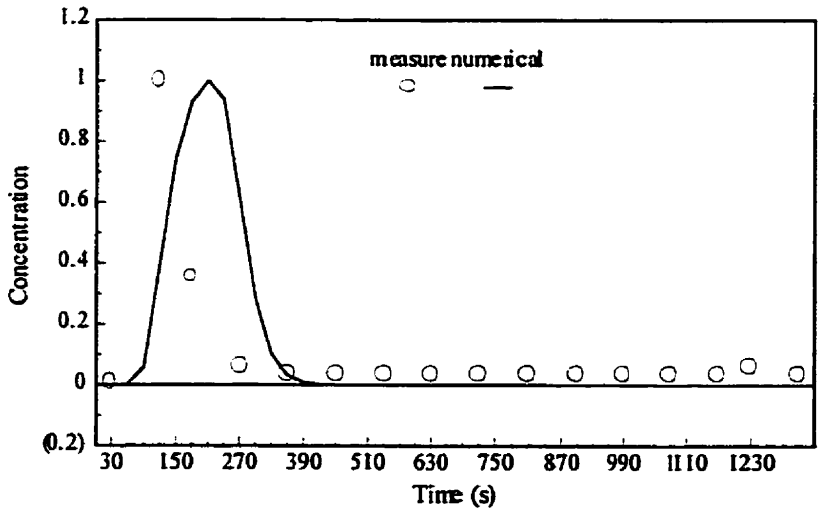

Position A

Figure 5.15 Comparison between measured concentration with numerical results for KCl test(1) for experiment 2

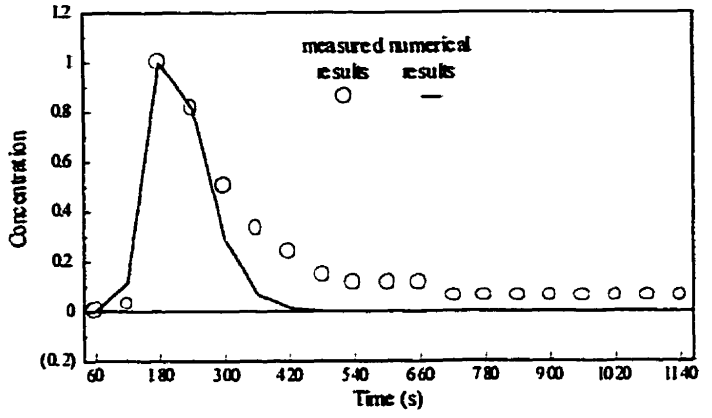

Outlet

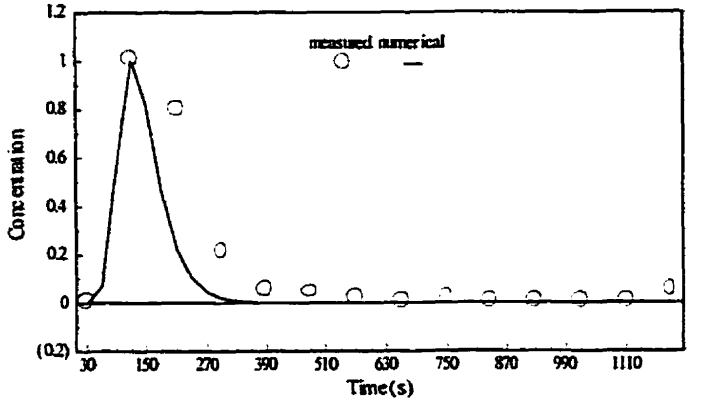

Position A

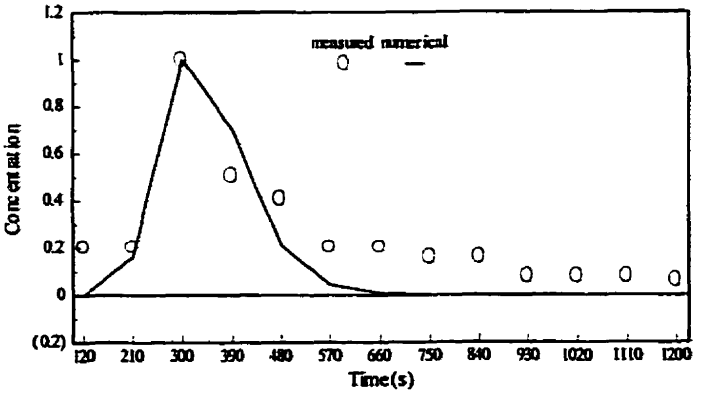

Position B

Figure 5.16 Comparison between measured concentration with numerical results for KCl test(2) for experiment 2

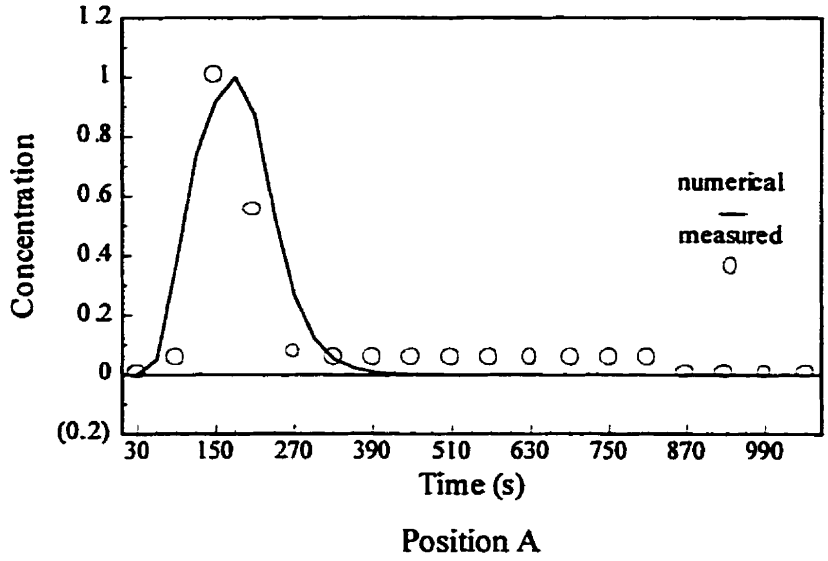

Position A

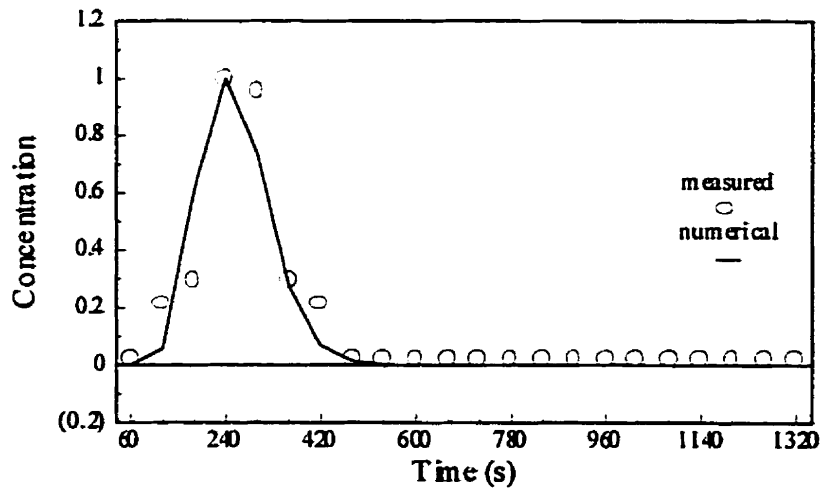

Outlet

Figure 5.17 Comparison between measured concentration with numerical results for Glycerol-phosphate test (3) for experiment 2

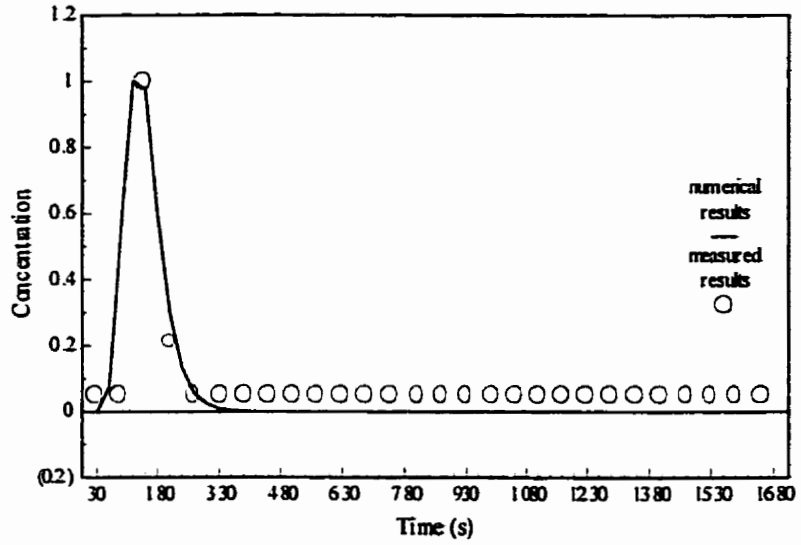

Position A

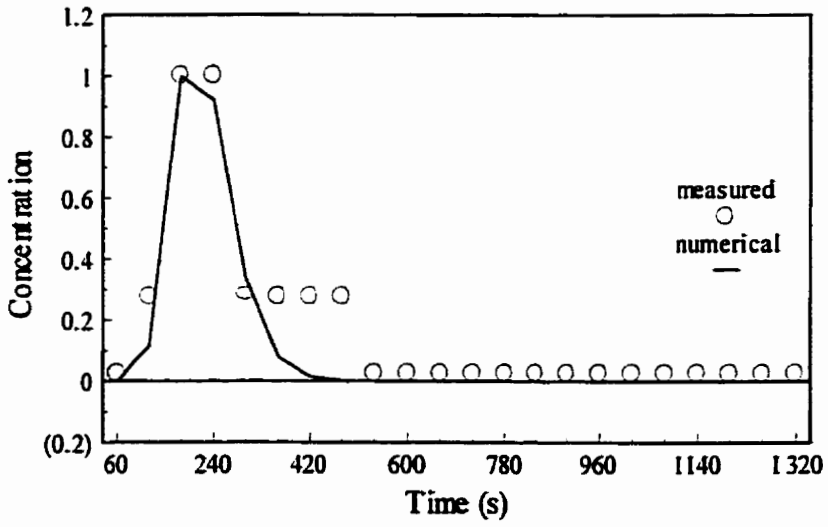

Outlet

Figure 5.18 Comparison between measured concentration with numerical results for Glycerol-phosphate test (4) for experiment 2

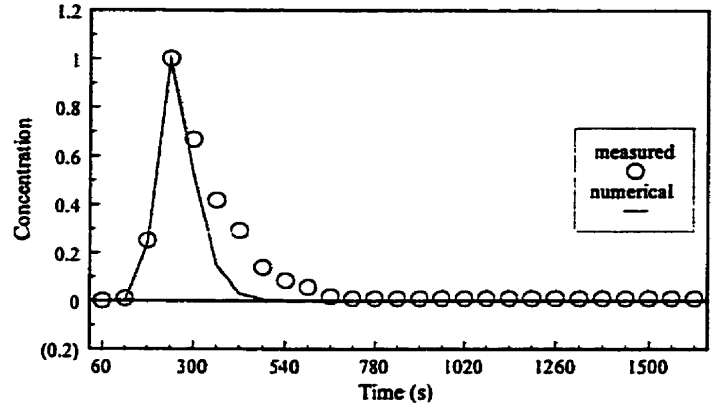

Outlet

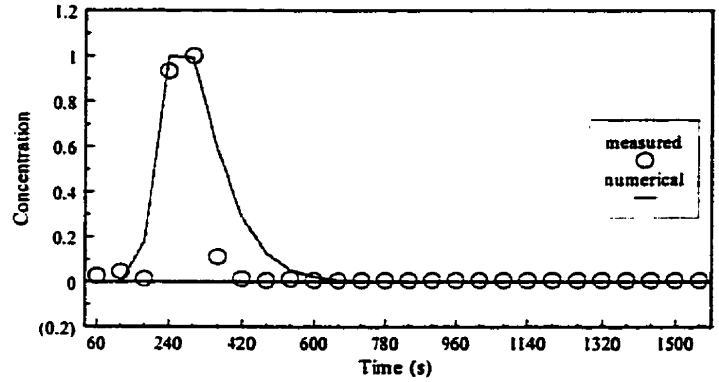

Position A

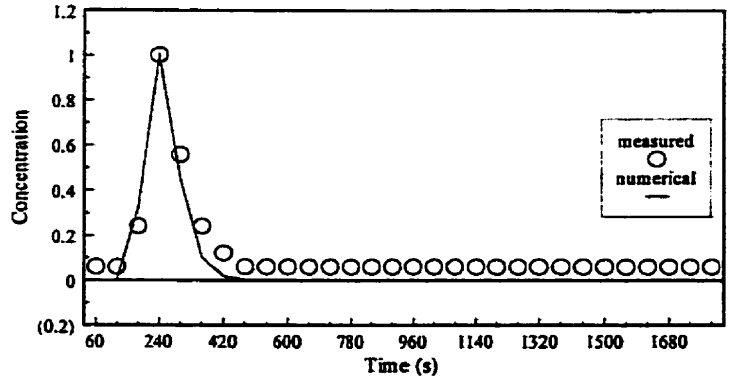

Position B

Figure 5.19 Comparison between measured concentration with numerical results for $CaCl_2$ (k2 = 0.0001) test (5) for experiment 2

CHAPTER 6: RESULTS AND SENSITIVITY ANALYSIS

6.1 Generalities

In this study, a two dimensional mathematical model for pollutant washoff has been developed and numerical solutions obtained. The governing differential equations for the hydrodynamic model consists of the two horizontal-momentum equations and the continuity equation, these equations being based on the depth-integrated Navier-Stokes equations. The hydraulic effects of bottom friction, shear stress and turbulence, as well as infiltration, dissolution and adsorption have been included. The bed shear stress and the friction factor are represented by the empirical equation of Manning, while a turbulent kinematic eddy viscosity and surface mass transfer coefficient have been included. The dissolution process is described by the solubility rate equation, which depends on the solubility of the pollutant and bed shear stress. The infiltration factor is evaluated by using both Horton's and Green-Ampt equations. The transport and migration of pollutant are estimated by using the advection-diffusion equation with the adsorption factor being evaluated by using three adsorption rate models. The solution of the transport advection-diffusion equation proceeds independently of the equation for the overland flow.

At a given time step, after obtaining the distribution of hydraulic variables from the equations of overland flow with infiltration and the results from solubility rate and adsorption equations which are solved individually, the pollutant transport equation is solved to predict the spatial and temporal distribution of pollutant. The solution procedure is indicated in Figure 6.1.

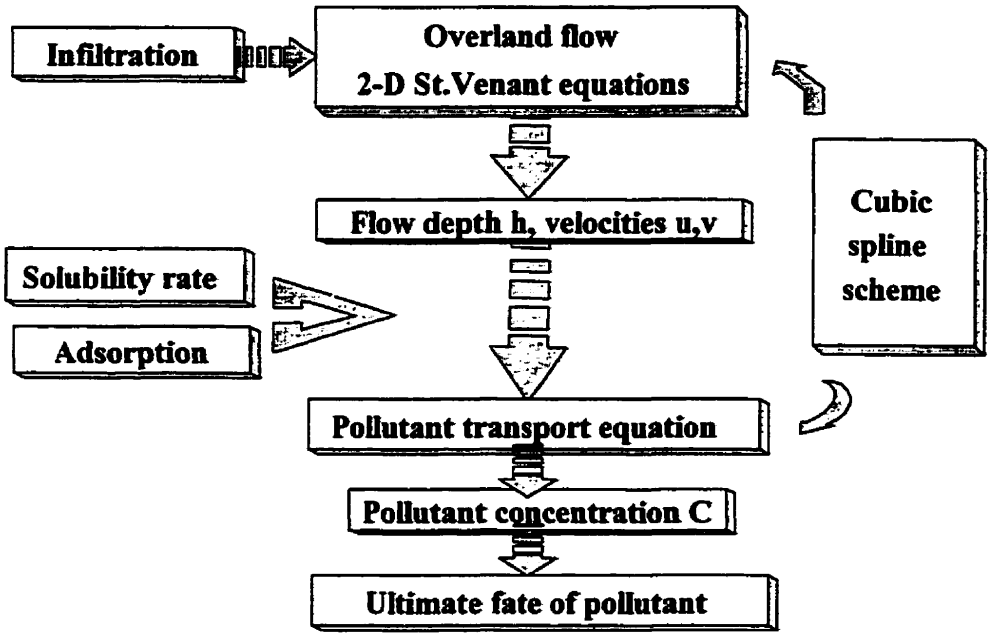

Figure 6.1 Sketch of solution procedure

An alternating cubic spline integration scheme, based on the technique of Wang and Kahawita (1983a), has been used for solving the set of equations consisting of the shallow water wave equations and the pollutant transport equation. As indicated earlier, the scheme employs a piecewise cubic spline representation, with a set of finite

difference equations located at each spline. The method allows both nonuniform or uniform grids to be employed. Explicit or implicit formulations are possible, with the latter being incorporated into a SADI (Spline Alternating Direction Implicit) procedure. For a mathematical model to find useful application, it is essential that some numerical experimentation, to determine the sensitivity of the results to various input parameters, be realized. In this study, the behavior of pollutant washoff with the combined effects of adsorption and infiltration has been investigated. Two different cases of initial pollutant mass distribution were simulated: solid pollutant applied at a single discrete location, and uniformly applied solid pollutant. Finally, several tests were made to illustrate application of the model.

6.2. Sensitivity Analysis of Model Parameter

For the sensitivity analysis, the pollutant solubility, the reaction rate constant and finally the dispersion coefficient were chosen as the salient parameters for the sensitivity analysis.

Pollutant dissolution is not only affected by physical effects but also affected by chemical effects, such as, solubility and reaction rate constant. The solubility of a solid reflects the extent to which the solid is favored in a dissolution process. The solubility depends on the properties of the pollutant and on the temperature. The results obtained

in this study involve the assumption that temperature is kept constant during the process of dissolution and no new substance is created. This assumption is based on the experimental measurement. During the process of experiment, the measured room temperature is close to the measured water temperature. In order to determine the sensitivity of the model with respect to the solubility, several simulations were carried out.

Reaction rate constant is the reciprocal of turbulent Schmidt number, it is presumed to depend only on the solubility characteristics of the pollutant. Since no work has been experimentally done to estimate its value, the sensitivity analysis is necessary to indicate how the reaction rate constant influence the shape and magnitude of the pollutant concentration distribution.

For a system with fluid motion, mass transport is generally entailed by advection and diffusion. This combined flux may be described mathematically by combining the advection flux and the diffusion flux. However, diffusion alone does not fully account for mixing during mass transport. Mechanical dispersion in many systems is usually more important. Logically, if dispersion is to be incorporated in to the advection-diffusion equation, it should be reflected in the velocity term. Unfortunately, it has not been possible to do this in a simple way. Instead the coefficient of hydrodynamic

dispersion is introduced to incorporate the combined effect of diffusion and mechanical dispersion (Domenico and Schwartz, 1990).

The coefficient of hydrodynamic dispersion is the sum of the coefficient of bulk diffusion and mechanical dispersion. However, questions remain as to what is a realistic range of values for the coefficient of dispersion. A large amount of research in developing relations for the dispersion coefficient has been realized in rivers and estuaries. Most of this work indicates that it is highly variable and cannot be accurately modeled outside a laboratory situation. In addition, a variety of laboratory column experiments have been done in groundwater systems by previous researchers. The main emphasis of their effort has been to estimate dispersivity values from field experiments. They indicate that many dispersion studies have suffered from errors related to the collection and interpretation of field data. Thus many of the published estimates of dispersivity should not be considered transferable to other sites. They also indicate that in current practice, the majority view still involves assuming that dispersivity values are constant (Domenico and Schwartz, 1990). In overland flow, no work has been done to estimate dispersion coefficients. Consequently, the numerical tests reported here have been limited to some assumed constant values for the dispersion coefficient. The dispersion coefficient is an important parameter that influences the spatial spread of the pollutant cloud. Consequently, overestimates or underestimates of its value will create variability in the concentration distribution which ultimate affects the amount of

pollutant that will infiltrate into the subsurface and the amount that is transported by the groundwater. Therefore, it is necessary to analyze the sensitivity of the estimated dispersion coefficient to indicate the variation in the results that may be obtained.

6.2.1 Solubility

Solubility is the maximum amount of a solute that may be dissolved in a solvent so that a saturated solution is obtained. The symbol C* in this study indicates solubility which is given in grams of the substance in 100g of the solvent at a particular temperature. In order to illustrate the important effect of solubility, different values of solubility were used, corresponding approximately to Potassium chloride (KCl), Calcium chloride ($CaCl_2$), β-Glycero-phosphate, Barium Oxide (BaO) and 1:1:1,Trichloroethane (TCA). Table 6.1 lists the solubility of the various compounds. Figures 6.2 and 6.3 demonstrate the two-dimensional spatial distribution of concentration for BaO and TCA at times 500s and 2500s. As expected, peak concentrations are obviously affected by solubility, however the "spread" of the pollutant "cloud" referred to the peak concentration is relatively unaffected since the determining factor for this would be the horizontal dispersivity. Figure 6.2 (a) shows the pollutant concentration distribution using BaO, and (b) illustrates that using TCA at time 500s. Figure 6.3 (a) (b) demonstrates the effect using BaO and TCA at time 2500s. Figure 6.4 was plotted using different solubilities and two fixed values for reaction rate constant and dispersion coefficient. It is evident

that the peak concentration of pollutant with the larger solubility is higher than that with smaller solubility, and with increasing time, the maximum concentration decreases. A summary of the results is shown in Table 6.1.

Table (6.1) Summary of Solubility Test Results

Name of Pollutant	Solubility (kg/m^3)	Maximum Concentration (kg/m^3) at t = 500s
BaO (Barium Oxide)	34.8	0.00281
TCA(1:1:1 Trichloroethane)	1.25	0.000101.
$C_3H_7O_6PNa_2$	660	0.0598
(β - Glycerophosphate)		
$CaCl_2$ (Calcium Chloride)	745	0.0675
KCl (Potassium Chloride)	375	0.0323

For the numerical experiment, the test domain consisted of an area of 100m by 100m, comprised of 20 by 20 grid cells providing an equal spacing of 5m. The time step used was $\Delta t = 1s$. A bed slope of 0.008 in both the x- and y-directions, a constant Manning roughness coefficient of 0.04 and a constant rainfall intensity 0.000038m/s for a duration of 1000s was specified. The diffusion coefficient and the reaction rate constant assumed were $0.5m^2/s$ and 0.00001 respectively. The results were obtained using the cubic spline implicit scheme.

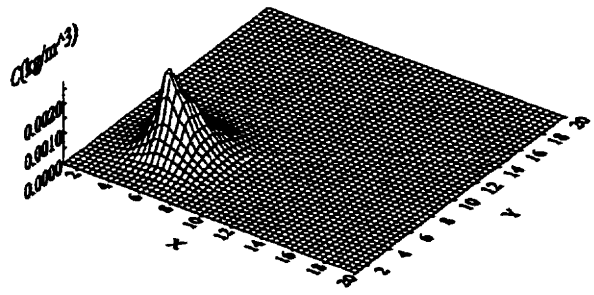

(a) Solubility of BaO = 34.8 kg/m^3

Maximum concentration C = 0.00281kg/m^3

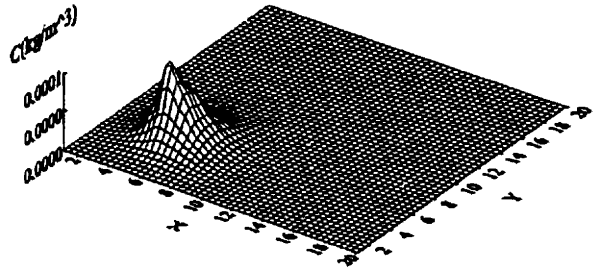

(b) Solubility of TCA = 1.25 kg/m^3

Maximum concentration C = 0.000101kg/m^3

Figure 6.2 Influence of solubility on concentration distribution,

Time = 500s, dc = 0.5, k = 0.00001

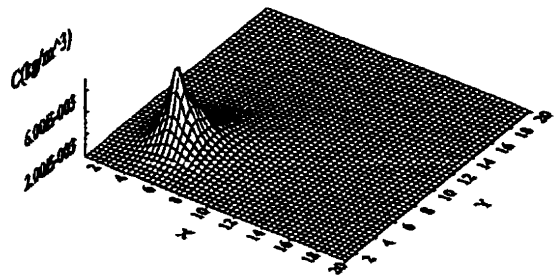

(a) Solubility of BaO = 34.8 kg/m^3

Maximum concentration C = 0.00723kg/m^3

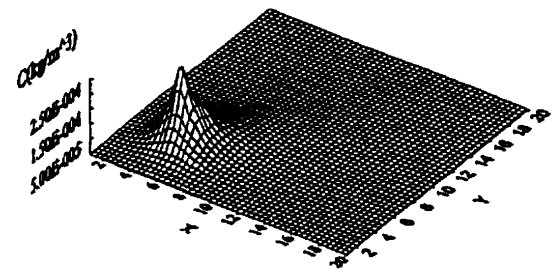

(b) Solubility of TCA = 1.25 kg/m^3

Maximum concentration C = 0.000260kg/m^3

Figure 6.3 Influence of solubility on concentration distribution,

Time = 2500s, dc = 0.5, k = 0.00001

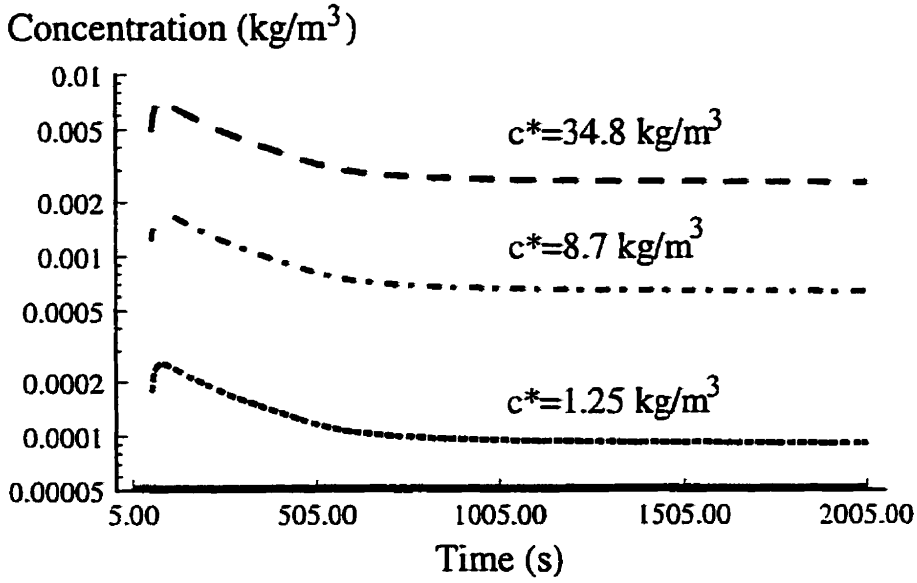

Figure 6.4 Plots of maximum concentration vs.time for the different compounds

6.2.2 Reaction rate constant

The model was run to test the sensitivity of the reaction rate constant for the Barium Oxide, whose solubility is 34.8 kg/m^3, while the diffusion coefficient was kept constant at 0.5 m^2/s. The same computational domain as in the previous test was used. Figure 6.5 (a) and (b) illustrates the sensitivity of the reaction rate constant, (values of 0.001 and 0.00001 were used) at time 500s, respectively, while Figure 6.6 (a) and (b) illustrates this sensitivity at time 2500s. The results indicate that the larger the reaction rate constant, the faster the dissolution of the (surface applied) solid pollutant and the higher the peak concentration in the runoff. Table 6.2 summarizes the tests involving the reaction rate constant.

In addition, numerical tests for the reaction rate constant were made using Glycerophosphate with solubility $100kg/m^3$. Figure 6.7 is the normalized maximum concentration plotted versus time. The four curves in this figure were obtained using reaction rate constants of 0.0005, 0.0001, 0.00005 and 0.00001. The effect of the reaction rate constant on the dissolution process is quite marked. This is because the reaction rate constant has a significant influence on the delay time of the dissolution process. These curves were also used to compare with the experimentally measured data which is represented as circles. By comparing the simulation results with experimental data, a best fit value of reaction rate constant may be found, in this case 0.0001.

Table (6.2) Comparison of the Effect of Reaction Rate Constant

Solubility C* BaO	Reaction Rate Constant	Maximum Concentration (kg/m^3) at t = 500s	Maximum Concentration (kg/m^3) at t = 2500s
34.8(kg/m^3)	0.001	0.0718706	0.00286733
34.8(kg/m^3)	0.0001	0.0270738	0.00296562
34.8(kg/m^3)	0.00001	0.00281227	0.00723495

In this numerical simulation, the test domain consisted of an area of 17m by 10m with $\Delta x = \Delta y = 1m$. The time step used was $\Delta t = 1s$. A bed slope of 0.019 and 0 in the x- and y-directions, respectively was imposed. A constant Manning roughness coefficient of 0.05 and a constant rainfall intensity 0.000185m/s for a duration of 1320s was specified. The dispersion coefficient assumed was $0.1 m^2/s$. An examination of the results from the numerical tests clearly indicates the significant influence of the reaction rate constant. The comparison between the numerical simulation and experimental results provide useful information on the simple methodology to be followed for the determination of the reaction rate constant on the basis of experiments.

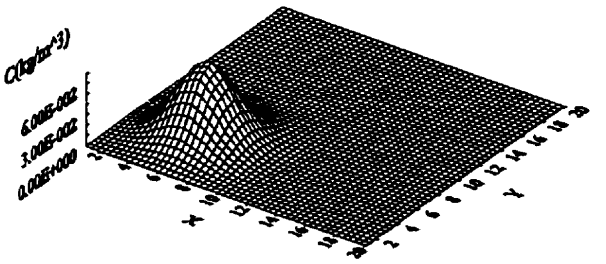

(a) Reaction rate constant k = 0.001,

Maximum concentration C = 0.0719kg/m^3

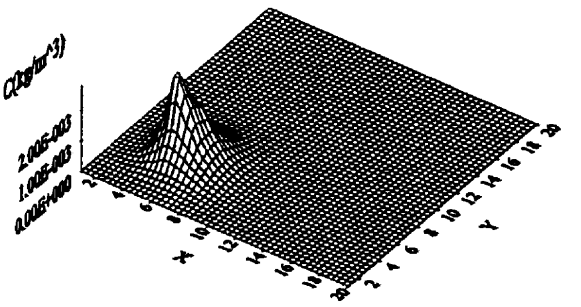

(b) Reaction rate constant k = 0.00001,

Maximum concentration C = 0.00281kg/m^3

Figure 6.5 Sensitivity tests for reaction rate constant, Time = 500s,

C* = 34.8, dc = 0.5

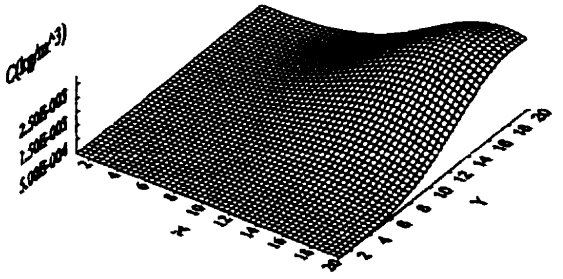

(a) Reaction rate constant k = 0.001,

Maximum concentration C = 0.00287kg/m^3

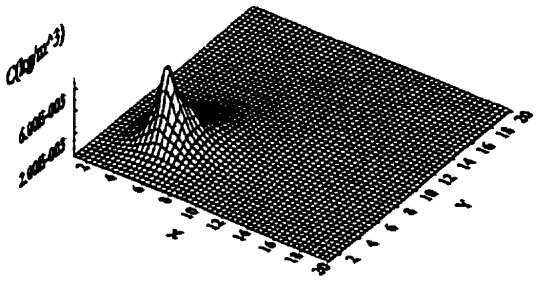

(b) Reaction rate constant k = 0.00001,

Maximum concentration C = 0.00723kg/m^3

Figure 6.6 Sensitivity tests for reaction rate constant, Time = 2500s,

C* = 34.8, dc = 0.5

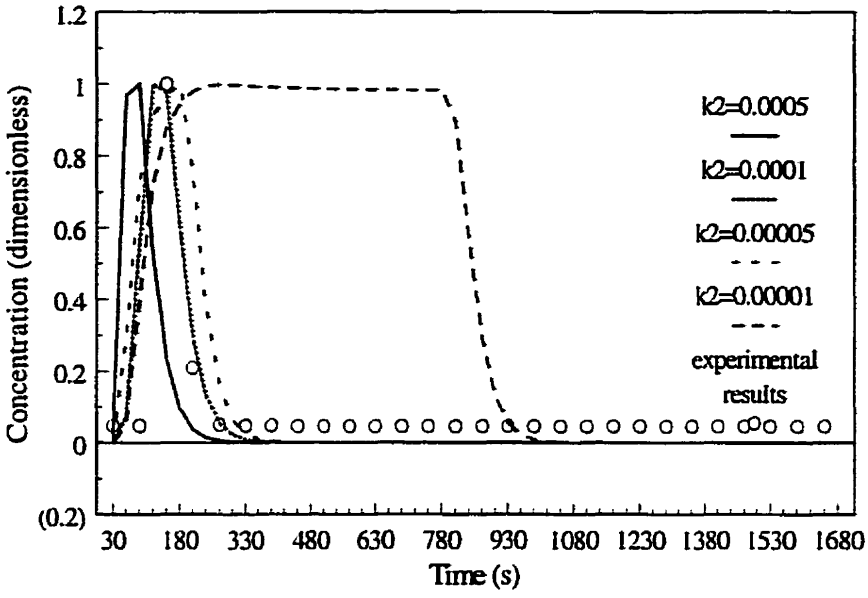

Figure 6.7 Sensitivity of reaction rate constant for Glycerophosphate

6.2.3 Dispersion coefficient

The influence of the diffusion coefficient, evaluated using numerical tests, is illustrated in Figures 6.8 and 6.9. The results obtained generally confirm the expected behavior. In Figure 6.8 (a) and (b), diffusion coefficients of 0.2 m^2/s and 1.0 m^2/s respectively have been used and the results presented at a time of 500 seconds. In Figure 6.9 (a) and (b), the results are presented at time 2500s for the same two values of dispersion coefficients. Not surprisingly, the larger diffusion coefficient results in lowering the peak concentration in the runoff. This is because as the mass moves along with the moving water, it also spreads out. The contaminant mass occupies an increasingly longer length

thereby decreasing in concentration with time. The migration of the peak concentration of the pollutant with a smaller diffusion coefficient is faster than that with the larger diffusion coefficient. Furthermore, since the plume is further spread out, a quantity of pollutant infiltrated into the soil will be affected thus changing the way in which the pollutant is redistributed between groundwater and surface water. Figure 6.10 is a simple representation of relationships between maximum pollutant concentration and time with different diffusion coefficient values: dc = 0.1, 0.3, 0.5, 0.7 and 1.0, respectively. From the figure, it is clear that small changes of dispersion coefficient could result in significant variability in the spreading of the pollutant. The results described were obtained using the implicit cubic spline scheme. For purposes of comparison, the same computations were repeated using the explicit formulation of the scheme. The results were virtually indistinguishable from those obtained using the implicit scheme. The principal hydraulic conditions used in the simulation were the same as those used in the solubility test. The results of the diffusion coefficient tests are summarized in Table 6.3

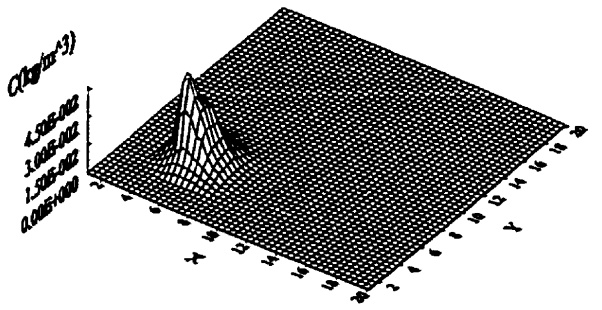

(a) Diffusion coefficient dc = 0.2

Maximum concentration C(max) = 0.0477 kg/m^3

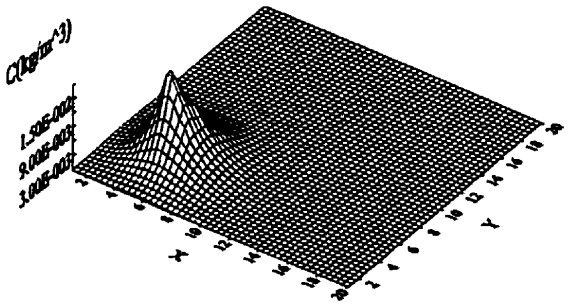

(b) Diffusion coefficient dc = 1.0

Maximum concentration C(max) = 0.0184 kg/m^3

Figure 6.8 Comparison of the effect of diffusion coefficient,

Time = 500s, C* = 357.5

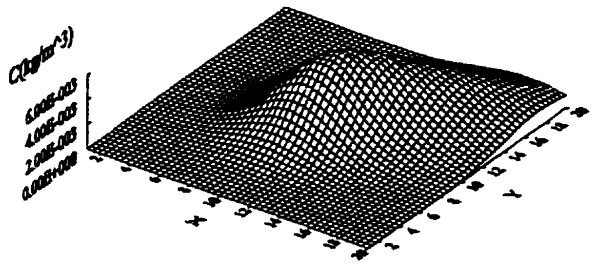

(a) Diffusion coefficient dc = 0.2

Maximum concentration C(max) = 0.00605 kg/m^3

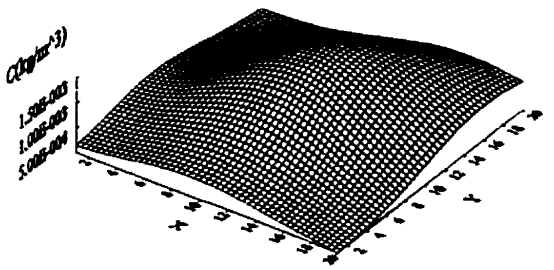

(b) Diffusion coefficient dc = 1.0

Maximum concentration C(max) = 0.00153 kg/m^3

Figure 6.9 Comparison of the effect of diffusion coefficient,

Time = 2500s, C* = 357.5

Table (6.3) Summary of the Dispersion Coefficient Tests

Time S	Diffusion Coefficient m^2/s	Maximum Concentration kg/m^3
500	0.2	0.0476
500	1.0	0.01827
2500	0.2	0.0061
2500	1.0	0.00153

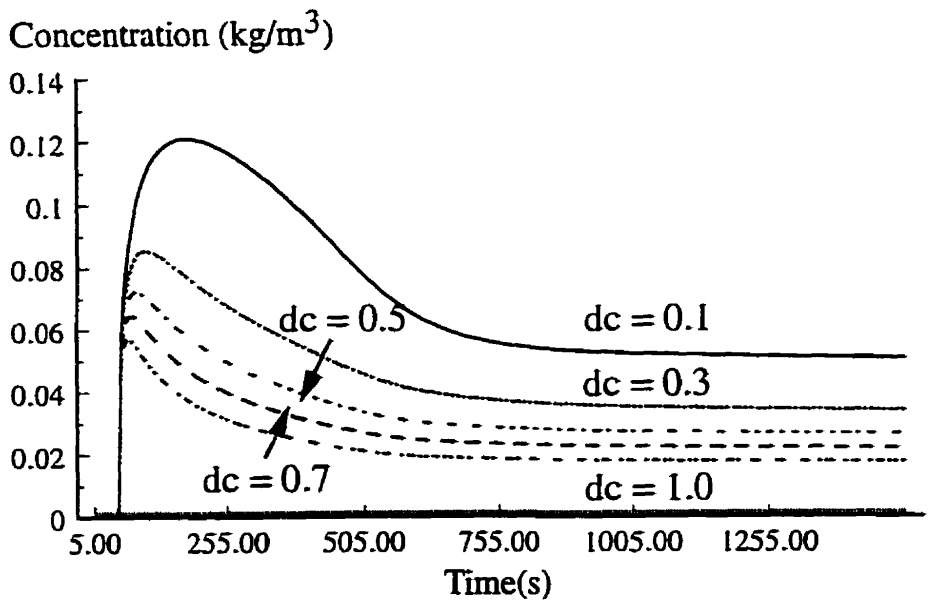

Figure 6.10 The effect of diffusion coefficient for the pollutant, with $c^* = 357.5$ and $k = 0.00001$

6.3 Results

6.3.1 Infiltration

Infiltration is that process by which precipitation moves downward through the surface of the earth and replenishes soil moisture, recharges aquifers, and ultimately supports streamflows during dry periods (Viessman et al. 1989). However, the role infiltration plays not only in affecting runoff quantities but also in carrying pollutant concentration into the subsurface, hence the amount of pollutant infiltrating into the soil, is of great interest in this project. Figure 6.11 shows the temporal evolution of infiltrated pollutant. When rainfall begins, the rainwater infiltrates into the soil with a concentration of pollutant close to its saturated value. The infiltration rate decreases with time as the surface layer reaches saturation. When the rainfall intensity exceeds the infiltration capacity, ponding occurs, ultimately leading to the initiation of overland flow. At this point in time, the pollutant is dissolved in the runoff and diluted. The concentration of the pollutant infiltrating into the soil decreases as time increases. In the figure, the minus sign indicates the downward direction of the pollutant infiltrated. The numerical results provide quantitative information on how infiltration rate affects the pollutant penetration into the soil. As seen earlier, this penetration is affected by dispersion. These results lead to the conclusion that the amount of pollutant that infiltrats into the soil depends on the infiltration rate, the infiltrated area involved, duration time and concentration of pollutant.

6.3.2 Adsorption

To simulate pollutant adsorption, the assumption is made that the original soil contains no pollutants, and that the soil is not detached by rainfall impact and entrained into the flow. Figure 6.12 shows the amount of pollutant adsorbed at different time steps. The simulation conditions are as follows: the domain is two-dimensional measuring 100 by 100m. It is overlaid with a 20 by 20 mesh, in which $\Delta x = \Delta y$. The rainfall rate is 0.000038 m/s. Bed slopes are 0.086 in both the x- and y-directions. The Manning coefficient is 0.025, solubility 357.5kg/m^3 and diffusion coefficient 0.4m^2/s. 525kg of solid pollutant is initially applied at one grid cell. The simulation results confirm the generally expected behavior, namely that with increasing time, the amount of adsorbed pollutant decreases. The computational results also show that the mass loss from the source occurs initially during the infiltration, since the decrease in concentration would be attributed to adsorption onto the soil. This loss can be quite significant. A comparison using three adsorption models, resulted in no important differences being noted. This indicates that the effect of adsorption in the presence of surface flow is smaller than for subsurface flow.

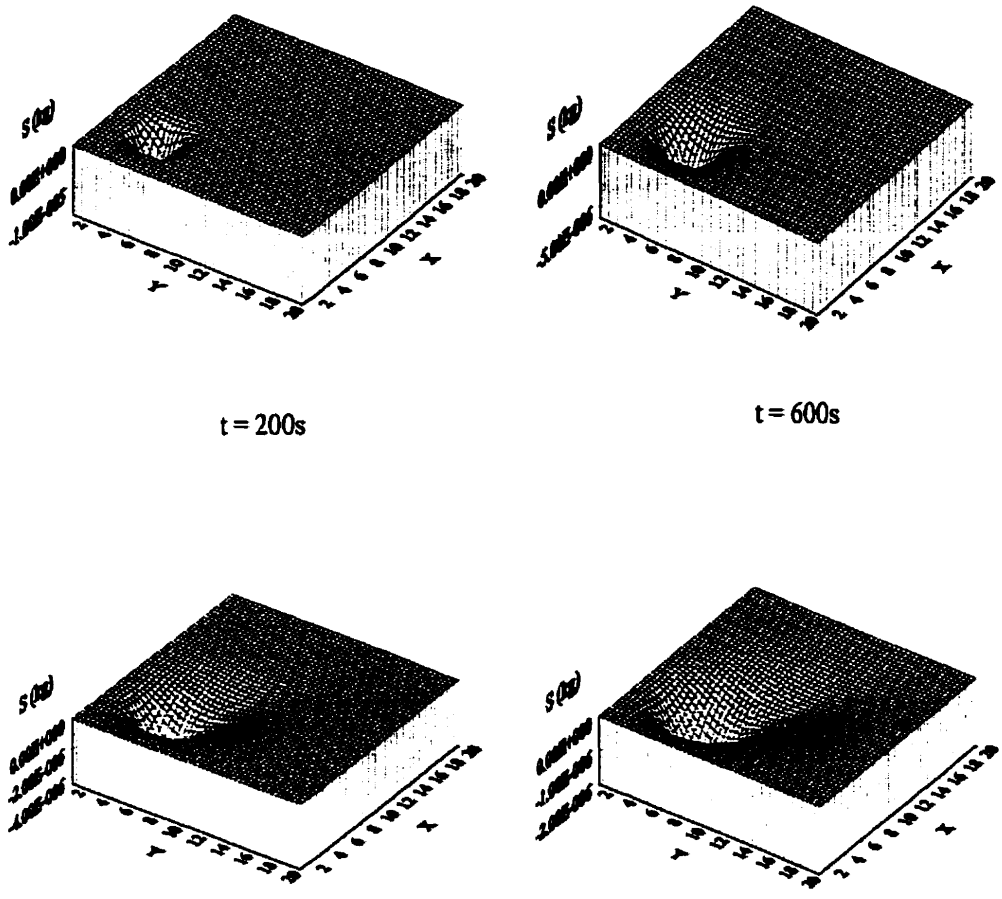

t = 200s

t = 600s

t = 1000s

t = 2200s

Figure 6.11 Pollutant infiltrated at time 200s, 600s, 1000s and 2000s

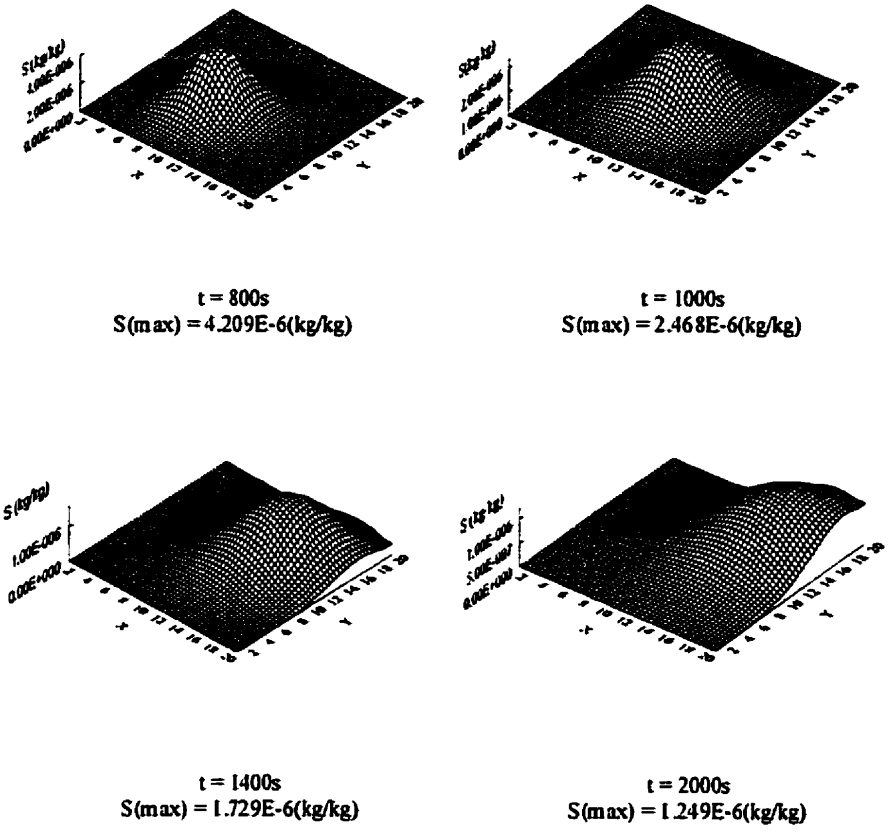

t = 800s
S(max) = 4.209E-6(kg/kg)

t = 1000s
S(max) = 2.468E-6(kg/kg)

t = 1400s
S(max) = 1.729E-6(kg/kg)

t = 2000s
S(max) = 1.249E-6(kg/kg)

Figure 6.12 Amount of pollutant adsorbed at time 800s, 1000s, 1400s and 2000s

6.3.3 Two initial conditions for pollutant distribution

In this investigation, two cases of surface-applied pollutants are studied. The first case deals with a solid pollutant applied on a spot of upstream land surface, whereas the second case considers the solid pollutant to be uniformly applied throughout the domain. Figure 6.13 shows the time evolution of pollutant concentration for the first case. Figure 6.14 shows the time evolution of pollutant concentration for the second case. Clearly, when the pollutant is applied at one location, the initiation of rainfall results in dissolution near the point of application resulting in peak concentration being situated near the upstream. Subsequently, the combined effect of advection and dispersion results in the position and magnitude of the peak concentration being carried downstream with attenuation of the peak. When the pollutant is uniformly applied, the pollutant is uniformly dissolved in the runoff at the beginning. With increase of time, the pollutant concentration migrates and accumulates downstream where it finally leaves the domain. The peak concentration always occurs at the downstream end.

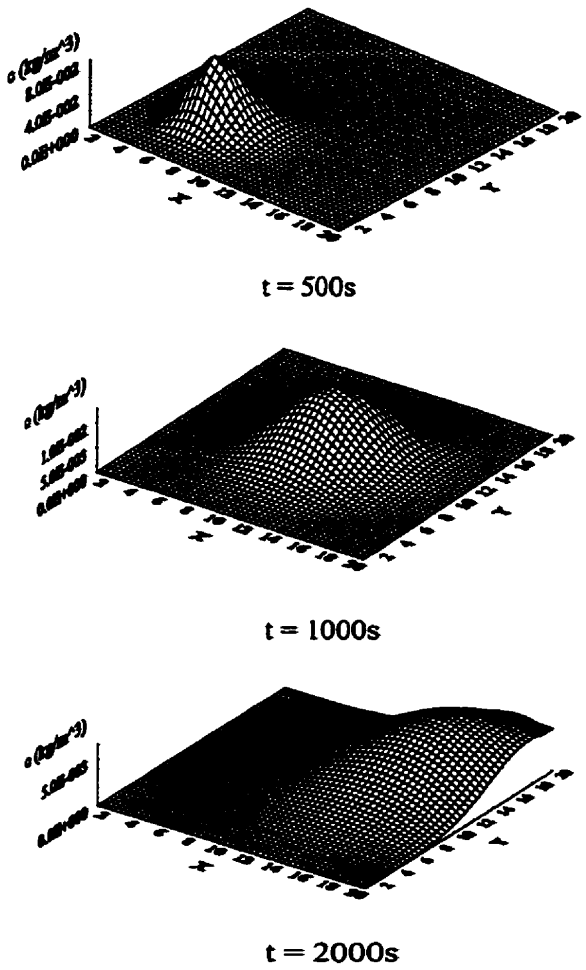

t = 500s

t = 1000s

t = 2000s

Figure 6.13 Time evolution of pollutant concentration in the case of initial pollutant applied on one spot

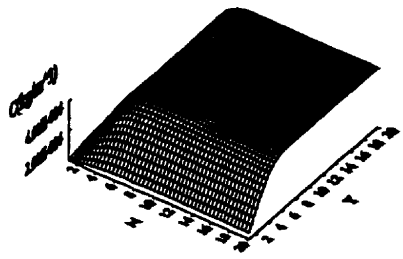

t = 500s
Cmax = 0.000403(kg/m^3)

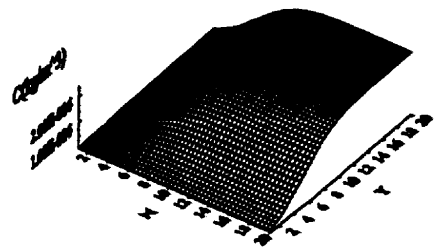

t = 1000s
Cmax = 0.000243(kg/m^3)

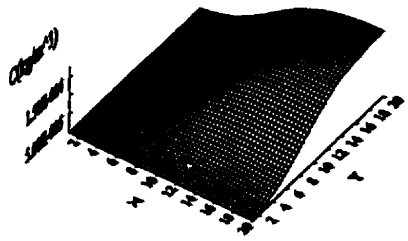

t = 1500s
Cmax = 0.00017934(kg/m^3)

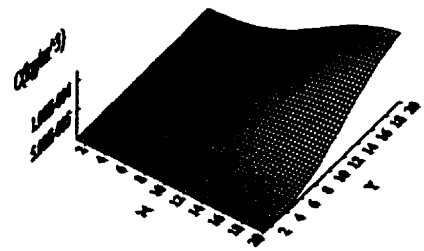

t = 2000s
Cmax = 0.00011997(kg/m^3)

Figure 6.14 Time evolution of pollutant concentration in the case of initial pollutant uniformly applied

6.3.4 Ultimate fate of surface applied pollutant simulated by the numerical model using Cubic Spline integration with implicit and explicit formulation

Several numerical simulations were conducted to generate the general results for predicting the ultimate fate of surface applied pollutant. Two formulations implicit and explicit of the cubic spline integration scheme with different numerical properties and computational efficiencies were employed. The simulations were performed involving different aspects. Figure 6.15 shows the amount of pollutant infiltrated before ponding time. Figure 6.16 shows the amount of pollutant infiltrated after ponding time. Figure 6.17 shows the amount of pollutant remained and dissolved in water. Figure 6.18 shows the amount of pollutant wash-out. Figure 6.19 shows the amount of pollutant adsorbed and Figure 6.20 shows the amount of runoff. In all these figures, the mark solid circles represent the results obtained by using explicit scheme and the mark stars represent the results obtained by using implicit scheme. These numerical tests confirm that the difference between the explicit and implicit cubic spline schemes is negligible. The implicit cubic spline scheme is therefore preferable owing to its computational efficiency. These two schemes are also used to simulate the ultimate fate of surface applied pollutant. In addition, different mesh sizes are used in the tests. Figure 6.21 shows the pollutant migration produced by using different grids, 15 by 20.

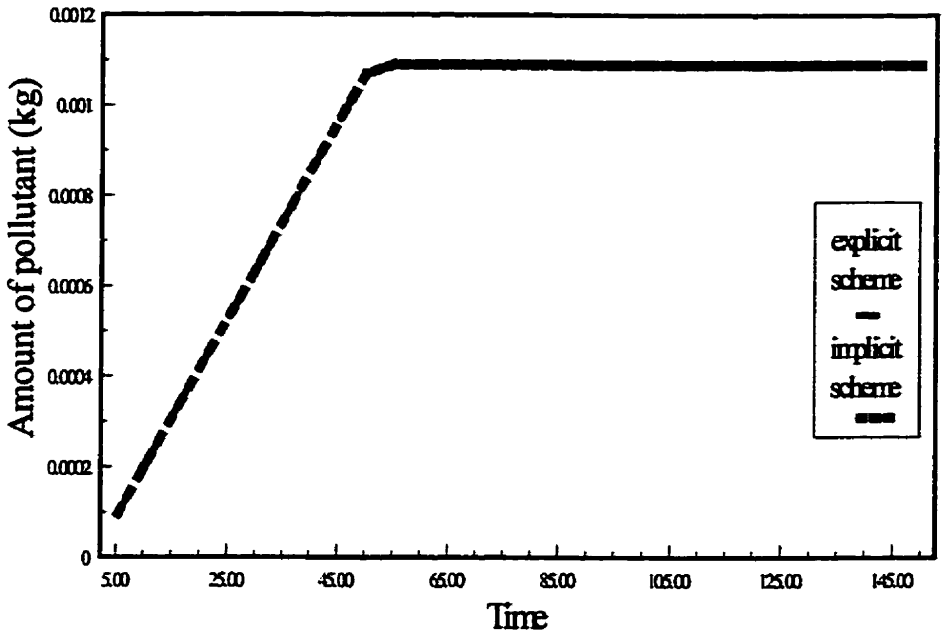

Figure 6.15 Amount of pollutant infiltrated before ponding using both implicit and explicit schemes

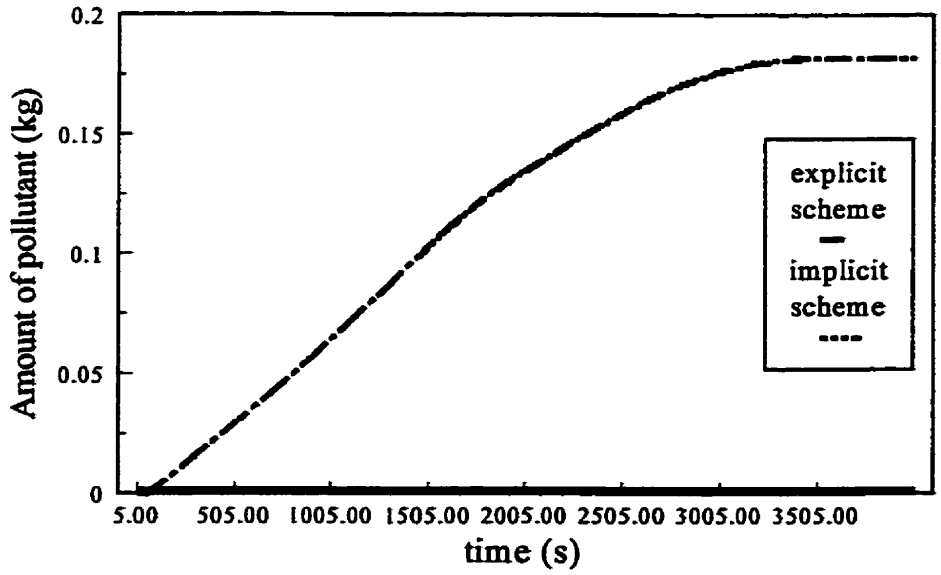

Figure 6.16 Amount of pollutant infiltrated after ponding using both implicit and explicit schemes

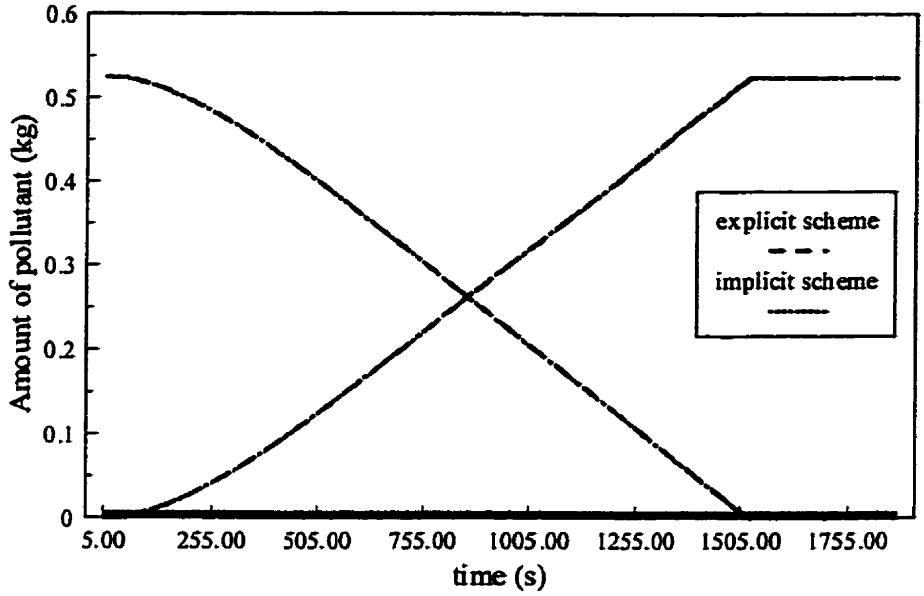

Figure 6.17 Amount of pollutant remaining and dissolved using both implicit and explicit schemes

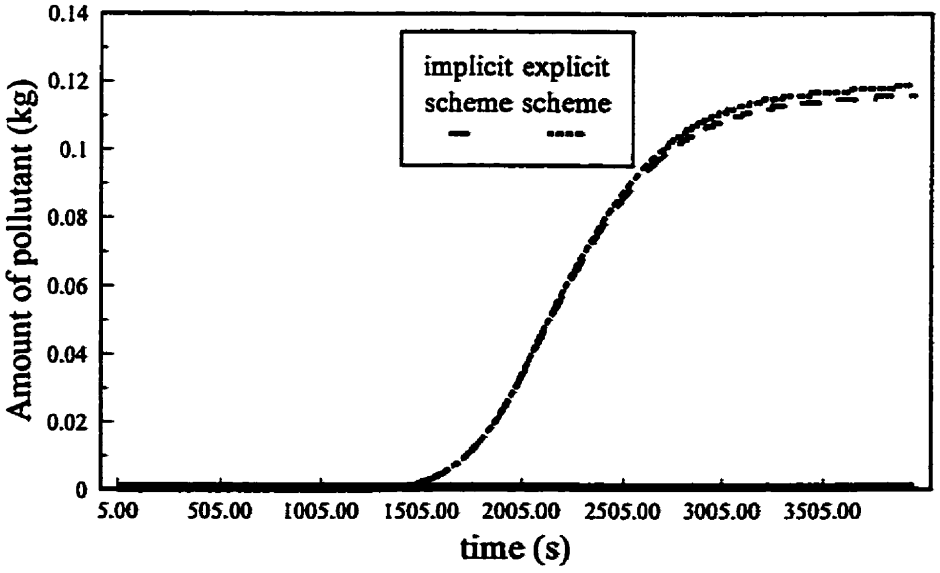

Figure 6.18 Amount of pollutant washed out using both implicit and explicit scheme

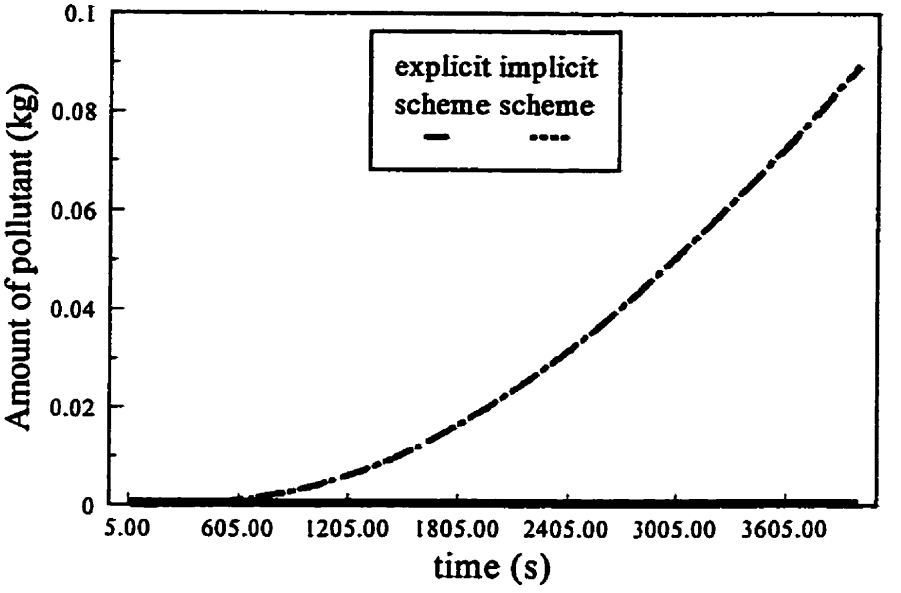

Figure 6.19 Amount of pollutant adsorbed using both implicit and explicit schemes

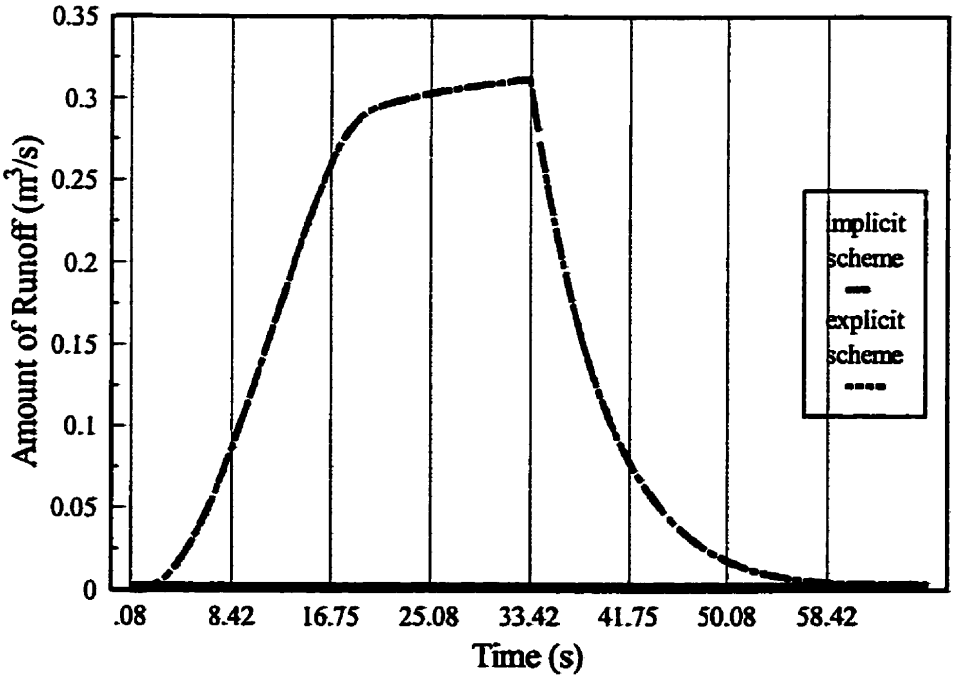

Figure 6.20 Amount of runoff using both implicit and explicit schemes

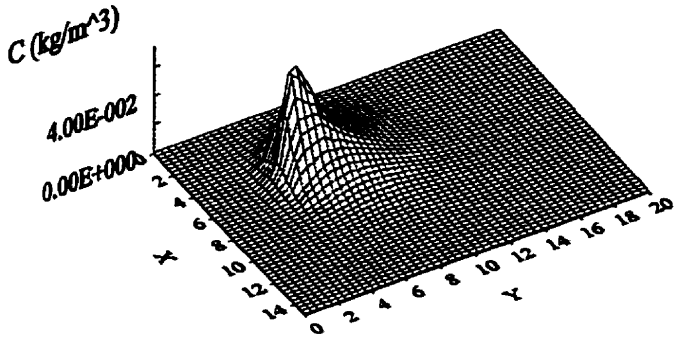

t = 500s, Cmax = 0.0746(kg/m^3)

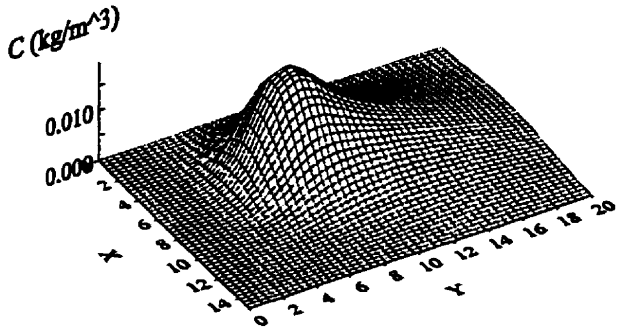

t = 1000s, Cmax = 0.0198(kg/m^3)

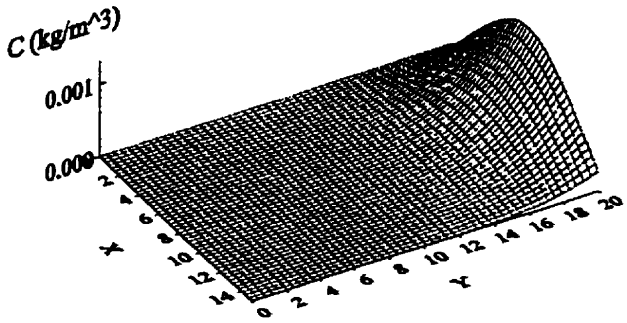

t = 2000s, Cmax = 0.000662(kg/m^3)

Figure 6.21 Pollutant concentration migration with different mesh size

6.3.5 Pollutant migration

Following the preceding analysis, Figure 6.22 shows the time evolution of pollutant concentration in the x-y plane. The pollutant concentrations are obtained at time 250s, 500s, 750s, 1000s and 2000s, respectively. These figures show that the pollutant migration depends on many factors, such as flow depth, flow velocities, bed shear stress, dissolution and dispersion, as well as solubility. Due to the effect of solubility, pollutant dissolved during the process of runoff initiation, results in the apprerance of a concentration peak. Pollutant is continuously dissolved and dispersed around the point of application. The peak concentration migrates downstream due to the effect of advection. Finally, the pollutant is completely washed out and leaves the domain by infiltration and advection. These results adequately describe the general behavior of the migration process of the pollutant.

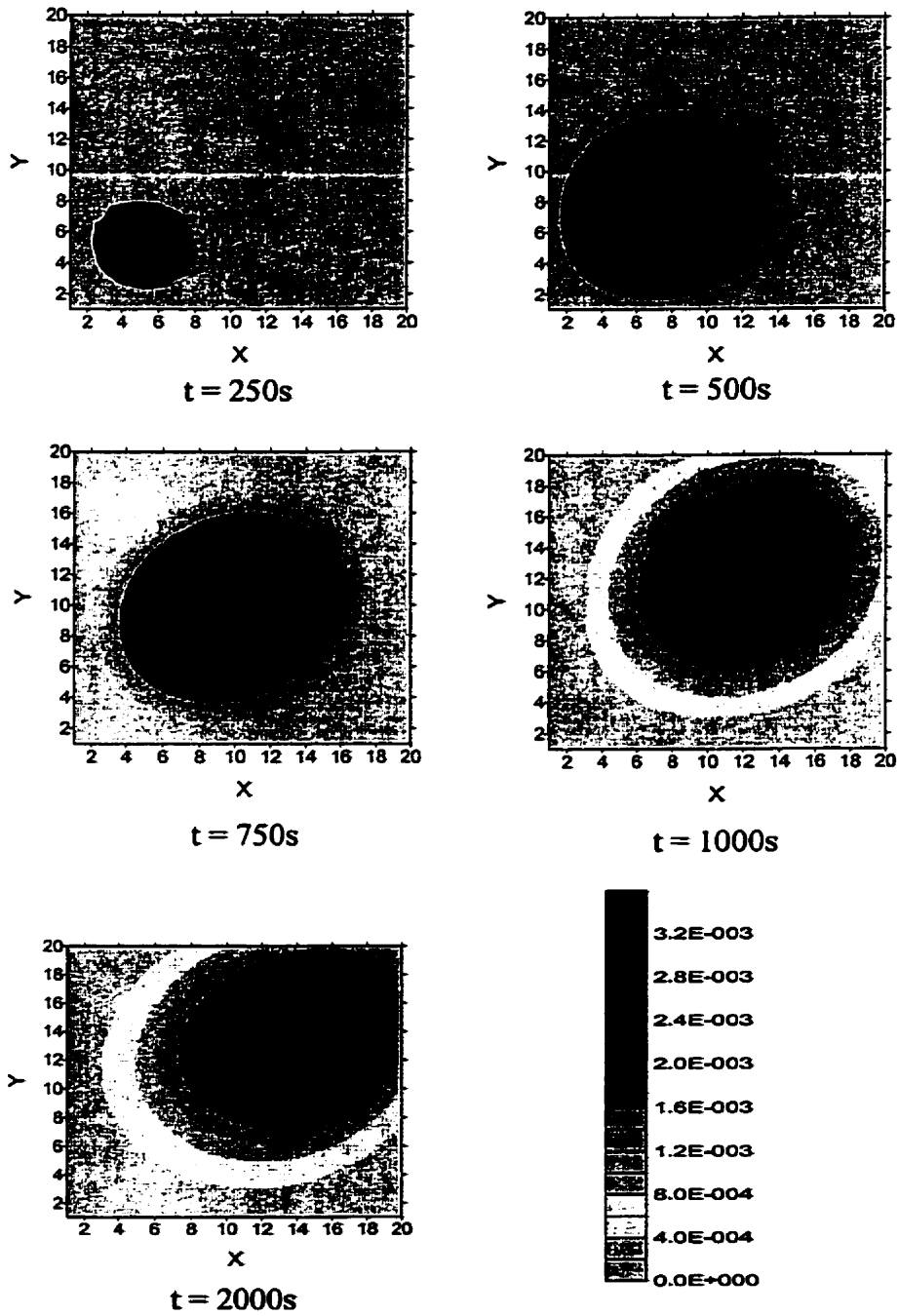

Figure 6.22 Time evolution of pollutant concentration on x-y plan

CHAPTER 7: CONCLUSIONS

This dissertation has focused on the development of a numerical model to simulate pollutant washoff from soil surface in the presence of infiltration and adsorption effects. A solubility rate equation to model the dissolution of the pollutant has been developed based on the analogy between mass and momentum transfer. The final set of governing equations which includes the advection-diffusion equation for the pollutant transport has been solved numerically using an adaptation of the cubic spline integration scheme. The model allows explicit incorporation of variable surface roughness, infiltration, and different pollutant characteristics. The applicability of the model to two-dimensional pollutant washoff in overland flow has been demonstrated with the effects of infiltration, dissolution, diffusion and different substances being incorporated. The overall performance of the model is very satisfactory. The model may be used as a predictive tool to generate useful results concerning the ultimate fate of a surface applied pollutant.

The present sections of the numerical model have been verified by comparison with analytical equations and published field data. Due to the non-existence of comprehensive published data on pollutant washoff, a series of experiments were conducted at the Ecole Polytechnique, covering two main areas: rainfall/runoff relationships and pollutant transport in overland flow. The numerical model was then further evaluated using these data sets. The good correspondence obtained between the

numerical results and experimental data confirms that the numerical model is a reliable tool for predicting pollutant transport in overland flow.

Considerable effort on developing the numerical techniques for this investigation was spent. From the quality of the results obtained, it may be concluded that the cubic spline scheme is an attractive and flexible solution technique for the numerical solution of the model in terms of its high accuracy, lower computational time and ease of application.

The sensitivity test of model parameters indicates that the solubility and reaction rate constant are the significant parameters that influence the process of pollutant dissolution. The dimensionless reaction rate constant k_2 is presumed to depend only on the solubility characteristics of the pollutant.

There are some improvements that can be made to refine the model. A laboratory calibration for dispersion value is needed. Based on the actual behavior, the relations for the dispersion coefficient may be expressed as functions of overland flow and soil parameters in the transport model. Additional laboratory testing needs to be done on infiltration and adsorption; this will ensure that application of the complete numerical model to real cases may be realized.

REFERENCES

AKAN, A. Q. (1986). Time of concentration of overland flow, Journal of Irrigation and Drainage Engineering, 112(4), 283-292.

AKAN, A. Q. (1987). Pollutant washoff by overland flow, Journal of Environmental Engineering, 113(4), 811-824.

AKAN, A. O. and YEN, B. C. (1981). Mathematical model of shallow water flow over porous media, Journal of the Hydraulics Division, 107(4), 479-494.

AMEIN, M. (1968). An implicit method for numerical flood routing, Water Resources Research, 4(4), 719-726.

ARAL, M. M. and LIAO, B. (1996). Analytical solutions for two-dimensional transport equation with time-dependent dispersion coefficients, Journal of Hydrologic Engineering, 1(1), 20-32.

BARONE, F. S., ROWE, R. K. and QUIGLEY, R. M. (1992). A laboratory estimation of diffusion and adsorption coefficients for several volatile organics in a natural clayey soil, Journal of Contaminant Hydrology, 10, 225-250.

BOSMA, W. J. P. and VAN DER ZEE, S. E. A. T. M. (1992). Analytical approximations for nonlinear adsorbing solute transport in layered soils, Soils. J. Contam. Hydrol., 10, 99-118.

BRESLER, E. (1973). Simultaneous transport of solutes and water under transient unsaturated flow conditions, Water Resource Research, 9(4), 975-986.

BURDEN, R. L. and FAIRES, J. D. (1993). Numerical analysis, fifth edition, PWS-KENT Publishing Company, Boston, 133.

CELORIE, J. A., VINSON, T. S., WOODS, SANDRA L. and ISTOK, J. D. (1989). Modeling solute transport by centrifugation, Journal of Environmental Engineering, 115(3), 513-526.

CHEN, Y. P. and FALCONER, R. A. (1992). Advection-diffusion modeling using the modified QUICK scheme, Department of Civil Engineering, University of Bradford, Bradford BD7 1DP U.K. 1171-1196.

CHOW, V. T. and BEN-ZVI, A. (1973). Hydrodynamic modeling of two-dimensional watershed flow, Journal of the Hydraulics Division, 99(11), 2023-2040.

CHU, S. T. (1978). Infiltration during an unsteady rain, Water Resources Research, 14(3), 461-466.

CLAPP, R. B. and HORNBERGER, G. M. (1978). Empirical equations for some soil hydraulic properties, Water Resources Research, 14(4), 601-604.

CORRADINI, C., FLORISA, M. and SMITH, R. E. (1994). Modeling infiltration during complex rainfall sequences, Water Resources Research, 30(10), 2777-2784.

DOMENICO, P. A. and SCHWARTZ, F. W. (1990). Physical and chemical hydrogeology, John Wiley & Sons, Inc., 475.

FALCONER, R. A. and LIU, S. Q. (1988). Modeling solute transport using QUICK scheme, Journal of Environmental Engineering, 114(1), 3-19.

FENNEMA, R. J. and CHAUDHRY, M. H. (1990). Explicit methods for 2-D transient free-surface flows, Journal of Hydraulic Engineering, 116(8), 1013-1034.

FREEZE, R. A. and CHERRY, J. A. (1979). Groundwater, Prentice-Hall, Inc., 75.

GARCIA, R. and KAHAWITA, R. (1986). Numerical solution of the St.Venant equations with the MacCORMACK finite-difference scheme, International Journal for Numerical Methods in Fluids, 6, 259-274.

GARCIA-NAVARRO, P. and SAVIRON, J. M. (1992). McCormack's method for the numerical simulation of one-dimensional discontinuous unsteady open channel flow, Journal of Hydraulic Research, 30(1), 95.

GOVINDARAJU, R. S., KAVVAS, M. L. and JONES, S. E. (1990). Approximate analytical solutions for overland flows, Water Resources Research, 26(12), 2903-2912.

GREEN, W. H. and AMPT, G. A. (1911). Studies on soil physics, 1, The flow of air and water through soils, Journal of Agricultural Science, 4, 11-24.

GUPTA, R., RUDRA, R. and DICKINSON, T. (1998). Modeling infiltration with varying hydraulic conductivity under simulated rainfall conditions, Journal of the American Water Resources Association, 34(2), 279-287.

HOLDEN, A. P. and STEPHENSON, D. (1995). Finite difference formulations of kinematic equations, Journal of Hydraulic Engineering, 121(5), 423-426.

HOLLY, F. M. JR. and PREISSMANN, A. (1977). Accurate calculation of transport in two dimensions, Journal of the Hydraulics Division, 103(11), 1259-1277.

HOLTAN, H. N. (1965). A model for computing watershed retention from soil parameters, Journal of Soil Water Conservation, 20(3), 91-94.

HORTON, R. E. (1935). Surface runoff phenomena: Part I, Analysis of the Hydrograph, Horton Hydrol. Lab. Pub. 101.

HROMADKA, T. V., MCCUEN, R. H. and YEN, C. C. (1987). Comparison of overland flow hydrograph models, Journal of Hydraulic Engineering, 113(11), 1422-1440.

JAMES, W. P., WARINNER, J. and REEDY, M. (1992). Application of the Green-Ampt infiltration equation to watershed modeling, Water Resources Bulletin, 28(3), 623-635.

JAQUE, D. T. and BALL, J. E. (1994). Numerical simulation of advective-diffusion mass transport, Journal of Hydroscience and Hydraulic Engineering, 11(2), 49-56.

KATOPODES, N. and STRELKOFF, TH. (1979). Two-dimensional shallow water-wave models, Journal of The Engineering Mechanics Division, Proceedings of ASCE, 105(2), 317-333.

KATZ, D. M., (1995). Effects of surface roughness and rainfall impact on overland flow, Journal of Hydraulic Engineering, 121(7), 546-553.

KAWAHARA, M. and YOKOYAMA, T. (1980). Finite element method for direct runoff flow, Journal of the Hydraulics Division, 106(4), 519-533.

KHAN, A. R., I. R. AL-WAHEAB and AL-HADDAD, A. (1996). A generalized equation for adsorption isotherms for multi-component organic pollutants in dilute aqueous solution, Journal of Environ. Tech., 17, 13-23.

KOMATSU, T., OHGUSHI, K. and ASAI, K. (1997). Refined numerical scheme for advective transport in diffusion simulation, Journal of Hydraulic Engineering, 123(1), 41-50.

LEONARD, B. P. (1979). A stable and accurate convective modeling procedure based on QUADRATIC upstream interpolation, Computer Methods in Applied Mechanics and Engineering., 19(1), 59-98.

LI, CH. W. (1990). Advection simulation by Minimax-Characteristics method, Journal of Hydraulic Engineering, 116(9), 1138-1144.

LIGGETT, J. A. and WOOLHISER, D. A. (1967). Difference solutions of the shallow-water equation, Journal of the Engineering Mechanics Division, 93(2), 39-71.

LIN, B. L. and FALCONER, R. A. (1997). Tidal flow and transport modeling using ULTIMAT QUICK scheme, Journal of Hydraulic Engineering, 123(4), 303-314.

LUK, G. K. Y., LAU, Y. L. and WATT, W. E. (1990). Two-dimensional mixing in rivers with unsteady pollutant source, Journal of Environmental Engineering, 116(1), 125-143.

MEIN, R. G. and LARSON, C. L. (1973). Modeling infiltration during steady rain, Water Resources Research, 9(2), 384-394.

MELNYK, T. W., (1985). Effects of sorption behavior on contaminant migration, Atomic Energy of Canada Limited, Whiteshell Nuclear Research Establishment.

MORRIS, E. M. and WOOLHISER, D. A. (1980). Unsteady one-dimensional flow over a plane: partial equilibrium and recession hydrographs, Water Resources Research, 16(2), 355-360.

MULLEM, J. A. V. (1991). Runoff and peak discharges using Green-Ampt infiltration model, Journal of Hydraulic Engineering, 117(3), 354-370.

PHILIP, J. R. (1965). The theory of infiltration, Soil Sci., 84, 257-264.

RAWLS, W. J., BRAKENSIEK, D. and MILLER, N. (1983). Green-Ampt infiltration parameters from soils data, Journal of Hydraulic Engineering, 109(1), 62-70.

ROACHE, P. J. (1972). On artificial viscosity, Journal of Computational Physics, 10(2), 351-366.

SELROOS, J.-O. and CVETKOVIC, V. (1992). Modeling solute advection coupled with sorption kinetics in heterogeneous formations, Water Resource Research, 28(5), 1271-1278.

SIEMONS, J. (1970). Numerical methods for the solution of diffusion-advection equation, Technical report, Delft Hydraulics Laboratory, Ecole Polytechnique, 3.

SINGH, V. P. (1995). Computer Models of watershed Hydrology, Water Researches Publications, 783-808.

SUNDSTROM, D. W. and KLEI, H. E. (1979). Wastewater treatment, Prentice-hall, Inc., 244-245.

TAYFUR, G., KAVVAS, M. L., GOVINDARAJU, R. S. and STORM, D. E. (1993). Applicability of St.Venant equations for two-dimensional overland flows over rough infiltration surfaces, Journal of Hydraulic Engineering, 119(1), 51-63.

VAN DER ZEE, S. E. A. T. M. (1990). Analytical traveling wave solutions for transport with nonlinear and nonequilibrium adsorption, Water Resources Research, 26(10), 2563-2578.

VAN GENUCHTEN, M. TH., DAVIDSON, J. M. and WIERENGA, P. J. (1973). An evaluation of kinetic and equilibrium equations for the prediction of pesticide movement through porous media, Soil Sci. Soc. A.P., 38, 29-35.

VIESSMAN, W. JR., LEWIS, G. L. and KNAPP, J. W. (1989). Introduction to hydrology, Third Edition, Harper & Row, Publishers, Inc., 68.

WANG, P. (1985). Spline-Lax-Wendroff scheme and Spline-Leap-Frog scheme, ACTA Aerodynamic SINICA., China, 3, 90-95.

WANG, P. (1987). The method of fractional steps for solving Navier-Stokes equations using parameter splines, ACTA Aerodynamic SINICA., China, 5(3), 218-225.

WANG, P. and KAHAWITA, R. (1983a). Numerical integration of partial differential equations using cubic splines, International Journal of computer Math., 13, 271-286.

WANG, P. and KAHAWITA, R. (1983b). Cubic spline techniques in numerical models of estuarine circulation, ACTA Aerodynamic SINICA., China, 3, 17-29.

WANG, P. and KAHAWITA, R. (1984). The numerical solution of Burgers' equation using splines, ACTA Aerodynamic SINICA., China, 2, 11-18.

WOOD, W. L. and ARNOLD P. D. (1990). On the Box scheme for overland flow calculations, Communications in Applied Numerical Methods, 6, 323-325.

WU, J. K. (1997). A wave equation model to solve the multidimensional transport equation, International Journal for Numerical Methods in Fluids, 24, 423-439.

YAN, M. (1995). Modeling pollutant transport in overland flow with infiltration, M. S. Thesis, École Polytechnique de Montréal, Canada.

YAN, M. and KAHAWITA, R. (1997). Modeling pollutant transport in overland flow with infiltration, 27th IAHR Congress, San Francisco, CA, August 10-15, the Proceeding of 27th Congress of the International Associate for Hydraulic Research: Water for a Changing Global Community, Vol.5, 347-351.

YAN, M. and KAHAWITA, R. (1998). Modeling of simultaneous hydrologic, chemical and pollutant transport processes, 1998 Western Pacific Geophysics Meeting, Taipei, July 21-24, the Proceeding of 1998 Western Pacific Geophysics Meeting, w28.

ZHANG, W. H. and CUNDY, T. W. (1989). Modeling of two-dimensional overland flow, Water Resources Research, 25(9), p2019-2035.

ZOPPOU, C. and KNIGHT, J. H. (1997). Analytical solutions for advection and advection-diffusion equations with spatially variable coefficients, Journal of Hydraulic Engineering, 123(2), p144-148.

APPENDIX

APPENDIX 1: Frequently Used Cubic Spline Formulation

Basic form of cubic spline scheme

$$y_i^{k+1} = F_i^{k+1} + R_i^{k+1} m_i^{k+1} + Q_i^{k+1} M_i^{k+1}$$

Where y represents a function, m and M are first derivative and second derivative, respectively, R represents a coefficient of first derivative and Q represents a coefficient of second derivative.

Explicit scheme

When explicit scheme is employed, the function h^{k+1}, u^{k+1}, v^{k+1} and c^{k+1} may be solved directly, and then m_i and M_i may be solved using basic relation of cubic spline.

A tridiagonal system for the first derivative m_i is as follows:

$$A_i m_{i-1}^{k+1} + B_i m_i^{k+1} + C_i m_{i+1}^{k+1} = D_i \qquad i = 1,2,...,m$$

$$A_i = \frac{1}{\Delta x_i}$$

$$B_i = 2\left(\frac{1}{\Delta x_i} + \frac{1}{\Delta x_{i+1}}\right)$$

$$C_i = \frac{1}{\Delta x_{i+1}}$$

$$D_i = \frac{3(y_{i+1} - y_i)}{\Delta x_{i+1}^2} + \frac{3(y_i - y_{i-1})}{\Delta x_i^2}$$

$$\begin{bmatrix} [B_1] & [C_1] & & & & & & \\ [A_2] & [B_2] & [C_2] & & & & & \\ & \ddots & \ddots & \ddots & & & & \\ & & \ddots & \ddots & \ddots & & & \\ & & & \ddots & \ddots & \ddots & & \\ & & & & [A_{m-2}] & [B_{m-2}] & [C_{m-2}] & \\ & & & & & [A_{m-1}] & [B_{m-1}] \end{bmatrix} \begin{bmatrix} [m_1] \\ [m_2] \\ \vdots \\ \vdots \\ \vdots \\ [m_{m-2}] \\ [m_{m-1}] \end{bmatrix} =$$

$$\begin{bmatrix} [D_1 - A_1 \cdot m_0] \\ [D_2] \\ \vdots \\ \vdots \\ \vdots \\ [D_{m-2}] \\ [D_{m-1} - C_{m-1} \cdot m_m] \end{bmatrix}$$

And second derivative may be written as follows:

$$M_i = -\frac{4m_i}{\Delta x_{i+1}} - \frac{2m_{i+1}}{\Delta x_{i+1}} + 6\frac{y_{i+1} - y_i}{\Delta x_{i+1}^2}$$

Implicit Scheme

The basic form for the implicit scheme is the same as for explicit scheme:

$$y_i^{k+1} = F_i + R_i m_i^{k+1} + Q_i M_i^{k+1}$$

There are three ways to get the solution by using the implicit scheme,

a) A tridiagonal system for the function y_i:

$$A_i y_{i-1}^{k+1} + B_i y_i^{k+1} + C_i y_{i+1}^{k+1} = D_i \qquad i = 1,2,\ldots,m$$

$$A_i = \frac{e_i \Delta x_i}{6 \cdot c_i} - \frac{1}{\Delta x_i}$$

$$B_i = \frac{d_i \Delta x_i}{6 \cdot c_i} + \frac{e_{i+1}(\Delta x_i + \Delta x_{i+1})}{3 \cdot c_{i+1}} - \frac{R_{i+1}(\Delta x_{i+1}^2 + 3 \cdot R_i \Delta x_{i+1} - 6 \cdot Q_i)}{36 \cdot c_{i+1}} + \frac{\Delta x_i + \Delta x_{i+1}}{\Delta x_i \cdot \Delta x_{i+1}}$$

$$C_i = \frac{d_{i+1}(\Delta x_i + \Delta x_{i+1})}{3 \cdot c_{i+1}} - \frac{R_i(2 \cdot \Delta x_{i+1}^2 - 3 \cdot R_i \cdot \Delta x_{i+1}) - 6 \cdot Q_i \cdot (\Delta x_{i+1} - R_{i+1}))}{36 \cdot c_{i+1}} - \frac{1}{\Delta x_{i+1}}$$

$$D_i = \frac{a_i \Delta x_i}{6 c_i} + \frac{a_{i+1}(\Delta x_i + \Delta x_{i+1})}{3 c_{i+1}} - \frac{F_{i+1}(2 R_i \Delta x^2{}_{i+1} - 6 Q \Delta x_{i+1}) + F_i R_{i+1} \Delta x^2{}_{i+1}}{36 c_{i+1}}$$

$$a_i = \frac{F_i R_{i-1} \Delta x_i}{6} + F_{i-1}\left(\frac{R_i \Delta x_i}{3} + Q_i\right)$$

$$c_i = \frac{R_i R_{i-1} \Delta x_i^2}{36} - \frac{(R_i \Delta x_i + 3 Q_i)(R_{i-1} \Delta x_i - 3 Q_{i-1})}{9}$$

$$d_i = R_{i-1}\left(\frac{\Delta x_i}{6} - \frac{R_i}{2} - \frac{Q_i}{\Delta x_i}\right)$$

$$e_i = R_i\left(\frac{\Delta x_i}{3} + \frac{R_{i-1}}{2}\right) + Q_i\left(1 + \frac{R_{i-1}}{\Delta x_i}\right)$$

$$\Delta x = x_i - x_{i-1}$$

The following relations give the solution algorithm for the first derivative,

$$m_0^{k+1} = \frac{d_0 b_1 - d_1 b_0}{a_0 b_1 - a_1 b_0}$$

$$m_i^{k+1} = \frac{d_i - a_i m_{i-1}^{k+1}}{b_i} \qquad i \neq 0$$

Where

$$a_0 = -R_0 + \frac{4Q_0}{\Delta x_1}$$

$$b_0 = -\frac{2Q_0}{\Delta x_1}$$

$$d_0 = F_0 - y_0^{k+1} - 6Q_0 \frac{y_1^{k+1} - y_0^{k+1}}{\Delta x_1^2}$$

$$a_i = -\frac{2Q_i}{\Delta x_i}$$

$$b_i = -R_i - \frac{4Q_i}{\Delta x_i}$$

$$d_i = F_i - y_i^{k+1} - 6Q_i \frac{y_i^{k+1} - y_{i-1}^{k+1}}{\Delta x_i^2}$$

By using the basic relation of cubic spline, the second derivative may be computed,

$$M_i = -\frac{4m_i}{\Delta x_{i+1}} - \frac{2m_{i+1}}{\Delta x_{i+1}} + 6\frac{y_{i+1} - y_i}{\Delta x_{i+1}^2}$$

A single tridiagonal system for the first derivative m_i:

$$A_i m_{i-1}^{k+1} + B_i m_i^{k+1} + C_i m_{i+1}^{k+1} = D_i \qquad i = 1,2,\ldots,m$$

$$A_i = \frac{1}{3 \cdot \Delta x_i} - \frac{2Q_i + 4Q_{i-1} - R_{i-1}\Delta x_i}{\Delta x_i^3 \Delta_i}$$

$$B_i = \frac{2}{3}\left(\frac{1}{\Delta x_i} + \frac{1}{\Delta x_{i+1}}\right) - \frac{2Q_{i+1} - 4 \cdot Q_i - R_i \Delta x_{i+1}}{\Delta x_{i+1}^3 \Delta_{i+1}} - \frac{2Q_{i-1} + 4Q_i + R_i \Delta x_i}{\Delta x_i^3 \Delta_i}$$

$$C_i = \frac{1}{3\Delta x_{i+1}} - \frac{2Q_i + 4 \cdot Q_{i+1} + R_{i+1}\Delta x_{i+1}}{\Delta x_{i+1}^3 \Delta_{i+1}}$$

$$D_i = \frac{F_{i+1} - F_i}{\Delta x_{i+1}^2 \Delta_{i+1}} + \frac{F_i - F_{i-1}}{\Delta x_i^2 \Delta_i}$$

$$\Delta_i = 1 + 6\left(\frac{Q_i + Q_{i-1}}{\Delta x_i^2}\right)$$

The following simple relations give the solution for function,

$$u_0^{k+1} = \frac{d_0 b_1 - d_1 b_0}{a_0 b_1 - a_1 b_0}$$

$$u_i^{k+1} = \frac{d_i - a_i u_{i-1}^{k+1}}{b_i}; \qquad i \neq 0$$

Where

$$a_0 = 1 + \frac{6Q_0^{k+1}}{\Delta x_1^2}$$

$$b_0 = -\frac{6Q_0^{k+1}}{\Delta x_1^2}$$

$$d_0 = F_0^{k+1} + R_0^{k+1} m_0^{k+1} - Q_0^{k+1}\left(\frac{2m_1^{k+1} + 4m_0^{k+1}}{\Delta x_1}\right)$$

$$a_i = -\frac{6Q_i^{k+1}}{\Delta x_i^2}$$

$$b_i = 1 + \frac{6Q_i^{k+1}}{\Delta x_i^2}$$

$$d_i = F_i^{k+1} + R_i^{k+1} m_i^{k+1} + Q_i^{k+1}\left(\frac{2m_{i-1}^{k+1} + 4m_i^{k+1}}{\Delta x_i}\right)$$

By using the same basic relation of cubic spline, the second derivative may be solved.

c) Derivation of the scalar set of equations containing Second derivatives only

$$A_i M_{i-1}^{k+1} + B_i M_i^{k+1} + C_i M_{i+1}^{k+1} = D_i \qquad i = 1,2,\ldots,m$$

Where

$$A_i = \frac{\Delta x_i}{6} + \frac{R_i + 2R_{i-1}}{6\Delta x_i} - \frac{Q_{i-1}}{\Delta x_i \Delta_i}$$

$$B_i = \frac{\Delta x_i + \Delta x_{i+1}}{3} - \frac{R_{i+1} + 2R_i}{6\Delta_{i+1}} + \frac{2R_i + R_{i-1}}{6\Delta_i} + Q_i\left(\frac{1}{\Delta_{i+1}\Delta x_{i+1}} + \frac{1}{\Delta_i \Delta x_i}\right)$$

$$C_i = \frac{\Delta x_{i+1}}{6} - \frac{2R_{i+1} + R_i}{6\Delta_{i+1}} - \frac{Q_{i+1}}{\Delta x_{i+1}\Delta_{i+1}}$$

$$D_i = \frac{F_{i+1} - F_i}{\Delta_{i+1}\Delta x_{i+1}} - \frac{F_i - F_{i-1}}{\Delta_i \Delta x_i}$$

$$\Delta_i = 1 - \frac{R_i - R_{i-1}}{\Delta x_i}$$

Using the following equations may solve the function y,

$$y_0^{k+1} = \frac{d_0 b_1 - d_1 b_0}{a_0 b_1 - a_1 b_0}$$

$$y_i^{k+1} = \frac{d_i - a_i u_{i-1}^{k+1}}{b_i}; \qquad i \neq 0$$

Where

$$a_0 = 1 + \frac{R_0^{k+1}}{\Delta x_1}$$

$$b_0 = \frac{R_0^{k+1}}{\Delta x_0}$$

$$d_0 = F_0^{k+1} - R_0^{k+1}\left(\frac{\Delta x_1}{6} M_1^{k+1} + \frac{\Delta x_1}{3} M_0^{k+1}\right) + Q_0^{k+1} M_0$$

$$a_i = \frac{R_i^{k+1}}{\Delta x_i}; \qquad i = 1,2,\ldots,m$$

$$b_i = 1 - \frac{R_i^{k+1}}{\Delta x_i}$$

$$d_i = F_i^{k+1} + R_i^{k+1}\left(\frac{\Delta x_i}{3}M_i^{k+1} + \frac{\Delta x_i}{6}M_{i-1}^{k+1}\right) + Q_i^{k+1}M_i^{k+1}$$

By using the same basic relation of cubic spline, the second derivative may be solved.